

RL-TR-96-203
Final Technical Report
December 1996



SEMICONDUCTOR LASER LOW FREQUENCY NOISE CHARACTERIZATION

National Aeronautics and Space Administration

Dr. Lute Maleki and Dr. Ronald T. Logan

DTIC QUALITY INSPECTED 3

APPROVED FOR PUBLIC RELEASE; DISTRIBUTION UNLIMITED.

19970218 050

**Rome Laboratory
Air Force Materiel Command
Rome, New York**

This report has been reviewed by the Rome Laboratory Public Affairs Office (PA) and is releasable to the National Technical Information Service (NTIS). At NTIS it will be releasable to the general public, including foreign nations.

RL-TR-96-203 has been reviewed and is approved for publication.

APPROVED:



NORMAN BERNSTEIN
Project Engineer

FOR THE COMMANDER:



DONALD W. HANSON, Director
Surveillance & Photonics Directorate

If your address has changed or if you wish to be removed from the Rome Laboratory mailing list, or if the addressee is no longer employed by your organization, please notify RI/OCPC, 25 Electronic Pky, Rome, NY 13441-4514. This will assist us in maintaining a current mailing list.

Do not return copies of this report unless contractual obligations or notices on a specific document require that it be returned.

REPORT DOCUMENTATION PAGE

Form Approved
OMB No. 0704-0188

Public reporting burden for this collection of information is estimated to average 1 hour per response, including the time for reviewing instructions, searching existing data sources, gathering and maintaining the data needed, and completing and reviewing the collection of information. Send comments regarding this burden estimate or any other aspect of the collection of information, including suggestions for reducing this burden, to Washington Headquarters Service, Directorate for Information Operations and Reports, 1215 Jefferson Davis Highway, Suite 1204, Arlington, VA 22202-4302, and to the Office of Management and Budget, Paperwork Reduction Project (0704-0188), Washington, DC 20503.

1. AGENCY USE ONLY (Leave Blank)		2. REPORT DATE December 1996		3. REPORT TYPE AND DATES COVERED Final Nov 91 - Jun 95	
4. TITLE AND SUBTITLE SEMICONDUCTOR LASER LOW FREQUENCY NOISE CHARACTERIZATION				5. FUNDING NUMBERS C - FA875040013 PE - 63726F PR - 2863 TA - 92 WU - 50	
6. AUTHOR(S) Dr. Lute Maleki and Dr. Ronald T. Logan				8. PERFORMING ORGANIZATION REPORT NUMBER N/A	
7. PERFORMING ORGANIZATION NAME(S) AND ADDRESS(ES) National Aeronautics and Space Administration Jet Propulsion Laboratory Time and Frequency Systems Research Group 4800 Oak Grove Drive, Pasadena CA 91109-8099				10. SPONSORING/MONITORING AGENCY REPORT NUMBER RL-TR-96-203	
9. SPONSORING/MONITORING AGENCY NAME(S) AND ADDRESS(ES) Rome Laboratory/OCPC 25 Electronic Pky Rome NY 13441-4514				11. SUPPLEMENTARY NOTES RI. Project Engineer: Norman P. Bernstein/OCPC/(315) 330-3147	
12a. DISTRIBUTION/AVAILABILITY STATEMENT Approved for Public Release; Distribution Unlimited				12b. DISTRIBUTION CODE	
13. ABSTRACT (Maximum 200 words) This work summarizes the efforts in identifying the fundamental noise limit in semiconductor optical sources (lasers) to determine the source of 1/F noise and its associated behavior. In addition, the study also addresses the effects of this 1/F noise on RF phased arrays. The study showed that the 1/F noise in semiconductor lasers has an ultimate physical limit based upon similar factors to fundamental noise generated in other semiconductor and solid state devices. The study also showed that both additive and multiplicative noise can be a significant detriment to the performance of RF phased arrays especially in regard to very low sidelobe performance and ultimate beam steering accuracy. The final result is that a noise power related term must be included in a complete analysis of the noise spectrum of any semiconductor device including semiconductor lasers.					
14. SUBJECT TERMS Lasers, Optics, Phased Arrays, Optical Beam Formation				15. NUMBER OF PAGES 112	
				16. PRICE CODE	
17. SECURITY CLASSIFICATION OF REPORT UNCLASSIFIED		18. SECURITY CLASSIFICATION OF THIS PAGE UNCLASSIFIED		19. SECURITY CLASSIFICATION OF ABSTRACT UNCLASSIFIED	
				20. LIMITATION OF ABSTRACT UNLIMITED	

NSN 7540-01-283-5500

Standard Form 298 (Rev. 2/89)
Prescribed by ANSI Z39-18
298-102

TABLE OF CONTENTS

<i>Section</i>	<i>Title</i>	<i>Page</i>
I.	EXECUTIVE SUMMARY	2
II.	INTRODUCTION	4
III.	PHASE NOISE IN PHOTONIC RF ARRAYS	5
IV.	INFLUENCE OF MODULATION ON SEMICONDUCTOR NOISE	7
V.	MULTIPLICATIVE NOISE AND LASER LINEWIDTH	9
APPENDIX 1		
	EFFECTS OF PHASE NOISE FROM LASERS AND OTHER SOURCES ON PHOTONIC RF PHASED-ARRAYS	A-1
APPENDIX 2		
	PARTIAL-WAVE ANALYSIS OF MULTIPLICATIVE NOISE IN LASER AMPLIFIERS: APPLICATION TO LASER LINDWIDTH	B-1

1. EXECUTIVE SUMMARY

The objective of this task was to study the origin of the phenomena that contribute to the overall noise in photonic phased array systems. In particular, the task included the study and the characterization of the semiconductor laser low frequency noise and its $1/f$ behavior.

The approach adopted for this study included three parts. In the first, a comprehensive study of the effect of phase noise from lasers and other sources on photonic phased array systems was considered. This study considered the influence of additive, as well as multiplicative noise in photonic systems, and resulted in the important conclusion that the effect of uncorrelated multiplicative phase noise in a phased array system is diminished as the number of array elements is increased. The study further revealed that, by contrast, the additive phase noise of the array does not diminish with the number of elements. Thus for an array with a large number of elements, the overall signal-to-noise ratio will be independent of the size of the array. Results of this segments of the study pointed to the significance of including both the additive and multiplicative noise sources in system designs of photonic phased array antennas.

In the second segment, the influence of modulation on the noise of semiconductor lasers was experimentally determined. In particular, the dependence of the low-frequency noise on injection-current modulation in external cavity semiconductor lasers was examined. This noise can limit the performance of photonic sensors and phased array antenna systems, and can reduce the sensitivity of photonic and fiberoptic sensors.

The approach followed for the study of the $1/f$ noise in the spectrum of semiconductor lasers was the consequence of the need to examine the noise for a single mode laser, based on the findings of the second part of the study. This approach included a model of the laser as a noise-driven resonant amplifier. A dynamic partial wave model devised for this system was then used to obtain the spectrum of the output field of the laser. This model produced interesting and suggestive results, including a power-independent term in the Schawlow-Townes formula for the linewidth of the semiconductor laser, resulting from the multiplicative noise due to electron density fluctuations in the gain medium. The model, however, failed to directly account for the $1/f$ behavior in the spectrum as a consequence of the laser action.

2. INTRODUCTION

Noise is typically the limiting factor in the performance of photonic RF systems. The influence of noise in the stability of fiber optic distribution links, previously studied in detail at JPL, pointed to the need for a comprehensive examination of the influence of the phase noise of semiconductor lasers in photonic multi-element arrays. The Semiconductor Laser Low Frequency Noise Characterization task was aimed at addressing this problem.

The approach used in this task was devised to systematically consider the influence of low frequency noise of semiconductor lasers, both experimentally and analytically, and then develop a model for the origin of the $1/f$ noise in the laser spectrum. In this final report results of the study will be presented. The presentation is divided in three segments. In the first part the effect of the phase noise on the performance of phased arrays is analyzed. In the second part, the influence of modulation on the laser noise is reviewed, and experimental results are presented. The third segment includes the presentation of a model for the noise of the semiconductor lasers which yields the influence of the multiplicative noise on the linewidth manifested as an additional term to the Schawlow-Townes formula.

While the study did not reveal the origin of $1/f$ noise in the spectrum of semiconductor lasers, it laid important groundwork for future examination of this topic, which is difficult to analytically track, yet is of fundamental importance in the performance of photonic based RF systems.

3 Phase Noise in Photonic rf Arrays

The function of rf photonic phased arrays is fundamentally based on the phase control of individual elements. Thus any noise due to individual components in the system limit the system performance. Basically the total noise in the system is determined by the combination of both additive and multiplicative components. The additive term is produced by a variety of sources including the thermal noise of dissipative elements, the shot noise of the photodetectors, and the laser relative intensity noise (RIN). The additive term is readily measured and, in most instances, is easy to calculate; so its influence on the performance of the system is generally straightforward. The additive noise is always present in a system, and can be determined independent of the presence of any signal. The multiplicative noise originates from low frequency gain and path length instabilities, and is only present when the signal propagates in the system. This term usually has a $1/f^2$ behavior with frequency, and thus is typically dominant in frequency regimes close to the carrier.

Our model for the additive and multiplicative noise terms deals with the uncorrelated components. The model is given in detail in Appendix I and essentially generalizes the case of noise for a single element with unity gain to the case of a phased array with M elements. The analysis leads to the conclusion that for uncorrelated white Gaussian noise, the SNR for an M element array is given by,

$$SNR = \frac{\langle |E_0|^2 \rangle}{\frac{\langle |\delta\phi(t)|^2 \rangle E_0^2}{M} + \langle |N(t)|^2 \rangle}, \quad (1)$$

where SNR is the signal-to-noise ratio of the M element array, E_0 is the amplitude of the input signal, $\delta\phi(t)$ is the multiplicative phase noise, and $N(t)$ is the additive noise term. In the above expression $\langle \rangle$ represent time averaging.

From the above equation it is readily concluded that the additive term in the SNR remains constant, independent of the number of elements in the array. The multiplicative term, by contrast, does depend on the number of arrays, and is reduced by factor M. As M increases, the multiplicative noise term reduces to a negligible factor, and the noise performance of the array is determined by the additive noise contribution, only.

As mentioned above, laser RIN is a multiplicative noise source. Thus in designing photonic rf arrays the use of the above equation permits the determination of the type of the laser best suited for the particular system. Since the RIN for the injection current modulated lasers is generally much larger than that of the solid state YAG lasers, the combination of the additive noise level and the number of elements required will dictate which type will produce the highest performance in a given array.

4 Influence of Modulation on Semiconductor Laser Noise

In this task, the dependence of the low frequency intensity noise on injection-current modulation was studied. The results of an extensive literature search were employed to determine the most advantageous manner in which to proceed. It has been shown previously that low frequency intensity noise (0 - 1 GHz) in injection modulated semiconductor lasers is upconverted to the vicinity of an RF modulation signal. The heart of the problem, therefore, lies in determining the origin of the low frequency fluctuations in the laser diode, and how the low frequency noise is affected by injection current modulation.

Two competing views exist regarding the origin of the low frequency fluctuations in semiconductor lasers. One camp contends that low frequency intensity fluctuations are due to trapping of carriers in the semiconductor medium with a $1/f$ power law frequency spectrum, while the other view holds that competition between longitudinal modes of the laser diode causes an enhancement of low frequency fluctuations. The initial approach we adopted was to control the amount of coupling between longitudinal modes of the laser, and to observe the effect on the low-frequency fluctuations and close-to-carrier RF phase noise.

To investigate the effects of mode coupling, an external cavity semiconductor laser diode was constructed. The external cavity has the desirable effect of reducing the longitudinal mode frequency separation from approximately 450 GHz to 1 GHz, within the range of injection current modulation

frequencies. Then, the mode-coupling can be affected by injection current modulation at appropriate frequencies corresponding to the round trip light time of the cavity and its harmonics.

Testing of the external cavity semiconductor laser was performed under various conditions of bias current and modulation. Preliminary results employing mode-locking with a strong sinusoidal modulation at 1 GHz caused a reduction in the low frequency intensity noise of the laser diode in external cavity by approximately 10 dB. The cause of the noise reduction is presumed to be the reduction of competition between the lasing modes of the laser when mode-locked. However, an unexpected result was obtained when the 1/2 sub-harmonic of the mode-locking frequency (i.e., 500 MHz) was employed: the low frequency intensity noise was reduced by another 10 dB for frequencies above 5 kHz. These results were presented at the Third Annual DARPA Symposium on Photonics Systems for Antenna Applications (PSAA-III), on January 20th 1994 in Monterey California, in a paper entitled: "Influence of Modulation on Noise in Semiconductor Lasers," by R.T. Logan Jr. and L. Maleki.

5 Multiplicative Noise and Laser Linewidth

A theoretical model for the mode-competition noise reduction in a multi-mode laser was developed and computer simulations were performed. The model is based on a Fabry-Perot cavity containing a medium with a time-varying index of refraction. In the simulation, the center frequency and amplitude of the dominant mode was tracked to estimate the frequency and

intensity fluctuation power spectra. The computer random-number generator was used to simulate index of refraction variations with a white power-spectral-density; the model appeared to generate $1/f^\alpha$ -type noise similar to that observed in the laser, and proportional to the noise amplitude.

This initial theoretical result served as tentative confirmation of the mode-competition hypothesis. Theoretically, then, the $1/f$ noise should disappear completely if mode-competition was completely suppressed by perfect mode-locking. It should also disappear in the case of a purely single-mode laser. However, further searching of the literature, and experience revealed that a residual level of $1/f$ noise is often observed even in single-mode distributed-feedback laser diodes. The computer model was applied to the single-mode laser diode again, incorporating index of refraction variations with a white power-spectral-density. Again, $1/f$ -type frequency and intensity fluctuations were observed in the simulated output.

To verify the computer result, an analytic solution was derived for the problem of the fluctuations of the transmission of a resonant cavity due to variations in the feedback parameters. The analytic model is an extension of a linear feedback system model that includes the effects of time-variation of the feedback components. In this linear model, the transmitted wave at any time instant is comprised of a summation of "partial waves" that have existed in the cavity for various lengths of time. In the case of no feedback fluctuations, the partial waves may be summed analytically, and the familiar Fabry-Perot cavity result is obtained. As the Q of the cavity is increased, more partial waves are stored in the cavity. However, when the feedback parameter is fluctuating, the output wave is a summation of many partial

waves that have sampled the feedback fluctuations over increasing lengths of time. It is seen through this analysis that in a high-Q cavity, the fluctuations of the cavity are amplified by the fact that many partial waves make up the output wave at any instant, and each partial wave carries a history of the cavity fluctuations with it.

The analytic model results serve to confirm and explain the computer simulation results. The fluctuations of the output wave due to refractive index variations with white power spectral density acquire a $1/f^2$ power spectral density at frequencies above the -3 dB point of the cavity, but remain white at frequencies within the cavity bandwidth. This noise enhancement effect may explain why high-Q cavities typically have relatively poor long-term stability.

The linear model is not sufficient to model an oscillator, such as a laser. However, it provides interesting new insights into the effects of noise in resonators and resonant amplifiers. In the next phase of work, the time-varying feedback and partial wave model was incorporated into a non-linear analysis of the resonant cavity above the oscillation threshold. This formalism entailed modeling the laser as a noise driven resonant optical amplifier that has random gain and phase fluctuations. The model yields an additional power independent term in the Schawlow-Townes expression for the linewidth of the laser. As the power is increased, the model predicts a re-broadening of the linewidth, as generally observed in the case of semiconductor lasers.

The study also included an analysis of electron density fluctuations in the laser gain medium, from which the spectral power density of noise due to these fluctuations was obtained. Finally, the results were used to obtain

an estimate of the minimum linewidth of the semiconductor laser.

This segment of the work is the basis for the dissertation of R. T. Logan, which will be submitted in the future in partial fulfillment for the Ph. D. degree in Electrical Engineering, Electro-Physics at the University of Southern California. The portion of the dissertation supported in the task is presented in Appendix II.

APPENDIX I

EFFECTS OF PHASE NOISE FROM LASERS AND OTHER SOURCES ON PHOTONIC RF PHASED-ARRAYS

Ronald T. Logan Jr. and Lute Maleki

Jet Propulsion Laboratory, California Institute of Technology
4800 Oak Grove Drive, Pasadena, California 91109

ABSTRACT

The beam pattern of a linear phased-array antenna system employing a photonic feed network is analyzed using a model for the individual feed element noise including both additive and multiplicative equivalent noise generators. It is shown that uncorrelated multiplicative noise power of the individual feeds is reduced by a factor of N in the output of an N -element linear array. However, the uncorrelated additive noise of the individual feed paths is not mitigated, and therefore will determine the minimum noise floor of a large phased-array antenna.

1. INTRODUCTION

In phased-array antennas, the beam pattern depends critically on the phase control of the signals at the individual antenna elements. The ability to feed and adjust the phase of the microwave signals to the individual radiating elements using optical fiber and photonic components offers obvious advantages in size, weight, mechanical flexibility, and cross-talk, compared to metallic waveguides and phase-shifters. Various phased-array antenna system architectures with photonic feed networks have been proposed, however, the issues of phase stability and signal purity are not typically addressed in these proposals. Therefore, determination of the acceptable phase noise contribution of the individual active feed components has been problematic. In this paper, the general factors contributing to the phase stability of an array feed network are outlined, with particular attention paid to the type of noise encountered in photonic feed elements. It is shown that the analysis of array phase stability must consider both additive and multiplicative noise generation processes, and that the additive noise of the active feed components will limit the phase stability of a large phased-array.

2. PHASED-ARRAY SYSTEM MODEL

The general architecture of a phased-array antenna system comprised of M elements is depicted schematically in Figure 1. In this analysis, the phase noise contribution due to the array feed and antenna elements only is calculated. The

effects of the source phase noise will be common to all elements, and may be treated in the usual manner for a single antenna element.

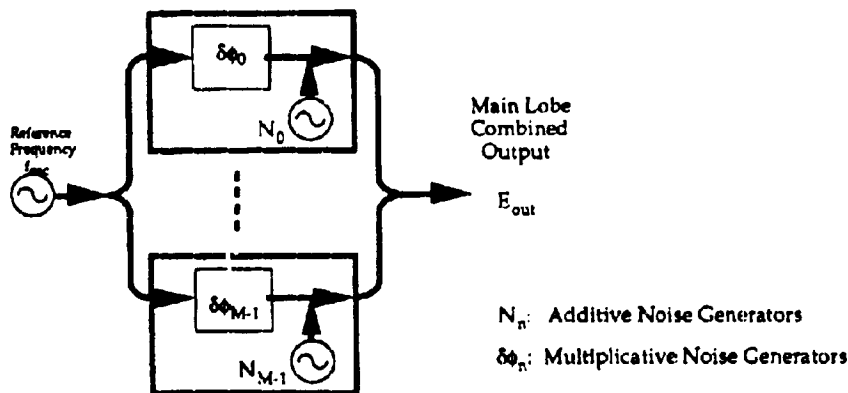


Figure 1. Noise Sources in M-Element Phased-Array Feed System

The feed system is driven by a common source oscillator whose power output is divided M ways. The phase delays required to point the antenna beam are generated in the separate feeds. To study the effect of noise on the elements, we assume a simple case in this model: the signals acquire equal delays in the feeds, and are then recombined in a second M-way power combiner. Thus, the output signal amplitude is scaled to be equal to the input signal amplitude, to facilitate comparison between a single-element antenna system and an array.

3. NOISE PROPERTIES OF PHOTONIC FEEDS

The photonic feed elements contain active components such as laser diodes, photodiodes, and amplifiers. The phase noise contribution of a microwave fiber optic feed system is therefore comprised of an additive noise term and a multiplicative noise term. Laser relative intensity noise (RIN), shot noise, and thermal (Johnson) noise are additive noise sources which are present at all times independent of signal level. Low frequency gain or path-length instabilities that modulate the microwave signal amplitude and phase are multiplicative noise sources that are only observed when a signal is present. As shown in Figure 2, additive noise usually determines the noise floor at higher offsets from the carrier frequency, but multiplicative noise often has a $1/f^\alpha$ power law characteristic, $1 < \alpha < 2$, so is typically dominant close to the microwave carrier frequency [1].

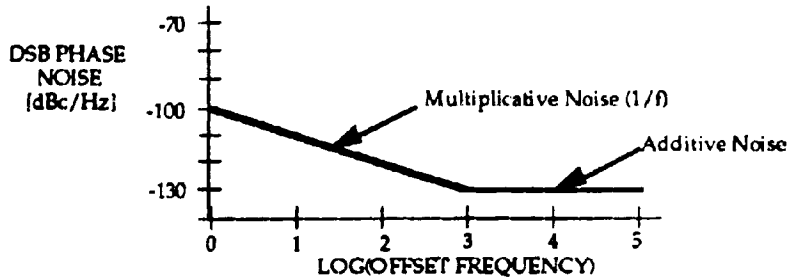


Figure 2. Typical Phase Noise of Photonic Feed System at 10 GHz

Additive noise sources due to thermal and shot processes or laser RIN are independent random processes and therefore can be assumed uncorrelated between the feed elements. Multiplicative noise may or may not be uncorrelated between elements, depending on its origin. For example, thermal expansion or vibration of all the optical fibers in the feed network may produce a phase modulation that is common to all elements, whereas, laser or amplifier-induced $1/f$ gain fluctuations will be uncorrelated between elements. Noise that is common to all the elements may be referred to the source oscillator and treated as if the array were a single element. In the analysis that follows, all of the noise sources in the individual feed elements are assumed to arise from independent random processes, so can be treated as uncorrelated sources.

It is noted that the multiplicative noise is not detectable by a standard noise figure measurement in the microwave signal frequency band. In fact, it is difficult in practice to predict the amount of multiplicative noise in an amplifier or laser diode, because the noise level may itself be a function of the modulation signal frequency or amplitude. Therefore, the amount of multiplicative phase noise is usually determined empirically.

4. ANALYSIS

We now proceed to calculate the effect of the noise added by the feed elements on the total array performance. Consider first a unity gain single feed element consisting of a fiber optic link and electronic amplifiers, with a microwave input signal $E_{in}(t) = E_0 e^{j\omega_0 t}$ of constant amplitude E_0 at microwave frequency ω_0 . The output signal amplitude for a single feed element may be written

$$E_{out}(t)e^{j\omega_0 t} = E_0 e^{j\omega_0 t} e^{j\delta\phi(t)} + N'(t) \quad (1)$$

where $N'(t)$ represents an additive Gaussian noise process with a white power spectral density from dc to well above ω_0 , and $\delta\phi(t)$ is a small multiplicative phase noise term. The multiplicative noise term can, in general, be complex and thus also represent gain fluctuations. Factoring out the sinusoidal variation at ω_0 yields the slow time-variation of the output field around the microwave carrier

$$\begin{aligned}
 E_{out}(t) &= E_o e^{j\delta\phi(t)} + N'(t) e^{-j\omega_o t} \\
 &= E_o e^{j\delta\phi(t)} + N(t)
 \end{aligned}
 \tag{2}$$

Limiting the analysis to a band of frequencies $\delta\omega$ in width around ω_o , the additive noise term can be written as a random phasor: $N(t) = N'(t) e^{-j\omega_o t} = \delta r(t) + j\delta i(t)$, where $|\delta i(t)| = |\delta r(t)|$, and are assumed to be independent Gaussian noise processes with white power spectral density from dc to $\delta\omega / 2$. Note that as the input signal amplitude E_o is decreased to zero in Equation (2), the multiplicative noise term vanishes, but the additive noise term $N(t)$ is unchanged.

The total array noise is now calculated by using the M individual feed element expressions from Equation (2) in the standard calculation [2] of the array output field. For a linear array at a steering angle ϕ , the field distribution in the far field of the array as a function of observation angle θ may be expressed as

$$E_{out}(\theta, \phi, t) = \sum_{n=0}^{M-1} \left(\frac{E_o}{\sqrt{M}} e^{j\delta\phi_n(t)} e^{j m(\pi \cos \theta - \phi)} + N_n(t) \right)
 \tag{3}$$

Figure 3 is the calculated radiation pattern for a linear array of ten antennas vs. observation angle θ when the steering angle $\phi = 0$.

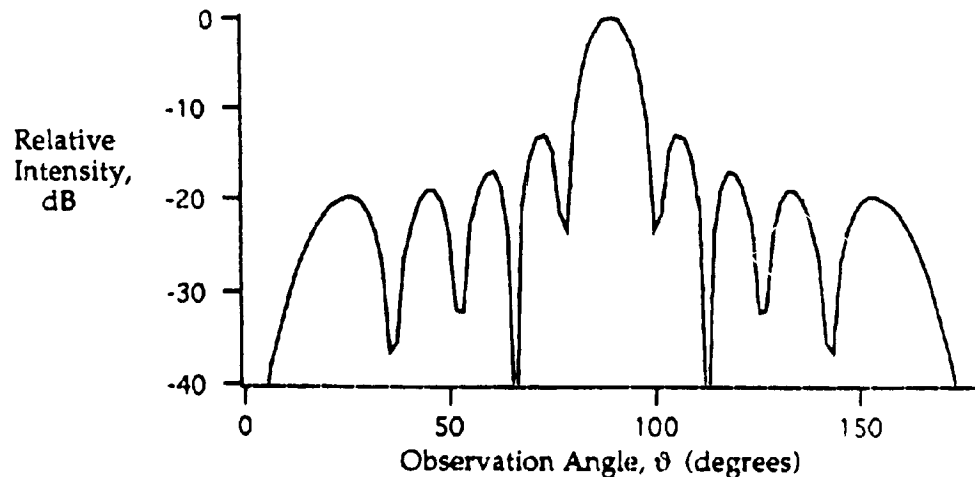


Figure 3. Calculated radiation pattern vs. observation angle for a 10-element linear array.

We wish to investigate the magnitude of the amplitude and phase fluctuations of the main lobe versus the number of elements in the array. If the noise sources in the feeds are uncorrelated, the statistics of the time-variation of the amplitude and phase of the main-lobe peak will be independent of the steering angle ϕ .

Therefore, for the purposes of this noise analysis, the array can be modeled simply as M equal-length feed systems sandwiched between two back-to-back ideal M -way power splitters, as depicted in Figure 1. Now, the output field amplitude is equal to the input field amplitude, independent of the number of elements M .

At the main lobe peak, $\pi \cos \theta = \phi$, and the signal amplitude at the output of the M -way coupler in Figure 1 corresponds to the main lobe peak amplitude of the antenna pattern, divided by \sqrt{M} . For small-angle phase noise $\delta\phi(t) \ll 1$ radian, the time variation of the output field can be written

$$E_{out}(t) = \frac{1}{\sqrt{M}} \sum_{n=0}^{M-1} \left(\frac{E_0}{\sqrt{M}} (1 + j\delta\phi_n(t)) + N_n(t) \right). \quad (4)$$

First consider the output of an "array" comprised of only one feed element with unity gain. In the above equation, this corresponds to the case of $M=1$. The output field is then given by

$$E_{out}(t) = E_0 + j\delta\phi(t)E_0 + N(t). \quad (5)$$

which is just the same as the expression for a single feed given earlier in Equation (2), as required. The signal and noise power are proportional to the time-average of the squared-magnitude of the output voltage:

$$P_{out} \propto \left(\begin{aligned} &\langle E_0 E_0^* \rangle + \langle E_0 (j\delta\phi)^* E_0^* \rangle + \langle E_0 N^* \rangle \\ &+ \langle j\delta\phi E_0 E_0^* \rangle + \langle j\delta\phi E_0 (j\delta\phi)^* E_0^* \rangle + \langle j\delta\phi E_0 N^* \rangle \\ &+ \langle N E_0^* \rangle + \langle N (j\delta\phi)^* E_0^* \rangle + \langle N N^* \rangle \end{aligned} \right) \quad (6)$$

where the angle-brackets $\langle \rangle$ denote the time-average of the enclosed quantity, and the explicit time-dependence of the random functions has been dropped for clarity. For independent zero-mean noise processes, the time-average of products of the constant and random terms are zero, because we have assumed zero-mean random noise processes. Also, the average of the product of two uncorrelated terms, such as $\langle N(j\delta\phi)^* \rangle$, is zero. But the time-average of the square of any signal or noise term is non-zero. Thus, the ratio of signal to noise power (SNR) for one feed is

$$SNR|_{1\text{-element}} = \frac{\langle |E_0|^2 \rangle}{\langle |j\delta\phi(t)|^2 |E_0|^2 \rangle + \langle |N(t)|^2 \rangle}. \quad (7)$$

Similarly, for the case of M parallel feeds with independent equal-amplitude multiplicative and additive noise sources, the output field is given by

$$\begin{aligned} E_{out}(t) &= \frac{1}{\sqrt{M}} \left(\frac{E_0}{\sqrt{M}} (1 + j\delta\phi_0(t)) + N_0(t) + \frac{E_0}{\sqrt{M}} (1 + j\delta\phi_1(t)) + N_1(t) + \dots \right) \\ &= E_0 + \frac{E_0}{M} (j\delta\phi_0(t) + j\delta\phi_1(t) + \dots) + \frac{N_0(t)}{\sqrt{M}} + \frac{N_1(t)}{\sqrt{M}} + \dots \end{aligned} \quad (8)$$

The individual powers of equal-amplitude, independent (therefore uncorrelated) noise sources may be added linearly. Thus, the equivalent noise voltage due to the sum of M uncorrelated equal-amplitude noise sources is just \sqrt{M} times the amplitude of a single noise source. Since all cross-terms between uncorrelated noise sources average to zero, we can write the output field for an M -element array in terms of a single multiplicative noise source $\delta\phi(t)$ and a single additive noise source $N(t)$

$$E_{out}(t) = E_o + \frac{E_o j \delta\phi(t)}{\sqrt{M}} + N(t). \quad (9)$$

Now, the ratio of signal to noise power in the combined output of an M -element array is

$$SNR|_{M\text{-elements}} = \frac{\langle |E_o|^2 \rangle}{\frac{\langle |j\delta\phi(t)|^2 |E_o|^2 \rangle}{M} + \langle |N(t)|^2 \rangle}. \quad (10)$$

The multiplicative noise power is thus mitigated by a factor of M in the combined output of an M -element array, whereas the signal power and additive noise power are unchanged from the single-element case. Figure 4 illustrates these results for an array of ten elements compared to a single element.

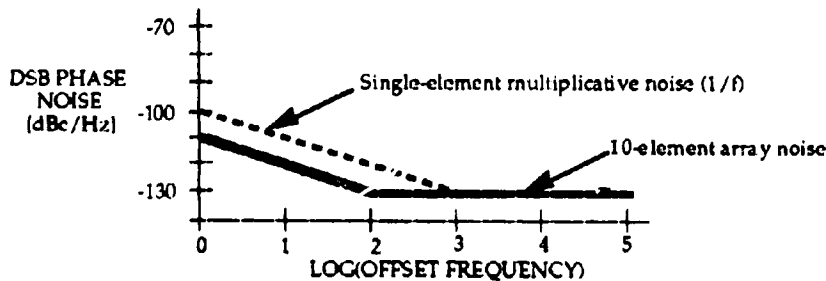


Figure 4. Comparison of Single-element and 10-element Phase Noise

The close-to-carrier $1/f^\alpha$ multiplicative noise of the combined array output is reduced by 10 dB compared to the noise of an individual element. The white additive noise power further from the carrier is unchanged from the single-element case. This behavior is analogous to the improved frequency stability obtained from an ensemble of oscillators, compared to the stability of a single oscillator. This property may therefore make phased-array antennas more desirable than single-element antennas for applications in which high levels of long-term phase stability are required. Alternatively, this property relaxes the requirements on multiplicative phase noise for the elements of a large phase array. It is emphasized that the additive noise requirements are not relaxed, however.

5. SUMMARY

It was shown that as the number of array elements M is increased, the effect of uncorrelated multiplicative phase noise of the feed elements on the total array stability is diminished. However, the uncorrelated additive noise of the feed elements is not diminished, so that the signal-to-noise ratio becomes independent of array size for large enough M . It is therefore important to quantify both the additive and multiplicative noise of the feed elements to correctly predict the total array phase stability.

6. ACKNOWLEDGEMENTS

This work described in this paper was carried out at the Jet Propulsion Laboratory, California Institute of Technology, and was sponsored by the United States Air Force Rome Laboratory and the National Aeronautics and Space Administration.

7. REFERENCES

1. R. T. Logan, G. F. Lutes, High Stability Microwave Fiber Optic Systems: Demonstrations and Applications, IEEE Frequency Control Symposium Hershey, Pennsylvania, 1992), pp. 310-316.
2. S. Ramo, J. R. Whinnery, T. Van Duzer, *Fields and Waves in Communication Electronics*. (John Wiley and Sons, New York, 1984).

APPENDIX II

Partial-wave Analysis of Multiplicative Noise in Laser Amplifiers: Application to Laser Linewidth

Ronald T. Logan Jr.

INDEX

APPENDIX II, List of Figures	B - 3
ABSTRACT	B - 4
CHAPTER 1, Introduction and Overview	B - 6
CHAPTER 2, General Analysis of Resonant Feedback System with Multiplicative Noise	B - 12
2.1 Review of Standard Linear Feedback Theory	B - 14
2.2 Linear System Analysis with Multiplicative Noise	B - 17
2.3 Small-angle multiplicative noise regime: linear approximation	B - 26
2.4 Large-angle multiplicative noise regime: numerical analysis.....	B - 36
2.5 Detailed description of simulation algorithm	B - 41
CHAPTER 3, Multiplicative noise in laser linewidth	B - 46
3.1 Analysis of effect of small-angle multiplicative noise on semiconductor resonant amplifier linewidth	B - 46
3.2 Onset of the large-angle regime	B - 50
3.3 Application of multiplicative noise model to laser linewidth	B - 51
3.4 Conclusion	B - 56
CHAPTER 4, References	B - 57

APPENDIX II - LIST OF FIGURES

<i>Figure No.</i>	<i>Title</i>	<i>Page</i>
1.	Analysis Basis Concept Diagram	B-60
2.	Output Field in Complex Plane for Net Gain, $K_o = 0.9$	B-61
3.	Output Field in Complex Plane for Net Gain, $K_o = 0.95$	B-62
4.	Output Field in Complex Plane for Net Gain, $K_o = 0.99$	B-63
5.	Output Field in Complex Plane for Net Gain, $K_o = 0.995$	B-64
6.	Output Field in Complex Plane for Net Gain, $K_o = 0.999$	B-65
7.	Output Intensity vs. Round Trips, $K_o = 0.9$	B-66
8.	Output Intensity vs. Round Trips, $K_o = 0.95$	B-67
9.	Output Intensity vs. Round Trips, $K_o = 0.99$	B-68
10.	Output Intensity vs. Round Trips, $K_o = 0.995$	B-69
11.	Output Intensity vs. Round Trips, $K_o = 0.999$	B-70
12.	Output Phase vs. Round Trips, $K_o = 0.9$	B-71
13.	Output Phase vs. Round Trips, $K_o = 0.95$	B-72
14.	Output Phase vs. Round Trips, $K_o = 0.99$	B-73
15.	Output Phase vs. Round Trips, $K_o = 0.995$	B-74
16.	Output Phase vs. Round Trips, $K_o = 0.999$	B-75
17.	Relative Probability vs. Intensity, $K_o = 0.90$	B-76
18.	Relative Probability vs. Intensity, $K_o = 0.95$	B-77
19.	Relative Probability vs. Intensity, $K_o = 0.99$	B-78
20.	Relative Probability vs. Intensity, $K_o = 0.995$	B-79
21.	Relative Probability vs. Intensity, $K_o = 0.999$	B-80
22.	Power Spectrum vs. Frequency, $K_o = 0.90$	B-81
23.	Power Spectrum vs. Frequency, $K_o = 0.95$	B-82
24.	Power Spectrum vs. Frequency, $K_o = 0.99$	B-83
25.	Power Spectrum vs. Frequency, $K_o = 0.995$	B-84
26.	Power Spectrum vs. Frequency, $K_o = 0.999$	B-85

Abstract

A general formalism is developed for analyzing the output field fluctuations of a resonant optical amplifier that has random gain and phase fluctuations by a modification of the partial wave model. The partial wave model provides an intuitive physical picture for the effect of multiplicative noise in the optical resonant amplifier. Then, by modelling a laser as a noise-driven resonant optical amplifier, it is shown that multiplicative noise generates an additional power-independent term in the Schawlow-Townes formula for the linewidth of the laser, and a re-broadening of the linewidth at high output power levels, as is typically observed in single-mode semiconductor lasers at high power levels. Time-varying complex gain constitutes a *multiplicative* gain and phase noise source that is transformed to the output field in a different way from *additive* noise sources, such as spontaneous emission. The formalism developed allows calculation of the transmitted field power spectra of amplitude and phase fluctuations due to multiplicative noise. It is shown that the effect of multiplicative noise on the transmitted optical field is enhanced as the net round-trip gain in the resonator is increased, so that the multiplicative noise ultimately determines the minimum linewidth for the resonant amplifier in the high-gain limit. A detailed analysis of electron density fluctuations in a semiconductor laser gain medium is also performed, from which the power spectral density of multiplicative phase noise due to electron number-density fluctuations in the gain medium is obtained. This result is then used in the multiplicative laser noise model to obtain an estimate of the minimum linewidth of a semiconductor laser. Although

the multiplicative noise analysis is applied to a resonant optical amplifier, the formalism is general and should be applicable to the analysis of other types of feedback systems perturbed by multiplicative noise.

1 Introduction and Overview

A formalism is developed for analyzing the output field fluctuations of a resonant optical amplifier with a time-varying complex gain medium, by a modified partial-wave model. A linear model of a laser as a noise-driven resonant optical amplifier is then modified using the results of the time-varying partial wave analysis. This new laser model provides an intuitive picture of a mechanism for power-independent linewidth and linewidth rebroadening in semiconductor lasers.

In a resonant amplifier, time-varying phase and gain constitute *multiplicative* noise sources whose effects are transformed to the output field in a different way from *additive* noise sources, which are typically treated as additional inputs to the system. The inclusion of multiplicative gain and phase fluctuations in a partial-wave analysis of an optical resonant amplifier is the principal novelty of this work. The partial wave model provides a simple physical picture for the effect of multiplicative noise in the optical resonant amplifier. The resonant amplifier is modeled as a delay-type feedback system (Figure 1) with input, output, and net round-trip loop gain less than unity, as shown in Figure 1. The output field at any time instant is comprised as a sum of partial waves; the "oldest" partial waves have travelled more times around the loop, so that the "memory" of the cavity extends further back in time. When no multiplicative noise is present, the width of the cavity resonance peak decreases as the net gain, and hence the cavity memory time, is increased. However, in the presence of multiplicative noise, the older partial waves accumulate progressively larger random phase fluctuations, leading to

increasing output field fluctuations. For high enough net round-trip gain, the multiplicative noise-induced fluctuations will dominate the output field fluctuations, and the linewidth will not decrease with further increases in net gain. Eventually, as the gain is increased further, the later partial waves accumulate so much phase that they begin to destructively interfere with the earlier partial waves, leading to large output fluctuations, and increasing linewidth.

By viewing the laser as a noise-driven resonant amplifier, and including the results of the partial-wave analysis, a model is obtained for the behavior of the laser with multiplicative noise as the net round-trip gain is varied. It is shown that multiplicative noise leads to an additional power-independent regime in the Schawlow-Townes formula for the linewidth of a laser at intermediate power levels, followed by linewidth rebroadening as the power is increased further. From this result, an estimated value of 120 Hz for the minimum power-independent linewidth of a typical single-mode DFB semiconductor laser due to electron number-density fluctuations is obtained.

Multiplicative noise arises in an optical feedback system when a multiplicative factor affecting the field, such as gain or round-trip phase, fluctuates in time. Additive noise arises from photons which are added randomly to the field, such as by spontaneous emission. In addition to the fundamental additive noise due to spontaneous emission, sources of multiplicative gain and phase fluctuation will always be present in the components of a laser system at some level. It has been shown [12] that statistical fluctuations in temperature and density can have significant effect on the optical phase of a wave passing through an optical fiber at a constant temperature T . For

example, in a fiber laser, this source of fluctuation constitutes a *fundamental* source of multiplicative phase noise that arises from the same thermodynamic considerations responsible for the unavoidable Johnson noise in electronic components, and is a basic consequence of the Fluctuation-Dissipation Theorem [16]. In other laser systems, the net gain and optical length of the laser cavity can fluctuate due to dye-stream width fluctuations, mirror vibrations, pump power fluctuations, or other technical factors. In typical laser systems, it is these *technical* sources of multiplicative noise that determine the actual observed linewidth [1], and not *fundamental* additive quantum noise due to spontaneous emission, as predicted by the well-known modified Schawlow-Townes formula [19], [21].

The Schawlow-Townes formula for laser linewidth predicts an inverse dependence on the output power given as

$$\delta\nu = (\delta\nu_c)^2 \pi \frac{h\nu}{P} \frac{N_2}{N_2 - N_1} \quad (1)$$

where $\delta\nu_c$ is the "cold cavity" linewidth determined by the losses, h is Planck's constant, ν is the oscillation frequency, P is the output power, and N_2 , N_1 are the populations of the upper and lower states of the atomic transition responsible for the optical gain. For large-scale gas lasers with high-reflectivity mirrors, equation (1) predicts linewidths on the order of several hertz for output powers in the milliwatt range. In real lasers, the observed linewidth typically several orders of magnitude larger than this quantum linewidth prediction, due to technical sources of noise.

A notable exception is the semiconductor laser. The combined effects

of large output coupling (i.e., low Q cavity) and amplitude-phase coupling through the carrier density [2], [3] yield a predicted fundamental quantum linewidth in the kHz to 100 MHz range for typical power levels. The prediction of the appropriately modified linewidth equation [2] for typical facet reflectivity of 32 percent yields an estimated linewidth of approximately 30 MHz at a power level of 10 milliwatts, and experiments are typically in good agreement with theory for lower power levels. However, a power-independent linewidth of several MHz [11], [22] and linewidth rebroadening [6], [5] in single-mode semiconductor lasers is typically observed at high output power, which is not predicted by the modified Schawlow-Townes relation. The excess linewidth is detrimental to applications requiring a high degree of coherence, such as atomic spectroscopy and coherent communications systems.

The origin of the excess linewidth in semiconductor lasers is not so clear as in the case of large-scale lasers, since the typical macroscopic technical sources of noise, such as mirror vibrations, dye stream fluctuations, and the like are absent. Early work on the power-independent linewidth attributed it to fundamental multiplicative refractive index fluctuations due to electron number-density fluctuations [11]. In that work, the transformation of refractive index variations δn to fluctuations of the laser frequency $\delta \nu$ was derived from the phenomenological relation

$$\frac{\delta \nu}{\nu} = \frac{\delta n}{n} \quad (2)$$

The refractive index fluctuations were included in a root-mean-square sense, derived from thermodynamic considerations regarding the number-density

fluctuations of the electrons contained in the active medium. However, this model can not explain the onset of linewidth rebroadening. In later work, various other mechanisms have been advanced to explain the origin of the power-independent linewidth, such as $1/f$ noise [22], and spatially-dependent temperature and carrier fluctuations [24]. Linewidth rebroadening has been explained in terms of excess carrier density in the confinement regions of quantum well lasers [5], and spatial hole burning [6]. These or other mechanisms, such as injection-current fluctuations, may be operative in various combinations in any particular laser. At present, however, there appears to be no uniform explanation of a mechanism responsible for both the power-independent linewidth and linewidth rebroadening in single-mode semiconductor lasers.

The dissertation is organized as follows: In Chapter 2, a discrete-time formula for the slowly-varying complex envelope of the output field is obtained, equation (16). Two regimes of the output fluctuations are examined: small-angle and large-angle. The small-angle approximation yields equation (30), which has the form of a finite-impulse-response filter acting on the multiplicative and input noise processes to produce the output fluctuations. From this expression, the impulse responses and frequency responses of the resonant amplifier for multiplicative and input fluctuations are obtained, finally yielding the output noise power spectrum, equation (46). In the limit of high net round-trip gain, this becomes equation (47), and the output fluctuation power spectrum is dominated by multiplicative noise. This is the mechanism for the power-independent linewidth. Numerical simulation results for the large-angle regime illustrate increasing amplitude and phase fluctuations due

to the random-walking phase and gain of the partial waves Figures 2 - 19. With increasing net gain, the probability distribution of the output intensity in the large angle regime moves to lower values as in 17 - 21 and the power spectrum broadens, (22 - 26) (This is the mechanism for the linewidth rebroadening.

In Chapter 3, for the small-angle regime, the output field power spectrum of the resonant amplifier is found to have a Lorentzian lineshape, that has width given by equation (52) for a multiplicative noise source that has white power spectrum. This result has the same form as the phenomenological result of equation (2). In the large-angle regime, the linewidth is predicted to broaden, which is not predicted by equation (2). The resonant amplifier analysis is finally applied to the laser by modelling it as a noise-driven resonant amplifier. The linewidth of the laser has a power-independent minimum for the small-angle regime, and rebroadens following the onset of the large-angle regime. A minimum linewidth for a typical semiconductor laser is estimated to be 120 Hz due to electron density fluctuations.

2 General Analysis of Resonant Feedback System with Multiplicative Noise

In this Chapter, the standard linear analysis of a delay-type feedback system is generalized to treat time-varying gain and phase perturbations of the components in the feedback system. The gain and phase coefficients multiply the complex amplitude of the field as it passes through the amplifying medium, so that *gain and phase fluctuations* constitute sources of *multiplicative noise*. First, to frame the discussion and define terminology, the basic analysis of a linear delay-type feedback system *without* multiplicative noise will be reviewed, and applied to the case of a resonant optical amplifier. The gain medium is treated as a linear amplifier operating below saturation. This amounts to a review of the standard treatment [4] of a resonant optical amplifier, from which the familiar Airy formula is obtained. Next, a discrete-time formalism, valid for a single oscillation mode at a cavity resonance frequency, is developed *including* multiplicative phase and gain fluctuations of the amplifying medium between the cavity mirrors.

In the standard analysis of a resonant cavity, the transmitted output field is computed from an infinite sum of partially-reflected fields inside the cavity, or "partial waves." Cavity resonances occur at discrete frequencies when all of the partial waves add constructively. For a perfectly stable cavity with net round-trip gain less than unity, an analytic form for this summation obtains. However, in the presence of multiplicative noise, the partial waves in the resonator will have randomly-varying phase and amplitude, so the usual

analytic summation is not applicable. Therefore, in the present analysis, the output field is computed as a random phasor summation of all the partial waves contained in the cavity at discrete instants of time. The case of an ideal noiseless input field is examined first to appreciate the effect of the multiplicative noise on the transmitted field. Then the more realistic case of an input field with phase and amplitude noise is treated.

Two regimes are examined: a small-angle linear regime, and a large-angle regime. In the small-angle regime, the fluctuating complex phase of the partial waves is less than 0.1 radians about the mean. In this regime, expressions for the output field amplitude and phase are analytically derived in terms of the power spectra of the multiplicative gain fluctuations and additive input fluctuations, and the net round-trip gain. But it is seen that the multiplicative noise is enhanced by the round-trip net gain, and that the resonant amplifier system acts like a linear finite-impulse-response filter in transforming the multiplicative fluctuations and the input field fluctuations to the output field. The impulse responses of the resonant amplifier for both multiplicative noise and input field noise are found to decay exponentially, leading to Lorentzian terms in the output field power spectrum. The familiar filtering characteristics of the Fabry-Perot cavity are obtained for the input additive fluctuations. The response for the multiplicative fluctuations is enhanced as the gain is increased, whereas the response for the input field fluctuations decreases with increasing gain. For large enough gain, the multiplicative noise dominates the output field fluctuations. It is shown that the enhancement of the multiplicative fluctuations limits the output power spectrum to a minimum width determined by the net round-trip gain and the

multiplicative noise strength, in contrast to the prediction of the standard analysis.

For the case of large-amplitude multiplicative noise exceeding the limits of the small-angle approximation, numerical simulations are performed using simulated noise time series. In this regime, the power transmission of the cavity with multiplicative phase fluctuations grows progressively more erratic with increasing net gain. For large enough net-gain, the phase of the output field "wraps around" more than 2π radians, causing discontinuous jumps of the output phase, and fast, spiky output amplitude fluctuations on time scales much faster than the cavity photon lifetime. Also, the probability distribution of the output intensity becomes more like that of a thermal source, and the power spectrum becomes broadened. In this regime, the impulse response is no longer exponentially decaying, but becomes erratic and enhanced at large times, resulting in enhancement of the low-frequency portion of the output field power spectrum.

Finally, it is noted that although the primary concern of this analysis is the optical resonant amplifier, the results of this analysis should be applicable to noise in other types of feedback systems.

2.1 Review of Standard Linear Feedback Theory

To begin the development, the standard analysis of a simple delay-type feedback system with linear, time-invariant components will be reviewed, and then applied to a resonant optical amplifier similar to the approach found in Siegman [4]. Consider the feedback system model of an optical cavity illus-

trated in Figure 1. The input, output, and internal states are electric fields with sinusoidal time dependence. The input field R incident from the left of Figure 1 is assumed to be a sinusoid of frequency ω and amplitude A_R .

$$R(\omega) = A_R e^{i\omega t}. \quad (3)$$

The output field $C(\omega)$ exiting to the right also has the same sinusoidal dependence. It is desired to compute the transfer characteristics of the feedback system from the input state $R(\omega)$ to the output state $C(\omega)$.

The system has an input coupler 1 on the left of Figure 1, and an output coupler 2 on the right. These couplers have branching ratio $\rho_{1,2}$ for the reflected amplitude, and $\gamma_{1,2}$ for the transmitted amplitude. The couplers are assumed to be lossless, so that $\gamma_{1,2}^2 + \rho_{1,2}^2 = 1$. The system has complex forward gain coefficient $G(\omega)$ and reverse gain coefficient $H(\omega)$. A crucial assumption is that the gains $G(\omega)$ and $H(\omega)$ are linear, so that the output field can be computed as a vector addition of partial waves. If the gain is non-linear, then mixing products will be generated at new frequencies. We will assume that the cavity behaves as a linear resonant amplifier, with the output field amplitude linearly related to the input field amplitude.

Throughout the remainder of the analysis, the explicit sinusoidal time dependence of $R(\omega)$, $C(\omega)$ etc., will be understood, and R , C etc. will be used instead. For a pure sinusoidal input field R that has been applied for an infinite time, the steady-state output field C is the summation of an infinite number of partial waves which may be written

$$C = (\gamma_1 \gamma_2) G R + (\gamma_1 \gamma_2) (\rho_1 \rho_2) G^2 H R + (\gamma_1 \gamma_2) (\rho_1 \rho_2)^2 G^3 H^2 R$$

$$\begin{aligned}
& +(\gamma_1\gamma_2)(\rho_1\rho_2)^4G^4H^3R + \dots \\
= & (\gamma_1\gamma_2)GR[1 + \rho_1\rho_2GH + (\rho_1\rho_2GH)^2 + (\rho_1\rho_2GH)^3 + \dots] \quad (4)
\end{aligned}$$

The term outside the square brackets represents the transmission of the input and output couplers $\gamma_1\gamma_2$, and the forward gain G for first one-way pass through the cavity. The terms inside the brackets represent the successive feedback terms which experience a net round-trip gain $\rho_1\rho_2GH$ on each trip through the cavity. For net gain $\rho_1\rho_2GH < 1$, the quantity inside the square brackets may be analytically summed, so that the output may be written

$$C = \frac{(\gamma_1\gamma_2)GR}{1 - (\rho_1\rho_2GH)} \quad (5)$$

Equation (5) has the form of the Airy formula obtained via the standard treatment of a resonant optical amplifier found in optics texts [4]. Identifying ρ_1, ρ_2 and γ_1, γ_2 as the mirror amplitude reflection and transmission coefficients, respectively, and setting $G = H = G_0 e^{-in\omega l/c}$ as the gain and phase experienced by a field for a one-way pass through the cavity of length l and index of refraction n , with c the speed of light in vacuum, the familiar transmission characteristic for a Fabry-Perot resonant amplifier is obtained:

$$T(\omega) = \frac{C}{R} = \frac{\gamma_1\gamma_2G_0e^{-in\omega l/c}}{1 - \rho_1\rho_2G_0^2e^{-i2n\omega l/c}} \quad (6)$$

The power transmission function is the magnitude-squared of this expression:

$$\frac{P_{out}(\omega)}{P_{in}(\omega)} = \frac{(\gamma_1\gamma_2G_0)^2}{1 + (\rho_1\rho_2G_0^2)^2 - 2\rho_1\rho_2G_0^2 \cos(2n\omega l/c)} \quad (7)$$

The resonant amplifier power transmission function is plotted in Figure 2 for facet reflectivities $\rho_1 = \rho_2 = 0.9$ and $G_0 = 1$. The system is resonant

at frequencies corresponding to integer multiples $m = 1, 2, \dots$ of the inverse round-trip time through the cavity $\tau = 2nl/c$:

$$\omega_m = \frac{2\pi m}{\tau}. \quad (8)$$

Equation (5) is the general form of the input-to-output transfer function for a delay-type feedback system as a function of frequency. This expression is valid for a system with no multiplicative noise, acting on sinusoidal input fields. As the feedback fraction is increased, the widths of the transmission peaks given by equation (7) decrease. The half-power amplification bandwidth of a resonance peak is [4]

$$\delta\nu \approx \frac{1 - \rho_1\rho_2G_0^2}{\rho_1\rho_2G_0^2} \frac{1}{\pi\tau}. \quad (9)$$

So, as the net round-trip gain approaches unity, the bandwidth of the resonant amplifier approaches zero.

2.2 Linear Feedback System Analysis with Multiplicative Noise

In this section, a general formalism will be developed for deriving the system output field C for the resonant amplifier of Figure 1 when the forward and reverse gains are perturbed by multiplicative noise. The multiplicative noise may be *fundamental* or *technical* in origin, as discussed previously. In the general case that G and H have non-negligible gain and phase fluctuations, the closed-form summation leading to equation (5) can not be applied. Instead, the partial waves must be explicitly summed to obtain the output

at each desired time instant t , and the amplitude and phase of the output field at the optical frequency ω_m , will fluctuate in time. This analysis will compute the slowly-varying complex envelope of the output field at a cavity resonance ω_m , or $C(\omega_m, t)$.

It is desired to analyze the fluctuations of the output amplitude and phase of $C(\omega_m, t)$ on time scales that are long compared to the period of the optical frequency ω_m . As will be described, this can be conveniently done by moving to a discrete-time picture of the system, breaking up time into discrete increments equal to the time delay for one round-trip through the cavity, τ . After the completion of this work, a similar approach was discovered in Reference [7] in which Z-domain techniques from digital systems theory were used to obtain the transmission and reflection characteristics of Fabry-Perot etalons versus the optical input frequency. However, in that work, no time-variation of the feedback coefficients was considered. Instead, the Z-domain analysis was used to simplify the difficult problem of computing the transmission and reflection characteristics of complicated multi-layer structures. In the present work, a similar discrete-time approach is used on a simple two-mirror Fabry-Perot structure, but extended to the case of time-varying gain coefficients to compute the noise properties of the output field.

For the special case of a feedback system operated near resonance, such as a Fabry-Perot optical cavity, the throughput is only appreciable in narrow bands of frequencies near the cavity resonances which occur at frequencies ω_m , as seen in the previous section. All other frequencies are heavily attenuated.

In many practical applications, such as the laser, the fluctuations of the cavity transfer function near a resonance fre-

quency are of primary interest, since they determine the long-term stability of the laser frequency. Also, the system operates at a single cavity resonance, so a full frequency domain analysis is not really necessary, and it is sufficient to analyze the effect of the gain coefficient fluctuations on the behavior of the cavity near the resonance frequency of interest.

Now, the resonant amplifier of Figure 1 will be analyzed near a single resonance frequency when the gain coefficients G and H are perturbed by noise. To keep the analysis simple and the results transparent, initially it will be assumed that the input state R is a pure sinusoid coincident with a resonance frequency, ω_m , with constant amplitude A_R , as defined in equation (3). Later, the more realistic case of an input field with additive noise will be treated. The input and output couplers 1 and 2 are assumed to be identical, so that $\rho_1 = \rho_2 = \rho$ and $\gamma_1 = \gamma_2 = \gamma$. It is assumed that the cavity length l is time-invariant, as is the nominal refractive index n . All phase or gain fluctuations are described by complex zero-mean random variables $\delta g(t)$ and $\delta h(t)$. The time-varying forward and reverse gain coefficients due to multiplicative noise are then modeled as

$$G(\omega_m, t) = G_o e^{-in\omega_m l/c} e^{-i\delta g(t)} = G_o e^{-in\omega_m l/c} G(t), \quad (10)$$

$$H(\omega_m, t) = H_o e^{-in\omega_m l/c} e^{-i\delta h(t)} = H_o e^{-in\omega_m l/c} H(t), \quad (11)$$

where G_o , H_o represent the static forward and reverse loss or gain, $e^{-in\omega_m l/c}$ is the static one-way phase shift added to a signal at frequency ω_m passing through the cavity. At a loop resonance ω_m , the static phase shift will satisfy the condition $n\omega_m l/c = 2\pi m$ radians, with m an integer. $\delta g(t)$ and $\delta h(t)$ are

complex random variables representing the time-varying phase and gain at frequency ω_m . These may be written

$$\delta g(t) = \delta g'(t) + i\delta g''(t) \quad (12)$$

$$\delta h(t) = \delta h'(t) + i\delta h''(t) \quad (13)$$

where the real parts $\delta g'(t)$ and $\delta h'(t)$ represent phase fluctuations, and the imaginary parts $\delta g''(t)$ and $\delta h''(t)$ represent gain fluctuations. The statistical description and any correlation of the real and imaginary parts will depend in detail on the physics of the gain medium.

The transformation from a continuous-time representation to the discrete-time representation is accomplished by considering the static phase shifts $e^{-i\omega_m t/c}$ as delay elements of duration $\tau/2$, as illustrated in Figure 3, and representing the continuous-time gain variations of $G(t)$ and $H(t)$ as a discrete-time random sequence of complex values G_t and H_t with dc gain G_o and H_o :

$$G_t = G_o e^{-i\delta g_t} = G_o G_t. \quad (14)$$

$$H_t = H_o e^{-i\delta h_t} = H_o H_t. \quad (15)$$

separated by time-intervals τ . (Throughout the rest of the analysis, discrete-time variables will be denoted with a subscripted time index, e.g., X_t , to distinguish them from continuous-time quantities: $X(t)$). In this discrete-time picture, $C(\omega_m, t)$ is assumed to be a pure sinusoid at loop resonance

frequency ω_m , with slowly-varying amplitude and phase fluctuations, which will be referred to as C_t .

Now, we apply this discrete-time definition of the gain to the linear analysis of the previous section to obtain an expression for the output field C_t . At time increment t , the forward gain coefficient is G_t , the reverse gain is H_t , and the input state is R_t . For notational clarity, it is understood throughout that time index $t - j$ refers to time $t - j\tau$, since time has been quantized in units of the round-trip time in the cavity τ . The output state is then written

$$\begin{aligned}
 C_t &= \gamma^2 G_t R_t + \gamma^2 \rho^2 G_t H_{t-1} G_{t-1} R_{t-1} \\
 &\quad + \gamma^2 \rho^4 G_t H_{t-1} G_{t-1} H_{t-2} G_{t-2} R_{t-2} + \dots \\
 &= \gamma^2 G_t [R_t + \rho^2 H_{t-1} G_{t-1} R_{t-1} \\
 &\quad + \rho^4 H_{t-1} G_{t-1} H_{t-2} G_{t-2} R_{t-2} + \dots] \quad (16)
 \end{aligned}$$

It is assumed that the dc forward and reverse gains and static phase are identical, so that $G_o = H_o$. This assumption is equivalent to requiring the loss (or gain) and time-of-flight to be equal for both directions of propagation in the optical cavity. This is a good assumption for a Fabry-Perot cavity, since the light passes through the same physical medium in both directions, but may not be valid for other cavity geometries. It is further assumed that the gain fluctuation rate is slow compared to the time-of-flight τ for a round-trip in the cavity. Then, it is valid to assume the forward and reverse gain fluctuations are equal over any round-trip time interval τ , so the round-trip gain may be written $G_t H_t = H_t^2$. Then, defining the time-varying net round-trip gain to be $\rho^2 H_t^2 = K_t$, the output field at time t is given by the infinite

series:

$$C_t = \gamma^2 H_t [R_t + K_{t-1} R_{t-1} + K_{t-1} K_{t-2} R_{t-2} + \dots]. \quad (17)$$

To analyze the characteristics of the gain coefficient fluctuations on the output field, first the case of an ideal noiseless input field will be examined. The input state is taken to be a constant $R_t = R$ for all times t , so it may be factored out of equation (17). Then, the output field C_t is expressible as an infinite sum of partial waves in the cavity at any given time instant t :

$$C_t = \gamma^2 H_t R [1 + K_{t-1} + (K_{t-1} K_{t-2}) + (K_{t-1} K_{t-2} K_{t-3}) + \dots]. \quad (18)$$

This infinite series will be truncated to a finite number of M terms, as follows. If the gain fluctuations are small, then the amplitudes of the successive terms are determined by increasing powers of the static net round-trip gain coefficient, so that the j - 1st term is proportional to K_o^j . When the mean value of the net round-trip gain is less than unity, $K_o = \rho^2 H_o^2 < 1$, the infinite sum of K_o^j is equal to $1/(1 - K_o)$, as was used previously to derive the Airy formula. If a finite number of terms are used instead, the summation of K_o^j from $j = 0$ to $j = M$ is given by

$$\sum_{j=0}^M K_o^j = \frac{1 - K_o^{M+1}}{1 - K_o}. \quad (19)$$

The value of M is determined by requiring the difference between the infinite sum and the finite sum of $M + 1$ terms to be less than a small fraction ϵ of the value of the full infinite sum. This condition is written

$$\left(\frac{1}{1-K_o}\right) - \left(\frac{1-K_o^M}{1-K_o}\right) < \epsilon \left(\frac{1}{1-K_o}\right). \quad (20)$$

Then, solving for the required number of terms M yields

$$M > \frac{\ln(\epsilon)}{\ln(K_o)} - 1. \quad (21)$$

We shall require $\epsilon < 0.01$, or the difference between the finite sum and the infinite sum of less than 1 percent. For example, if $K_o = 0.9$, then from equation (21) we obtain $M > 43$. The time interval $M\tau$ is proportional to the memory of the feedback system, and increases as the net round-trip gain K approaches unity. However, it will be seen later that the value of M just derived is only valid in the case of small gain fluctuations.

The output field at any time t is a random phasor sum of the $M + 1$ partial waves. This expression may be cast in a more illuminating form by substituting the full form of the discrete gain coefficients for the K_t terms given by equation (15). Doing this and simplifying yields:

$$C_t = \gamma^2 H_o e^{-i(\delta h_t)} R [1 + \rho^2 H_o^2 e^{-2i(\delta h_{t-1})} + \rho^4 H_o^4 e^{-2i(\delta h_{t-1} + \delta h_{t-2})} + \dots + \rho^{2M} H_o^{2M} e^{-2i(\delta h_{t-1} + \delta h_{t-2} + \dots + \delta h_{t-M})}]. \quad (22)$$

Each successive term of this expression represents an individual partial wave that has travelled an increasing number of times through the cavity, and has thus experienced the gain and phase fluctuations δh_t over an increasing time span. For the case of no gain or phase fluctuations, (i.e., $\delta h_t = 0$ for all t .) this expression may be summed analytically, and collapses to the well-known

Airy formula for the Fabry-Perot transmission derived previously. But in the present form, each partial wave has a different random gain and phase, due to the multiplicative complex fluctuations δh_t .

From equation (22) it is seen that the phases of the successive partial waves are cumulative sums of the multiplicative noise process δh_t over increasing times. If δh_t is a white Gaussian complex noise process with zero mean and variance σ_h^2 , then the complex phases of the successive terms represent a random walk process. The variance of a random-walk process grows linearly with time, so the complex phase of the M th partial wave, $2(\delta h_{t-1} + \delta h_{t-2} + \dots + \delta h_{t-M})$, will have variance $\sigma_M^2 = 2M\sigma_h^2$.

There are two regimes which we may identify with respect to the phase-spreading of the partial waves in the output field summation of equation (22), which we shall denote as the small-angle and large-angle regimes. The small-angle regime corresponds to relatively weak multiplicative noise and/or low net round-trip gain, such that the root-mean-square complex phase of the last (i.e., $(M+1)$ st) partial wave is less than 0.1. In this case, the exponentials in equation (22) may be linearized by the small-angle approximation, and the summation for C_t may be obtained analytically, as will be shown.

The large-angle regime corresponds to the case when the the rms complex phase variance of the older partial waves exceeds 0.1. In this case, the small-angle approximation does not obtain, and the full phasor expression of equation (22) must be used to compute the output field C_t at each time increment t . For a large multiplicative noise variance σ_h^2 , and/or high net round-trip gain $K_o \rightarrow 1$, the random-walking phase fluctuations of the later partial waves may become large enough to cause destructive interference with

the earlier partial waves, causing large fluctuations of the output field amplitude and phase. Also, the random-walking gain fluctuations of the later partial waves will eventually cause significant deviations from the exponential decay of the partial waves given by K_0^j . This causes the value of M to increase, which leads to enhanced low-frequency fluctuations of the output field.

First, the small-angle regime will be analyzed. In this regime, the phase fluctuations of the output field due to multiplicative phase noise are enhanced as the net round-trip gain is increased. Then, the large-angle regime will be examined by computing the full phasor expression of equation (22) for constant multiplicative phase noise variance while progressively increasing the net round-trip gain. The transition from the small-angle to large angle regimes is marked by the onset of rapid, large fluctuations of the output field amplitude and phase, and a decrease in the average output power. The results obtained will be used to calculate the linewidth of the resonant amplifier in each regime. In the small-angle regime, it is found that the multiplicative phase noise leads to an output-power-independent contribution to the linewidth of the output field power spectrum. In the large-angle regime, the linewidth increases with increasing net gain. Both of these results are counter to the decreasing linewidth with increasing net gain expected from equation (9) for the standard analysis without multiplicative noise.

2.3 Small-angle multiplicative noise regime: linear approximation

In this section, the case of relatively weak multiplicative noise will be treated using a linear approximation. The last term of equation (22) represents the "oldest" partial wave that has travelled $M + 1$ round-trips in the cavity. The complex phase of this wave is an $M + 1$ -step random walk. The small-angle regime is defined as the case when the standard deviation of the complex phase for the $M + 1$ st partial wave is less than 0.1, or

$$\sqrt{2M}\sigma_h \leq 0.1 \quad (23)$$

where M is defined by equation (21). Then, the small-angle approximation for the exponential ($e^x \approx 1 + x$) can be used to linearize the expression for the fluctuating output field so that equation (22) may be rewritten:

$$C_t \approx \gamma^2 H_o (1 + i(\delta h_t)) R [1 + \rho^2 H_o^2 (1 + 2i(\delta h_{t-1})) + \rho^4 H_o^4 (1 + 2i(\delta h_{t-1} + \delta h_{t-2})) + \dots + \rho^2 M H_o^{2M} (1 + 2i(\delta h_{t-1} + \delta h_{t-2} + \dots + \delta h_{t-M}))]. \quad (24)$$

Substituting $K_o = \rho^2 H_o^2$ into this expression yields:

$$C_t = \gamma^2 H_o (1 + i(\delta h_t)) R [1 + K_o (1 + 2i(\delta h_{t-1})) + K_o^2 (1 + 2i(\delta h_{t-1} + \delta h_{t-2})) + \dots + K_o^M (1 + 2i(\delta h_{t-1} + \delta h_{t-2} + \dots + \delta h_{t-M}))]. \quad (25)$$

Expanding this expression will yield many terms of $O(\delta h^2)$, like $(\delta h_t^2 \delta h_{t-k})$, which are small compared to $O(\delta h)$, and so may be discarded, leaving

$$\begin{aligned}
C_t = & \gamma^2 H_o R [(1 + K_o + K_o^2 + \dots + K_o^M) + (1 + K_o + K_o^2 + \dots + K_o^M)(i\delta h_t) \\
& + (K_o + K_o^2 + \dots + K_o^M)(2i\delta h_{t-1}) + (K_o^2 + K_o^3 + \dots + K_o^M)(2i\delta h_{t-2}) \\
& + \dots + K_o^M(2i\delta h_{t-M})]. \tag{26}
\end{aligned}$$

The term proportional to δh_t is due to the phase fluctuation encountered in the first "half round-trip" through the cavity. All other terms represent "full round-trips" through the cavity, hence the factors of 2 appear in terms $\delta h_{t-1}, \delta h_{t-2}, \dots$ etc.

The summations of powers of K_o may be performed analytically using equation (19). The coefficients in equation (26) are then designated as a_k , where the coefficient of the first term is a_0 , defined as

$$a_0 = \sum_{j=0}^{(M+1)-1} K_o^j = \frac{1 - K_o^{M+1}}{1 - K_o} \tag{27}$$

and subsequent terms $a_k, k \geq 1$ may be written

$$\begin{aligned}
a_k &= a_0 - \sum_{j=0}^{k-1} K_o^j \\
&= \frac{1 - K_o^{M+1}}{1 - K_o} - \frac{1 - K_o^k}{1 - K_o} \\
&= \frac{K_o^k - K_o^{M+1}}{1 - K_o} \tag{28}
\end{aligned}$$

As $M \rightarrow \infty, a_k$ converges to

$$a_k = \frac{K_o^k}{1 - K_o} \tag{29}$$

Now, substituting the coefficients a_k into equation (26), for the present special case of a noiseless input R , the output field at any time instant t is seen to be a weighted summation of the multiplicative noise samples h_t over the time interval $t - M$ to t :

$$\begin{aligned} C_t &= \gamma^2 H_o R \{a_0 + a_0 i \delta h_t + a_1 i 2 \delta h_{t-1} + \dots + a_M i 2 \delta h_{t-M}\} \\ &= \gamma^2 H_o R \left[a_0 (1 + i \delta h_t) + \sum_{k=1}^M a_k i 2 \delta h_{t-k} \right]. \end{aligned} \quad (30)$$

Finally, the factor $1/(1 - K_o)$ may be factored out of this expression to yield

$$C_t = \frac{\gamma^2 H_o R}{1 - K_o} \left[1 + i \delta h_t + i K_o 2 \delta h_{t-1} + i K_o^2 2 \delta h_{t-2} + \dots + i K_o^M 2 \delta h_{t-M} \right]. \quad (31)$$

This expression represents the transformation of the multiplicative phase and gain fluctuations to the output field at every time instant t . The first term is the static gain of the resonant amplifier as given from the standard analysis leading to equation (5). Recall from equation (13) that δh_t is a complex-valued random series whose real and imaginary parts represent the time-varying gain and phase, respectively, of the amplifying medium. Physically, the real-valued coefficients a_k determine the contribution of the multiplicative phase and gain fluctuation at the previous time increment $t - k$ to the output at time increment t . It is apparent from equation (31) that for $|K_o| < 1$, the a_k magnitudes decrease exponentially with increasing k . Thus, noise events further removed in time from the time increment t have a diminishing effect on the output state. In this small-angle approximation,

noise events occurring at times prior to $t - M$ have no effect on the output, which is just an analytic statement of the finite memory time of the system.

In the analysis thus far, fluctuations of the input field R were not considered. In general, the input $R = R_t$ may also have a time-varying amplitude and phase. To treat this possibility, the input state is now defined in the continuous-time picture as a sinusoid with mean frequency coincident with a cavity resonance ω_m , perturbed by amplitude noise $\delta A(t)$ and phase noise $\delta\phi(t)$

$$R(t) = (A_R + \delta A(t)) e^{i(\omega_m t + \delta\phi(t))}. \quad (32)$$

Assuming $\delta\phi_t < 0.1$ radian, the small-angle approximation can again be employed, and the time-varying input field $R(t)$ may be manipulated into the discrete-time form:

$$\begin{aligned} R_t &\approx (A_R + \delta A_t) (1 + i\delta\phi_t) e^{i\omega_m t} \\ &= (A_R + iA_R\delta\phi_t + \delta A_t + i\delta A_t\delta\phi_t) e^{i\omega_m t} \\ &\approx A_R \left(1 + i\delta\phi_t + \frac{\delta A_t}{A_R} \right) e^{i\omega_m t} \\ &= A_R e^{i\omega_m t} (1 + \delta R_t) \\ R_t &= R_0 (1 + \delta R_t). \end{aligned} \quad (33)$$

where the term of $O(\delta A)(\delta\phi)$ was neglected, since it is small compared to the terms of $O(\delta A)$ and $O(\delta\phi)$, and the noise sources δA and $\delta\phi$ are assumed to be uncorrelated.

Now, this expression for the fluctuating input field is inserted into the full

form of equation (22) to obtain the output at every time increment t due to both input field fluctuations and multiplicative gain fluctuations:

$$\begin{aligned}
 C_t &= \gamma^2 G_t R_t + \gamma^2 \rho^2 G_t H_{t-1} G_{t-1} R_{t-1} \\
 &\quad + \gamma^2 \rho^4 G_t H_{t-1} G_{t-1} H_{t-2} G_{t-2} R_{t-2} + \dots \\
 &= \gamma^2 G_t [R_t + \rho^2 H_{t-1} G_{t-1} R_{t-1} \\
 &\quad + \rho^4 H_{t-1} G_{t-1} H_{t-2} G_{t-2} R_{t-2} + \dots] \\
 &= \gamma^2 G_t [R_t + K_{t-1} R_{t-1} + K_{t-1} K_{t-2} R_{t-2} + \dots]. \quad (34)
 \end{aligned}$$

Using manipulations similar to those used to derive equation (31) (the detailed algebra is relegated to an Appendix) a simplified expression for the complex output field amplitude is obtained:

$$\begin{aligned}
 C_t &= \frac{\gamma^2 H_o R}{1 - K_o} [1 + i\delta h_t + K_o i 2\delta h_{t-1} K_o^2 i 2\delta h_{t-2} + \dots + K_o^M i 2\delta h_{t-(M-1)} \\
 &\quad + (1 - K_o) (\delta R_t + K_o \delta R_{t-1} + K_o^2 \delta R_{t-2} + K_o^3 \delta R_{t-3} + \dots + K_o^M \delta R_{t-M})]
 \end{aligned}$$

The powers of K_o multiplying the δR terms may be defined as a set of coefficients b_k :

$$b_k = K_o^k. \quad (36)$$

The full expression for the output field can now be written more compactly as summations of the two noise processes δh_t and δR_t in terms of the coefficients a_k and b_k :

$$C_t = \gamma^2 H_o R \left[a_0(1 + \delta h_t) + \left(\sum_{k=1}^M a_k i 2 \delta h_{t-k} \right) + \left(\sum_{k=0}^M b_k \delta R_{t-k} \right) \right]. \quad (37)$$

This expression represents a linear approximation to the full form of equation (22) for the slowly-varying complex envelope of the output field C_t including both input field fluctuations and multiplicative phase and gain fluctuations. This linear approximation is valid in the small-angle regime as defined by equation (23).

Now, the power spectrum of the output field in the small-angle regime will be calculated. Equation (37) has the form of a finite-impulse-response filter operating on "input" processes δh_t and δR_t . For linear systems in general, the Fourier transform of the time impulse-response yields the output frequency response of the system [8]. For an input field noise source modeled by a Gaussian-distributed random process, the power spectrum of the output field is the product of the input noise power spectrum and the magnitude-squared of the system frequency response [?]. So, if the impulse responses, net round-trip gain K_o , and the analytical form of the power spectra of the multiplicative fluctuations $S_h(f)$ and the input field fluctuations $S_R(f)$ are known, then the output power spectrum $S_C(f)$ may be obtained analytically.

The impulse-responses of the resonant amplifier output to a delta-function of multiplicative noise δh_t or input noise δR_t are defined to be $\delta C_{h,t}$ and $\delta C_{R,t}$, respectively. The multiplicative impulse-response $\delta C_{h,t}$ is the decaying output field response given by equation (37) due to a delta-function multiplicative impulse in δh_t applied to the system at time $t = 0$:

$$\begin{aligned}
\delta C_{h,t} &= \gamma^2 H_o R 2a_t u_t \\
&= \left(\frac{2\gamma^2 H_o R}{(1 - K_o)} \right) K_o^t u_t \\
&= \frac{2\gamma^2 H_o R}{(1 - K_o)} e^{-\Gamma t} u_t
\end{aligned} \tag{38}$$

where the decay constant, and u_t is the unit step function, with $u_t = 0$ for $t < 0$, and $u_t = 1$ for $t \geq 0$, and it is assumed that t takes only integer values (i.e., time is normalized to increments of τ). The first half-round-trip ($k = 0$ term) was taken to be equal to a full round-trip. For $M > 100$ corresponding to $K_o > 0.95$, this introduces a small error of less than a 1 percent in the output sum. The response to an input field impulse in δR_t is obtained similarly as the response of equation (37) to a delta-function impulse in δR_t applied to the system at time $t = 0$:

$$\begin{aligned}
\delta C_{R,t} &= \gamma^2 H_o R b_t u_t \\
&= \gamma^2 H_o R K_o^t u_t \\
&= \gamma^2 H_o R e^{-\Gamma t} u_t.
\end{aligned} \tag{39}$$

The Fourier transforms of the impulse responses $\delta C_{h,t}$ and $\delta C_{R,t}$ yield the corresponding frequency responses $F_h(f)$ and $F_R(f)$, where f is the Fourier frequency. Both impulse responses represent decaying exponentials, leading to Lorentzian frequency responses given by

$$F_h(f) = \left(\frac{2\gamma^2 H_o R}{(1 - K_o)\Gamma} \right) \frac{1}{1 - i \frac{2\pi f}{\Gamma}} \tag{40}$$

and

$$F_R(f) = \left(\frac{\gamma^2 H_o R}{\Gamma} \right) \frac{1}{1 + i \frac{2\pi f}{\omega_c}} \quad (41)$$

where $\omega_c = \Gamma/\tau$ is the rolloff frequency of the Lorentzian response.

The power spectrum of the output field is comprised of three terms: a delta-function term due to the sinusoidal input R , and terms due to the multiplicative and input fluctuations. In the absence of multiplicative noise, and for a pure sinusoidal input field R at a resonance frequency ω_m , the output power spectrum $S_C(f)$ is a pure sinusoid of frequency ω_m , with magnitude given by the constant term in equation (37). This may be written as

$$\begin{aligned} S_C(f) &= (\gamma^2 H_o R a_0)^2 \delta(f) \\ &= \left(\frac{\gamma^2 H_o R}{1 - K_o} \right)^2 \delta(f) \end{aligned} \quad (42)$$

where the delta function is defined as $\delta(0) = 1$ and $\delta(x) = 0, x \neq 0$, and is centered on frequency ω_m . The Fourier frequency f is the offset in ω from the optical frequency ω_m . This is equivalent to the power gain at the peak of the resonant amplifier transmission \mathcal{F} given by equation (7). The noise processes δh_t and δR_t give rise to additional terms in the output power spectrum. It is assumed that the noise processes δh_t and δR_t are uncorrelated, so the power spectra due to each process may be added. The term due to multiplicative noise is the product of the multiplicative noise power spectral density $S_h(f)$ and the magnitude-squared of the frequency response $F_h(f)$. Similarly, the term due to the input noise is the product of

the input field noise power spectral density $S_R(f)$ and the magnitude-squared of the frequency response $F_R(f)$. The addition of equation (42) and the two noise terms yields the total output power spectrum:

$$S_C(f) = \left(\left(\frac{\gamma^2 H_o R}{1 - K_o} \right)^2 \delta(f) \right) + |F_h(f)|^2 S_h(f) + |F_R(f)|^2 S_R(f) \quad (43)$$

Substituting for the frequency responses $F_h(f)$ and $F_R(f)$ and subsequent simplification yields

$$\begin{aligned} S_C(f) &= \left(\left(\frac{\gamma^2 H_o R}{1 - K_o} \right)^2 \delta(f) \right) \\ &\quad + \left(\frac{2\gamma^2 H_o R}{(1 - K_o)\Gamma} \right) \left| \frac{1}{1 + i \frac{2\pi f}{\omega_c}} \right|^2 S_h(f) + \left(\frac{\gamma^2 H_o R}{\Gamma} \right) \left| \frac{1}{1 + i \frac{2\pi f}{\omega_c}} \right|^2 S_R(f) \\ &= \left(\frac{\gamma^2 H_o R}{1 - K_o} \right)^2 \left(\delta(f) + \frac{\frac{4}{(1 - K_o)^2}}{1 + \frac{(2\pi f)^2}{\omega_c^2}} S_h(f) + \frac{1}{1 + \frac{(2\pi f)^2}{\omega_c^2}} S_R(f) \right). \end{aligned} \quad (44)$$

Consider the last term of this expression due to the input noise δR . For low gain and/or low multiplicative noise, the signal-to-noise ratio inside the amplifier bandwidth will be the same as the input signal-to-noise ratio. Physically, the last term implies that the output field phase and amplitude exactly follows the input field phase and amplitude fluctuations for rates less than the cavity bandwidth ω_c , which is intuitively correct. For fluctuation rates faster than ω_c , the input field fluctuations are rolled off as $1/f^2$, as expected, since they lie outside the bandpass of the cavity. As the net gain K_o is increased, ω_c decreases, and the integrated noise power due to the input fluctuations decreases, implying a decreased spectral width of the output field.

The resonant amplifier therefore produces a narrowband output signal of high spectral purity from a broadband noise input when the net round-trip gain K_o is high. This is the expected behavior of a resonant amplifier as obtained from the standard analysis leading to equation (7), and is the basis of the linear model of the laser as a noise driven resonant amplifier [4], which we will return to later.

Now consider the second term of equation (44). It is seen that the second term due to multiplicative noise δh_i is multiplied by the factor $1/(1 - K_o)^2$ compared to the last term due to the input field fluctuations δR_i . What is significant about this is that as the net gain K_o is increased, given fixed levels of input fluctuations $S_R(f)$ and multiplicative fluctuations $S_h(f)$, eventually the output field power spectrum $S_C(f)$ will become dominated by the multiplicative noise. After this happens, the signal-to-noise ratio for Fourier frequencies less than ω_c will decrease with further increases in the net gain.

Making use of the fact that for $K_o \approx 1$, $\Gamma = |\ell n(K_o)| \approx (1 - K_o)$, the rolloff frequency may be approximated as $\omega_c^2 \approx (1 - K_o)/\tau$. Making this substitution in the second term of equation (44) yields

$$S_C(f)|_{K_o \rightarrow 1} = \left(\frac{\gamma^2 H_o R}{1 - K_o} \right)^2 \left(\delta(f) + \frac{4}{(1 - K_o)^2 + (2\pi f\tau)^2} S_h(f) + \frac{1}{1 + \frac{(2\pi f)^2}{\omega_c^2}} S_R(f) \right)$$

In the limit as $K_o \rightarrow 1$, the second term due to multiplicative noise overwhelms the last term, so the output power spectrum becomes

$$S_C(f) = \left(\frac{\gamma^2 H_o R}{1 - K_o} \right)^2 \left(\delta(f) + \frac{4}{(2\pi f\tau)^2} S_h(f) \right) \quad (46)$$

In the limit as $K_o \rightarrow 1$, the integrated multiplicative noise power given by the second term in equation (45) approaches a constant value, which implies that the spectral width of the output signal also becomes constant. This is in marked contrast to the prediction of the standard analysis [4] of equation (7), which predicts decreasing linewidth with increasing gain. In summary, for low net gain when the input field fluctuations are dominant, the width of the output power spectrum decreases with increasing gain. But as the net gain $K_o \rightarrow 1$, the multiplicative fluctuations eventually become dominant, and the power spectrum of the resonant amplifier approaches a constant value. Therefore, a minimum linewidth should be expected for resonant amplifiers operated at high gain in the presence of multiplicative noise. To the extent that the multiplicative fluctuations arise from fundamental thermodynamic processes [12], this minimum linewidth will be a fundamental limit.

2.4 Large-angle multiplicative noise: numerical analysis

In this section, the full phasor form of the output field given by equation (22) is analyzed in the large-angle regime, by numerical simulation using computer-generated random time series to represent the multiplicative noise. This approach is taken to investigate the behavior of the output field amplitude and phase when the variance of the complex phase of the older partial waves exceeds 0.1 radians, so the small-angle approximation which permits

the analytic derivation of equation (23) no longer obtains. The output field time series is computed for a noiseless input field R of unit amplitude at fixed cavity resonance frequency ω_m , for various values of the net round-trip gain. The calculations are performed for a $300\mu\text{m}$ -long Fabry-Perot semiconductor laser cavity, at $1.3\mu\text{m}$ wavelength, with equal facet power reflectivities $\rho^2 = 0.32$.

The real and imaginary parts of δh_t are assumed to be correlated, as is the case for phase and gain fluctuations arising from electron-number fluctuations in a semiconductor laser gain medium [10]. The real and imaginary parts of δh_t are written in terms of a common noise source δn_t representing fluctuations of the refractive index:

$$\begin{aligned} \delta h(t) &= \delta h'(t) + i\delta h''(t) \\ &= \left(1 + \frac{i}{\beta}\right) \left(\frac{\omega_m l}{c}\right) \delta n(t) \end{aligned} \quad (47)$$

The constant β relates the changes in the real and imaginary parts of the refractive index due to electron density fluctuations, and is a measure of the amount of amplitude-phase coupling for waves in the gain medium. It was shown [2], [3] that β is responsible for broadening of the semiconductor laser linewidth above the Schawlow-Townes prediction, and so β is typically referred to as the linewidth enhancement factor. The refractive index in a semiconductor laser gain medium is typically modeled as a linear function of the carrier density [?]. Thus, changes in the electron density due to injection current noise, thermal fluctuations, or electron-hole recombination processes cause correlated changes in the gain and phase of the amplifying medium via

β .

Computer simulations were run for increasing net round-trip gains $K_o = 0.9, 0.95, 0.99, 0.995,$ and 0.999 , which represents three orders of magnitude change in the net gain. For each value of K_o , an N -element complex vector of the fluctuating output field C_i is produced. For these net gain values, the total numbers M of partial-waves used in the summations were, respectively, $M = 50, 100, 500, 1000,$ and 5000 . The complex multiplicative noise process δh_i is simulated by a computer-generated Gaussian-distributed zero-mean random time series with standard deviation of $\sigma_N = 0.1$. This implies that the system is in the large angle regime for all of the net gain values tested. The computer produces a series of random values from a Gaussian distribution such that the rms value of an infinite number of such values would be σ_N .

The computed results for net round-trip gain of $K_o = 0.9, 0.95, 0.99, 0.995,$ and 0.999 are now discussed. To see the qualitative effect of the increasing net gain on the output, the real and imaginary parts of the output electric field C_i are displayed parametrically in the complex plane in Fig 2 - 6, for increasing values of K_o . In these plots, each of the N dots on the complex plane represents the computed position of the tip of the output field vector C_i . Figure 2 illustrates the case of net round-trip gain $K_o = 0.9$. The tip of the electric field vector describes an arc with maximum phase excursion of approximately ± 0.3 radians, but with relatively constant amplitude. As the gain is increased to $K_o = 0.95, 0.99, 0.995,$ and 0.999 , illustrated in Fig 2 - 6, the maximum phase excursion increases and the amplitude exhibits progressively larger fluctuations which appear as a swirling pattern in the

complex plane. If there were no multiplicative noise, all of the dots would fall on one point on the real axis, determined by the static gain $1/(1 - K_0)$. The small-angle regime treated previously represents small excursions about this point.

As the output field vector swirls around the complex plane, Figure 4e, the magnitude and phase change drastically. The phase and instantaneous intensity (magnitude-squared of the electric field) versus time for each value of net gain are plotted in Figures 7 - 16. As the net gain increases, the period and amplitude of both the intensity and phase fluctuations increase. At the lower gain values, the mean value of the intensity fluctuations is close to the value expected without multiplicative noise. However, as the gain is increased, the amplitude of the intensity fluctuations increase greatly. The intensity becomes more deeply modulated, and the mean value of the intensity moves to lower values. This behavior is more apparent from the probability distribution of the intensity, discussed below. As the net gain is increased, the phase fluctuation amplitude also increases (Fig 12-16) until eventually, the phase "wraps around" more than π radians.

The probability distribution of the power versus increasing net gain is plotted in Fig 17 - 21. At $K_0 = 0.9$, the probability distribution has developed a "tail" stretching to lower values of intensity. As the net gain increases, this tail becomes more pronounced, and the mean value of the probability distribution decreases. At high gain of $K_0 = 0.999$, the intensity probability distribution is peaked near zero, nearly resembling the probability distribution of a thermal emission source, or a below-threshold laser. The shift of the mean intensity to lower values is in qualitative agreement with a theoretical

Fokker-Planck analysis and experimental results obtained for a helium-neon laser with multiplicative loss noise [15]. This shift of the probability distribution to lower values with increasing gain is contrary to the behavior expected for the resonant amplifier without multiplicative noise. In the context of laser operation, this result implies that the mean value of the intensity probability distribution will initially grow as the gain is first increased, but eventually will reach a maximum value, and then begin to decrease.

In Fig 22 - 26 the power spectrum of the output field versus increasing net gain is plotted. The noise level progressively increases as the net gain is increased. This is not unexpected, given the increasingly large intensity and phase fluctuations of the output field as the net gain is increased. In the absence of multiplicative noise, the output power spectrum would be a delta-function, since no input noise source is included in the simulations.

It is noted that in all of these results, the variance of the multiplicative noise time-series was kept constant, and only the net gain was changed. While such a large value of multiplicative noise may not typically encountered in practice, these simulation results serve to illustrate the effects of increasing net gain on the output field. By using a relatively large value of multiplicative noise, it was possible to study the qualitative behavior of the output versus net gain using a manageable number of partial waves. In a semiconductor laser, net gains of $K_0 \approx 1 - 10^{-5}$ are typical, requiring approximately one million partial waves per time increment to simulate. To obtain a reasonable estimate of the output power spectrum, at least 1024 time increments need to be computed, which becomes computationally prohibitive.

2.5 Detailed description of simulation algorithm

For each value of K_o , the details of the simulation algorithm are as follows: First, a real-valued random noise vector δn_t of length $2N$ is generated. Then the complex vector δh_t of length $2N$ is generated according to equation (47). The cumulative sum of δh_t is then computed, resulting in another vector of length $2N$, that represents a complex random walk process. The indices of this vector are reversed, so that random-walk begins with the last ($2N$ th) element and moves to earlier times. This vector is called w . Then, the output field C_t is computed for each of the N time increments t by summing the $M + 1$ partial waves whose complex phases are given by the values of w . Thus, the first sample of C_t is computed by starting at the middle of the vector w (i.e., w_{N-1}), and using the previous M values. The complex phase of the first partial wave at time increment t is given by $w_{t+N-1} - w_{t+(N-2)}$, and the last partial wave has complex phase $w_{t+N-1} - w_{t+N-1-(M+1)}$. Then, the magnitude-squared and phase of C_t are computed. The magnitude-squared of C_t is proportional to the intensity of the output field at time t . The probability distribution (histogram) of the intensity is also computed. Finally, a Hanning (raised-cosine) windowing function is applied to the time series C_t and a complex fast-Fourier-transform (FFT) is performed on this time series. The magnitude squared of the FFT is the computed power spectrum of the output field.

responding frequency responses $F_h(f)$ and $F_R(f)$, where f is the Fourier frequency. Both impulse responses represent decaying exponentials, leading to Lorentzian frequency responses. The frequency response of the cavity to the multiplicative noise process is

$$F_h(f) = \left(\frac{2\gamma^2 H_o R}{(1 - K_o)\Gamma} \right) \frac{1}{1 + i\frac{2\pi f}{\omega_c}} \quad (2.40)$$

and the response to the input field fluctuations is

$$F_R(f) = \left(\frac{\gamma^2 H_o R}{\Gamma} \right) \frac{1}{1 + i\frac{2\pi f}{\omega_c}} \quad (2.41)$$

where $\omega_c = \Gamma/\tau$ is the rolloff frequency of the Lorentzian response, and the Fourier frequency f is the offset in Hz from the optical frequency ω_m .

The power spectrum of the output field fluctuations is comprised of two terms due to the multiplicative and input fluctuations. The carrier at the cavity resonance frequency ω_m is shifted to DC due to the discrete-time analysis, and has amplitude

$$S_C(0) = \left(\frac{\gamma^2 H_o R}{1 - K_o} \right)^2 \quad (2.42)$$

This is equivalent to the output power at the peak of the resonant amplifier transmission as derived previously in equation (2.5).

The noise processes δh_t and δR_t give rise to complex-valued terms in the output field. It is assumed that the noise processes δh_t and δR_t are uncorrelated, so the power spectra due to each process may be added. The term due to multiplicative noise is the product of the multiplicative noise complex power spectral density $S_h(f)$ and the magnitude-squared of the frequency response $F_h(f)$. Similarly, the contribution due to the input noise is the product of the input field noise complex

power spectral density $S_R(f)$ and the magnitude-squared of the frequency response $F_R(f)$. Therefore, the total output field noise power spectrum due to both input field fluctuations and multiplicative gain and phase fluctuations is:

$$S_C(f) = |F_R(f)|^2 S_R(f) + |F_h(f)|^2 S_h(f) \quad (2.43)$$

Substituting equations (2.40) and (2.41) for the frequency responses $F_h(f)$ and $F_R(f)$, and using the approximation when $K_o \approx 1$ that $\Gamma = |\ln(K_o)| \approx 1 - K_o$, yields the total output field power spectrum:

$$\begin{aligned} S_C(f) &= \left| \left(\frac{\gamma^2 H_o R}{\Gamma} \right) \frac{1}{1 + i \frac{2\pi f}{\omega_c}} \right|^2 S_R(f) + \left| \left(\frac{2\gamma^2 H_o R}{(1 - K_o)\Gamma} \right) \frac{1}{1 + i \frac{2\pi f}{\omega_c}} \right|^2 S_h(f) \\ &= \left(\frac{\gamma^2 H_o R}{1 - K_o} \right)^2 \left(\frac{1}{1 + \frac{(2\pi f)^2}{\omega_c^2}} S_R(f) + \frac{\frac{4}{(1 - K_o)^2}}{1 + \frac{(2\pi f)^2}{\omega_c^2}} S_h(f) \right). \end{aligned} \quad (2.44)$$

This is the general expression for the output field fluctuation power spectrum of a resonant amplifier including input field noise and multiplicative noise.

Consider now the first term of this expression due to the input noise ϵR . For low gain and/or low-level multiplicative noise, the signal-to-noise ratio for Fourier frequencies less than ω_c will be the same as the input signal-to-noise ratio. Physically, this implies that the output field phase and amplitude exactly follow the input field phase and amplitude fluctuations for fluctuation rates less than the cavity bandwidth ω_c , which is intuitively expected. For fluctuation rates faster than ω_c , the input field fluctuations are filtered by the cavity, and so are rolled off as $1/f^2$. As the net gain K_o is increased, the cavity corner frequency ω_c decreases, and the integrated output noise power due to the input fluctuations decreases, implying a decreased spectral width of the output field. The resonant amplifier therefore produces a narrowband

output signal of increasing spectral purity from a broadband noise input as the net round-trip gain K_o is increased. This is the expected behavior of a resonant amplifier as obtained from the standard analysis leading to equation (2.5), and is the basis of the linear model of the laser as a noise-driven resonant amplifier, to which we will return later.

Now consider the second term of equation (2.44). This term due to multiplicative noise is new, and not obtained from the standard analysis of the resonant amplifier. The multiplicative noise term is multiplied by the factor $1/(1 - K_o)^2$ compared to the first term due to the input field fluctuations. It is seen that as the net gain K_o is increased, given fixed levels of input fluctuations $S_R(f)$ and multiplicative fluctuations $S_k(f)$, eventually the output field power spectrum $S_C(f)$ will become dominated by the multiplicative noise term. After this happens, the signal-to-noise ratio for Fourier frequencies less than ω_c will decrease with further increases in the net gain.

Again, making use of the fact that for $K_o \approx 1$, $\Gamma = |dn(K_o)| \approx (1 - K_o)$, the roll-off frequency may be approximated as $\omega_c \approx (1 - K_o)/\tau$. Making this substitution in the second term of equation (2.44) yields

$$S_C(f)|_{K_o \rightarrow 1} \approx \left(\frac{\gamma^2 H_o R}{1 - K_o} \right)^2 \left(\frac{1}{1 + \frac{(2\pi f)^2}{\omega_c^2}} S_R(f) + \frac{4}{(1 - K_o)^2 + (2\pi f \tau)^2} S_k(f) \right). \quad (2.45)$$

In the limit as $K_o \rightarrow 1$, the corner frequency $\omega_c \rightarrow 0$, and the second term due to multiplicative noise overwhelms the first term. The output power spectrum then becomes

fluctuations and increasing linewidth make the large-angle regime something to be avoided, so that a prediction of the *onset* of the large angle regime is sufficient for most applications.

By the Wiener-Khinchin Theorem, the power spectrum of a stationary noise process is the Fourier transform of its auto-correlation function [9]. For the case of small-angle multiplicative phase noise, the amplitude fluctuations of the output field are small compared to the phase fluctuations, so the field auto-correlation function is determined primarily by the phase fluctuations. In the large-angle regime, large amplitude and phase fluctuations occur, as seen in the previous chapter. In this regime, the field auto-correlation function and linewidth are determined primarily by the amplitude fluctuations.

First, the amount of linewidth enhancement is calculated in the small-angle regime from the power spectral density of phase fluctuations obtained from the small-angle analysis. The small-angle fluctuations are found to lead to an output-power-independent Lorentzian power spectrum for the resonant amplifier. The power spectrum in the large-angle regime broadens with increasing net gain as the numerical results of the last chapter illustrated. The onset of the large-angle regime is derived from the net round-trip gain and the multiplicative noise variance.

3 Multiplicative noise in laser linewidth

3.1 Analysis of effect of small-angle multiplicative noise on semiconductor resonant amplifier linewidth

As discussed in the previous chapter, the multiplicative phase fluctuations in a semiconductor laser gain medium are larger than the gain fluctuations by the factor β . So, in the small-angle regime, the amplitude fluctuations of the field are small compared to the phase fluctuations. This is illustrated graphically in the complex plane in Figure 4a of the previous chapter. From the numerical simulation results at the onset of the large-angle regime, it is seen that the phase fluctuations are larger than the amplitude fluctuations of the field. This means that the multiplicative noise contribution to the output power spectrum $S_C(f)$ is primarily phase noise for a semiconductor laser amplifier in the small-angle regime.

The output field power spectrum is the Fourier transform of the field auto-correlation function. Following the development of Petermann [10], the output field power spectrum may be derived in terms of the frequency fluctuations of the field when the amplitude fluctuations are negligible. In this case, the field autocorrelation function may be obtained in terms of the frequency fluctuations of the output field [10] (See Appendix for detailed derivation):

$$\langle C(t)C^*(t-T) \rangle = \langle P \rangle e^{i(\langle \dot{\phi} \rangle T)} e^{-\frac{1}{2} \langle \Delta \phi^2 \rangle} \quad (48)$$

where P is the average output intensity, $\langle \dot{\phi} \rangle$ is the mean frequency offset from the mode frequency ω_m , and the mean square phase fluctuation $\langle \Delta \phi^2 \rangle$ is related to the power spectrum of the frequency fluctuations $S_\nu(f)$ as

$$\langle \Delta\phi^2 \rangle = T^2 \int_{-\infty}^{\infty} S_{\nu}(f) \frac{\sin^2(\pi f T)}{(\pi f T)^2} df. \quad (49)$$

The power density spectrum of the field is then obtained as

$$W_C(\omega) = \int_{-\infty}^{\infty} \langle C(t)C^*(t-T) \rangle e^{-i\omega T} dT. \quad (50)$$

These expressions relating the power density spectrum of the field to the frequency fluctuation power spectrum are valid as long as the the phase fluctuations exhibit a Gaussian probability distribution. The derivation of these results is detailed in the Appendix.

When the multiplicative noise contribution to the output power spectrum $S_C(f)$ (derived in the previous chapter) is predominantly phase noise, the power spectrum of instantaneous frequency fluctuations is related to the power spectrum of phase fluctuations as [18]

$$S_{C,\nu}(f) = f^2 S_C(f). \quad (51)$$

Substituting the previous result from the small-angle analysis for the power spectrum of output phase fluctuations, the power spectrum of the output frequency fluctuations for net gain K_o approaching unity may be written

$$S_{C,\nu}(f) = f^2 \frac{4}{(2\pi f\tau)^2} S_h(f) \quad (52)$$

The factors of f^2 cancel, leaving

$$S_{C,\nu}(f) = \frac{1}{(\pi\tau)^2} S_h(f) \quad (53)$$

The frequency fluctuation power spectrum thus has the same form as the power spectrum of multiplicative fluctuations $S_h(f)$.

Consider the special case when the power spectrum of multiplicative fluctuations $S_h(f)$ is white. Equation (53) then implies that the power spectrum of output frequency fluctuations, $S_{C,\nu}(f)$, is also white. In this case, the autocorrelation function of the field amplitude is (See Appendix)

$$\langle C(t)C^*(t-T) \rangle = \langle P \rangle e^{i\langle \phi \rangle T} e^{-\frac{|T|}{t_c}} \quad (54)$$

where $t_c = 2/S_{C,\nu}(0)$. The Fourier transform of this expression yields a Lorentzian-shaped spectrum:

$$W_C(\omega) = \frac{2t_c \langle P \rangle}{1 + ([\omega - \langle \dot{\phi} \rangle] t_c)^2} \quad (55)$$

which is centered around the optical frequency $\omega_m + \langle \dot{\phi} \rangle$, and has spectral width

$$\delta\nu|_{mult} = \frac{1}{\pi t_c} = \frac{S_{C,\nu}(0)}{2\pi} = \frac{1}{(2\pi)^3 \tau^2} S_h(0). \quad (56)$$

In the small-angle regime, the total linewidth has the functional form:

$$\delta\nu|_{tot} = \delta\nu + \delta\nu|_{mult} \quad (57)$$

where the first term on the right is the linewidth obtained from the standard analysis without multiplicative noise [4].

In the standard analysis of the resonant amplifier without multiplicative noise [4] discussed in the previous chapter, the linewidth is given by:

$$\delta\nu \approx \frac{1 - \rho_1 \rho_2 G_o^2}{\rho_1 \rho_2 G_o^2} \frac{1}{\pi\tau} \quad (58)$$

For $K_o \approx 1$, this may be written

$$\delta\nu \approx \frac{1 - K_o}{\pi\tau} \quad (59)$$

Some other useful relationships are:

$$\delta\nu = \frac{2\Gamma}{2\pi\tau} = \frac{\Gamma}{\pi\tau} = \frac{\omega_c}{\pi} \approx \frac{(1 - K_o)c}{2\pi nl} \quad (60)$$

The total linewidth of the resonant amplifier can finally be expressed in terms of the net gain K_o as the sum of the standard and multiplicative contributions

$$\delta\nu|_{tot} = \frac{(1 - K_o)}{\pi\tau} + \frac{K_o^2}{(2\pi)^3 \tau^2} S_n(0) \quad (61)$$

when $K_o \approx 1$. The first term from the standard analysis decreases with increasing net gain K_o , whereas the second term due to multiplicative noise approaches a constant as $K_o \rightarrow 1$.

A noise source that has a white power spectrum up to infinite frequency has a delta-function auto-correlation function, which is a useful mathematical model, but is not physically realistic. A more realistic model for a noise process has an exponential time-correlation proportional to $e^{-\alpha t}$, with correlation constant α . The Fourier transform of an exponentially-correlated noise source yields a Lorentzian power spectral density, which is white up to a Fourier frequency of approximately $f = \alpha$, and then rolls off as $1/f^2$ for higher frequencies. Then, for practical purposes, a white noise source may

be modeled as having a α larger than all Fourier frequencies of interest. In practice, the noise may be considered to be white if α is at least as large as the cavity mode spacing f_c , equation (56) may be used to estimate the linewidth.

When α is small, then the approximation of equation (56) is no longer valid, and the lineshape of the field power spectrum will not necessarily be Lorentzian. The lineshape must then be computed from the Fourier transform of the auto-correlation function of the electric field. The electric field auto-correlation function must be first be derived in terms of the frequency fluctuation power spectrum, as is done in reference [10].

3.2 Onset of the large-angle regime

From the numerical analysis of the previous chapter, it is seen that when the phase of the later partial waves exceeds the small-angle regime of 0.1 radians, the output amplitude and phase fluctuations increase dramatically, (Figures 2 to 16, previous chapter). In this regime, the linewidth of the resonant amplifier can no longer be determined from the phase fluctuations of the output field, as in the small-angle regime. As illustrated in Figures 8a-e, the power spectrum of the electric field becomes progressively noisier as the net gain is increased, corresponding to increased linewidth.

The large amplitude and phase fluctuations make this regime of operation undesirable, so avoiding the onset of this regime is of great practical interest. From the preceding numerical analysis, the onset of the large amplitude fluctuations just begins to occur for net gain of $K_o = 0.9$ and when the

multiplicative noise standard deviation is $\sigma_h = 0.1$ radians, as illustrated in Figures 4a and 5a. For this value of net gain, the number of partial waves to achieve 1 percent convergence of the output partial wave summation is computed to be approximately 45. So, the variance of the phase for the last (i.e., M th) partial wave at the onset of the large angle regime is

$$\sqrt{2M}\sigma_h \approx \sqrt{90} (0.1) \approx 1 \text{radian.} \quad (62)$$

So, to avoid rebroadening of the linewidth, the net gain should be kept below the value that causes the standard deviation of the M th partial wave to exceed the 0.1 radians, i.e., within the limits of the small-angle model, as discussed in the last chapter.

3.3 Application of multiplicative noise model to laser linewidth

In this section, the results of the small angle analysis for the effect of multiplicative noise in a resonant amplifier will be applied to a linear model of a laser to derive an analytic expression for the linewidth. The laser may be considered to be a resonant amplifier driven by an equivalent input noise source corresponding to the spontaneous emission in the active medium [19], & [20]. In this model, the presence of the constant amplitude spontaneous emission noise input field causes the net round-trip gain to saturate at a value slightly less than unity, resulting in a finite linewidth for the resonant amplifier. The ratio of the output intensity to the input noise intensity due to spontaneous emission determines the net round-trip gain. The wide-band

spontaneous emission noise is amplified within the narrow bandpass of the resonant amplifier, yielding the laser output. Thus, for high gain, the laser output field may be viewed as a wave of constant amplitude and frequency, on which small statistical amplitude and phase fluctuations due to the spontaneously emitted photons are superimposed. The modified Schawlow-Townes model [21] takes into account the damping effect of the saturated gain above threshold on the amplitude fluctuations, which results in a factor of two decrease in the linewidth above threshold. Although the linear laser model does not explicitly include damping of the amplitude fluctuations, its simplicity makes it easy to see the basic physics responsible for the linewidth and the results for the multiplicative noise are easily obtained.

In both the original and the modified Schawlow-Townes models, the linewidth at a given output power level is seen to arise from the *additive* noise source of the spontaneously emitted photons which add random amplitude and phase components to the output field. The power output of the laser increases as the saturation level of the gain medium (i.e., pumping) is increased, due to increased stimulated emission. However, since the spontaneous emission level is proportional to the gain, which is essentially unity above threshold, so it remains clamped at its saturated threshold value. Thus, the additive random phase contribution of the spontaneous photons becomes less significant as the power increases, resulting in an increasing signal-to-noise ratio and decreasing linewidth. Thus, by the the Schawlow-Townes model, it is predicted that the linewidth of a laser can be made arbitrarily small by operating the laser at an arbitrarily high optical power level. We now derive the linear laser linewidth model, including the effect of

multiplicative phase fluctuations.

Following the development of Siegman [4], the output power of the laser P is related to the spontaneous emission input noise power P_{sp} as

$$1 - RG_p = 2T \frac{P_{sp}}{P} \quad (63)$$

where R is the power reflection coefficient of the cavity mirrors, so that $R = \rho^2$, $T = \gamma^2 = 1 - R$ is the power transmission coefficient, and G_p is the power gain per round trip. The quantity $1 - RG_p$ is defined as the "saturation amplification" of the resonant amplifier. The spontaneous emission power per cavity mode can be written

$$P_{sp} = \frac{1}{2} h\nu \frac{c}{nl} \frac{N_2}{N_2 - N_1} (G_p - 1) \quad (64)$$

where h is Planck's constant, ν is the frequency of the light, c is the speed of light in vacuum, n is the average value of the refractive index, l is the length of the cavity, and N_2 and N_1 are the population of the upper and lower atomic levels. For low-loss mirrors, $R \approx 1$, and above lasing threshold the round-trip gain $RG_p \approx 1$, so $(G_p - 1) \approx (1 - R)$. Now, substituting this and equation (64) into equation (63), and assuming lossless mirrors, so that $T = 1 - R$, obtains

$$1 - RG_p = \frac{h\nu c}{P nl} \frac{N_2}{N_2 - N_1} (1 - R)^2. \quad (65)$$

From the development of the previous section, the linewidth of a resonant amplifier with gain is given by equation (61)

$$\delta\nu|_{tot} = \frac{(1 - K_o)}{\pi\tau} + \frac{1}{(2\pi)^3\tau^2} Sh_\phi(0). \quad (66)$$

The round-trip power gain RG_p is approximately 1, as is K_o , so we may approximate $1 - RG_p \approx 1 - K_o$. Making these substitutions for the saturated gain of the laser into the last expression then yields

$$\begin{aligned} \delta\nu &= \left(\frac{c(1 - R)}{2\pi nl} \right)^2 2\pi \frac{h\nu}{P} \frac{N_2}{N_2 - N_1} + \frac{1}{(2\pi)^3\tau^2} Sh_\phi(0) \\ &= (\delta\nu_c)^2 2\pi \frac{h\nu}{P} \frac{N_2}{N_2 - N_1} + \frac{1}{(2\pi)^3\tau^2} Sh_\phi(0) \end{aligned} \quad (67)$$

for the linewidth as a function of the output power, where $\delta\nu_c$ is defined as the "cold-cavity" linewidth, or the linewidth of the cavity with the gain medium removed. The first term of this expression is equivalent to the original formula derived by Schawlow and Townes for the linewidth of the laser, which is correct up to threshold, and displays the familiar $1/P$ dependence. Above threshold, this term is reduced by a factor of two due to the damping of the amplitude fluctuations by the saturated gain [21]. The second term represents the multiplicative phase noise of the laser, and is seen to be independent of the output power. This equation predicts that the laser linewidth should initially decrease linearly with increasing output power, but will finally reach a minimum value proportional to the multiplicative noise strength. If the gain is increased yet further, the linewidth begin to "rebroaden" at the onset of the large-angle regime. A minimum linewidth and linewidth rebroadening is typically observed in single-frequency laser diodes at high power levels, corresponding to high net round-trip gain. This model has the same power-

independent character as the linewidth derived by Welford and Mooradian [11] using the phenomenological expression of equation (2). But the formalism used to derive it also reveals that same mechanism can be responsible for both a power-independent linewidth and linewidth rebroadening, as is typically observed in single-mode semiconductor lasers.

It is well-known that semiconductor lasers exhibit a power-independent linewidth deviation from the modified Schawlow-Townes formula [11], [22]. As an application of this model, the minimum linewidth of a typical single-mode semiconductor laser will be estimated due to the effects of electron density fluctuations as derived in the next chapter. Consider a single-mode GaAs semiconductor laser amplifier of length $l = 250\mu\text{m}$, which implies round-trip time $\tau \approx 5$ picoseconds. Assume multiplicative phase fluctuations due to electron density fluctuations, as calculated in the next chapter, at a level of $Sh_{\nu}(0) = 10^{-18} \text{ rad}^2/\text{Hz}$ for a carrier density at threshold of 10^{18} cm^{-3} . Then from equation (67), the minimum linewidth for the laser is calculated to be 120 Hz. This is 30 times less than the lowest reported linewidth of 3.6 kHz for a single-mode laser diode. In other semiconductor lasers, the minimum observed linewidth is 2 to 4 orders of magnitude larger. This estimate of the minimum linewidth implies noise mechanisms other than electron-density fluctuations may be dominant in the lasers tested, but that the lowest reported value to date is not far from the minimum due to electron density fluctuations.

Various mechanisms have been advanced to explain the origin of the power-independent linewidth and linewidth rebroadening, including electron number-density fluctuations [23], spatial hole burning [6], and spatially-

dependent temperature and carrier fluctuations [24]. These or other mechanisms, such as injection-current fluctuations, may be operative in various combinations in any particular laser. Whatever the source, multiplicative phase and gain fluctuations in the active medium will cause a minimum linewidth for the output field emission spectrum due to the fact that the active medium experiences thermodynamic fluctuations that alter the refractive index [12]. Multiplicative optical phase fluctuations in the active medium due to temperature and density fluctuations arise from the same considerations responsible for Johnson noise in electronic components. Therefore, *multiplicative* noise represents a fundamental limit to the minimum linewidth achievable in a laser. When this limit is reached, further increases in gain, or decreases in cavity losses, will not afford decreased linewidth. In fact, the linewidth is predicted to rebroaden if the net gain is increased past the point that the large-angle regime is entered. Also, it is noted that the total effect of independent multiplicative noise sources is diminished as more sources are added in parallel. This means that the effects of multiplicative noise will be more pronounced in structures with small transverse dimensions, such as semiconductor lasers and optical fibers, as compared to bulk optical systems.

3.4 Conclusion

An expression relating the effect of the multiplicative fluctuations to the linewidth of a resonant amplifier was derived using the results of the previous small-angle analysis. The amount of linewidth enhancement is calculated in the small-angle regime from the power spectral density of phase fluctua-

tions obtained from the small-angle analysis. The small-angle fluctuations are found to lead to an output-power-independent Lorentzian power spectrum for the resonant amplifier. The power spectrum in the large-angle regime broadens with increasing net gain as the numerical results of the last chapter illustrated. The onset of the large-angle regime is derived from the net round-trip gain and the multiplicative noise variance. For the case of multiplicative phase noise, it is shown that this effect produces a minimum linewidth of the resonant amplifier, and qualitatively explains the phenomena of the power-independent linewidth and linewidth rebroadening in single-frequency semiconductor lasers.

4 References

References

- [1] R. Drever, et al., *Applied Physics B Photophysics And Laser Chemistry* 31, 97-105 (1983).
- [2] C. H. Henry, *IEEE Journal of Quantum Electronics* QE-18, 259-264 (1982). C. H. Henry, *Journal of Lightwave Technology* LT-4, 298-311 (1986). C. H. Henry, *IEEE Journal of Quantum Electronics* QE-19, 1391-1397 (1983).
- [3] K. Vahala, A. Yariv, *IEEE Journal of Quantum Electronics* QE-19, 1096-1101 (1983). K. Vahala, A. Yariv, *IEEE Journal of Quantum Electronics* QE-19, 1102-1109 (1983).

-
- [4] A. E. Siegman, Lasers. (University Science, Mill Valley, CA, 1986).
 - [5] H. Yamazaki, M. Yamaguchi, M. Kitamura. IEEE Photonic Tech. Lett. 6. 341-343 (1994).
 - [6] H. Olesen, B. Tromborg, H. E. Lassen, X. Pan, Electron. Lett. 28, 444 (1992).
 - [7] D. L. Macfarlane, E. M. Dowling, Journal Of The Optical Society Of America A Optics Image Science And Vision 11, 236-245 (1994).
 - [8] A. D. Poularikas, S. Seely, Signals and Systems. (PWS Engineering, Boston, 1985).
 - [9] J. W. Goodman, Statistical Optics. (Wiley, New York, 1985).
 - [10] K. Petermann, Laser Diode Modulation and Noise, T. Okoshi, Ed., Advances in Optoelectronics (Kluwer, Dordrecht, 1991), vol. 3.
 - [11] D. Welford, A. Mooradian, Appl. Phys. Lett. 40, 560-562 (1982).
 - [12] W. H. Glenn, IEEE Journal of Quantum Electronics 25, 1218-1224 (1989).
 - [13] J. M. Deutsch, Physical Review E 48, R4179-R4182 (1993).
 - [14] M. R. Young, S. Singh, Physical Review A 38, 238-244 (1988). M. R. Young, S. Singh, Opt. Lett. 13, 21-23 (1988).

- [15] S. Zhu, *Physical Review A* **41**, 1689-1694 (1990), S. Zhu, *Physical Review A* **45**, 3210-3215 (1992), S. Zhu, *Physical Review A* **45**, 8148-8153 (1992), S. Zhu, *Physical Review A* **47**, 2405-2408 (1993).
- [16] H. B. Callen, R. F. Greene, *Physical Review* **86**, pp. 702-710, (1952).
- [17] M. Born, E. Wolf, *Principles of Optics*. (Pergamon Press, Oxford, 1980).
- [18] J. A. Barnes, D. W. Allan, *Proc. IEEE* **34**, 176-178 (1966).
- [19] A. L. Schawlow, C. H. Townes, *Physical Review* **112**, 1940-1949 (1958).
- [20] E. I. Gordon, *Bell System Technical Journal* **43**, 507-539 (1964).
- [21] M. Sargent, M. O. Scully, W. E. Lamb, *Laser Physics*. (Addison-Wesley, Reading, Mass., 1974).
- [22] K. Kikuchi, *IEEE Jour. Quant. Elec.* **25**, 684-688 (1989).
- [23] D. Welford, A. Mooradian, *Appl. Phys. Lett.* **40**, 560-562 (1982).
- [24] R. J. Lang, K. J. Vahala, A. Yariv, *IEEE Jour. Quant. Elec.* **QE-21**, 443-451 (1985).

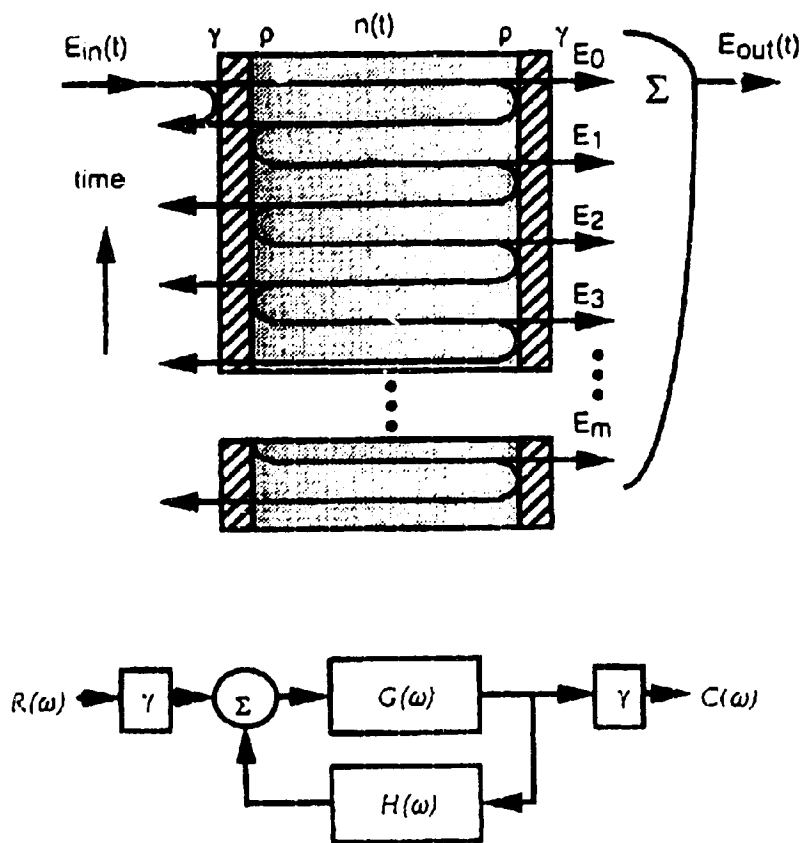


Figure -- 1. Analysis Basis Concept Diagram

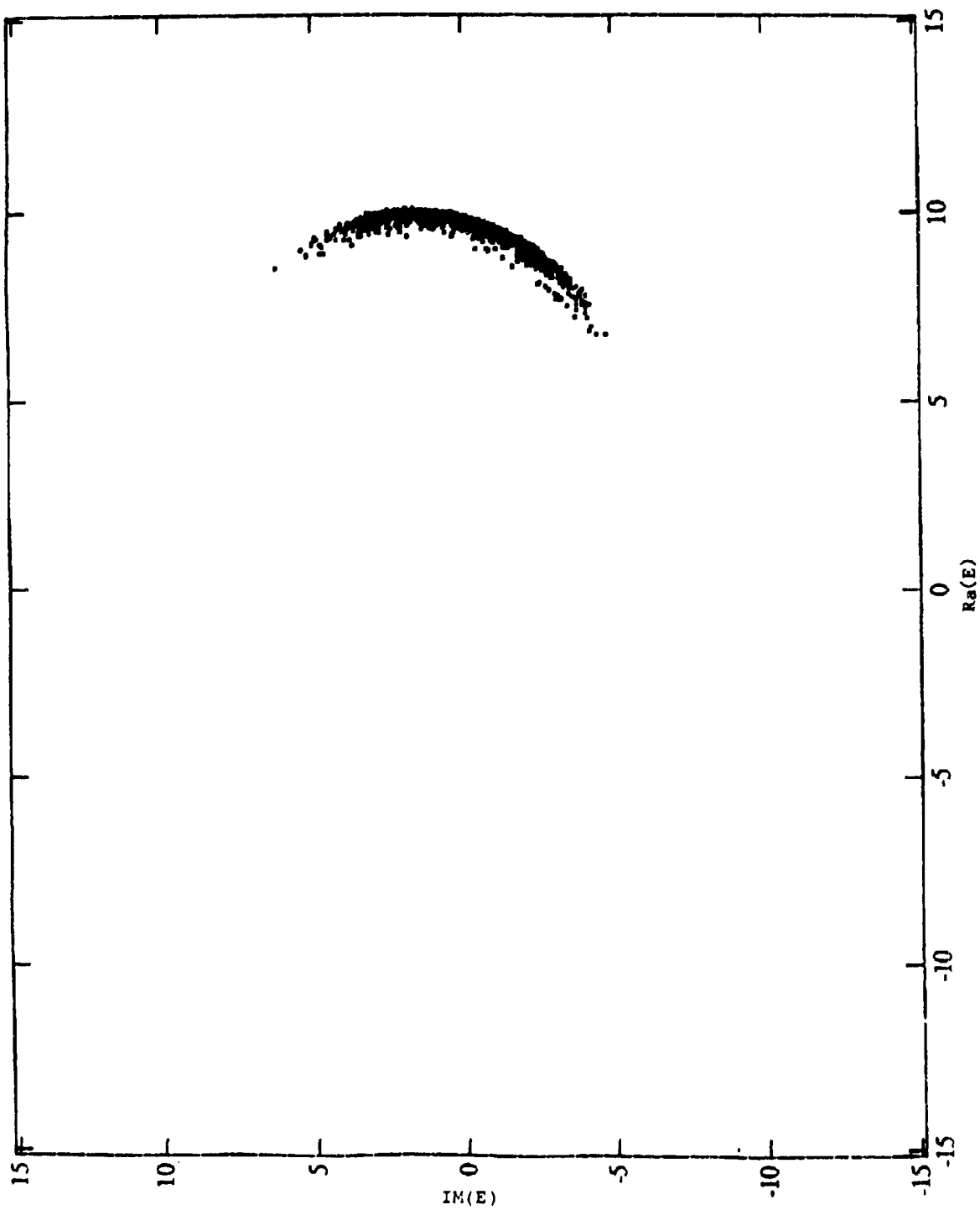


Figure - 2. Output Field in Complex Plane for Net Gain, $K_o = 0.9$

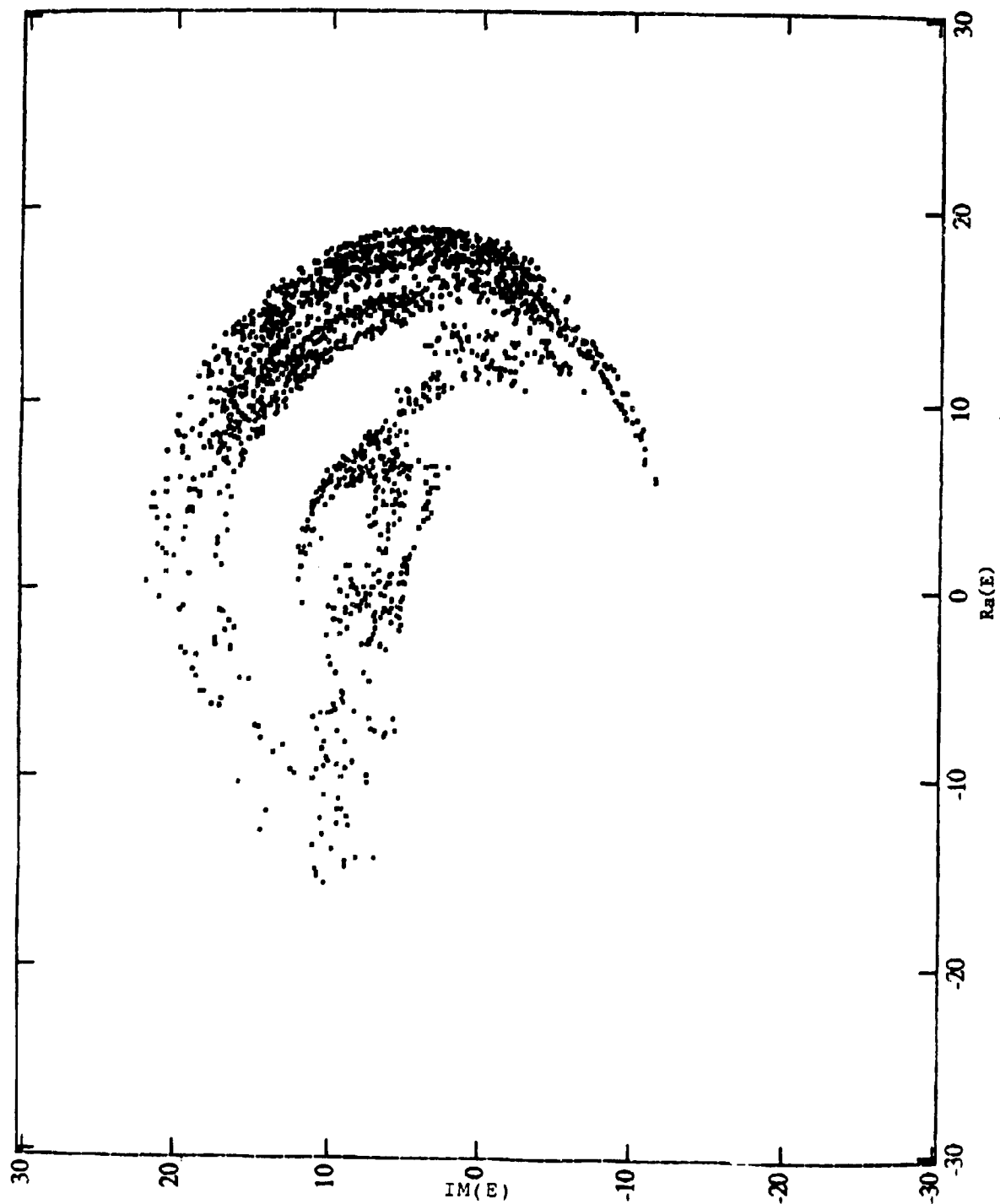


Figure - 2. Output Field in Complex Plane for Net Gain, $K_0 = 0.95$

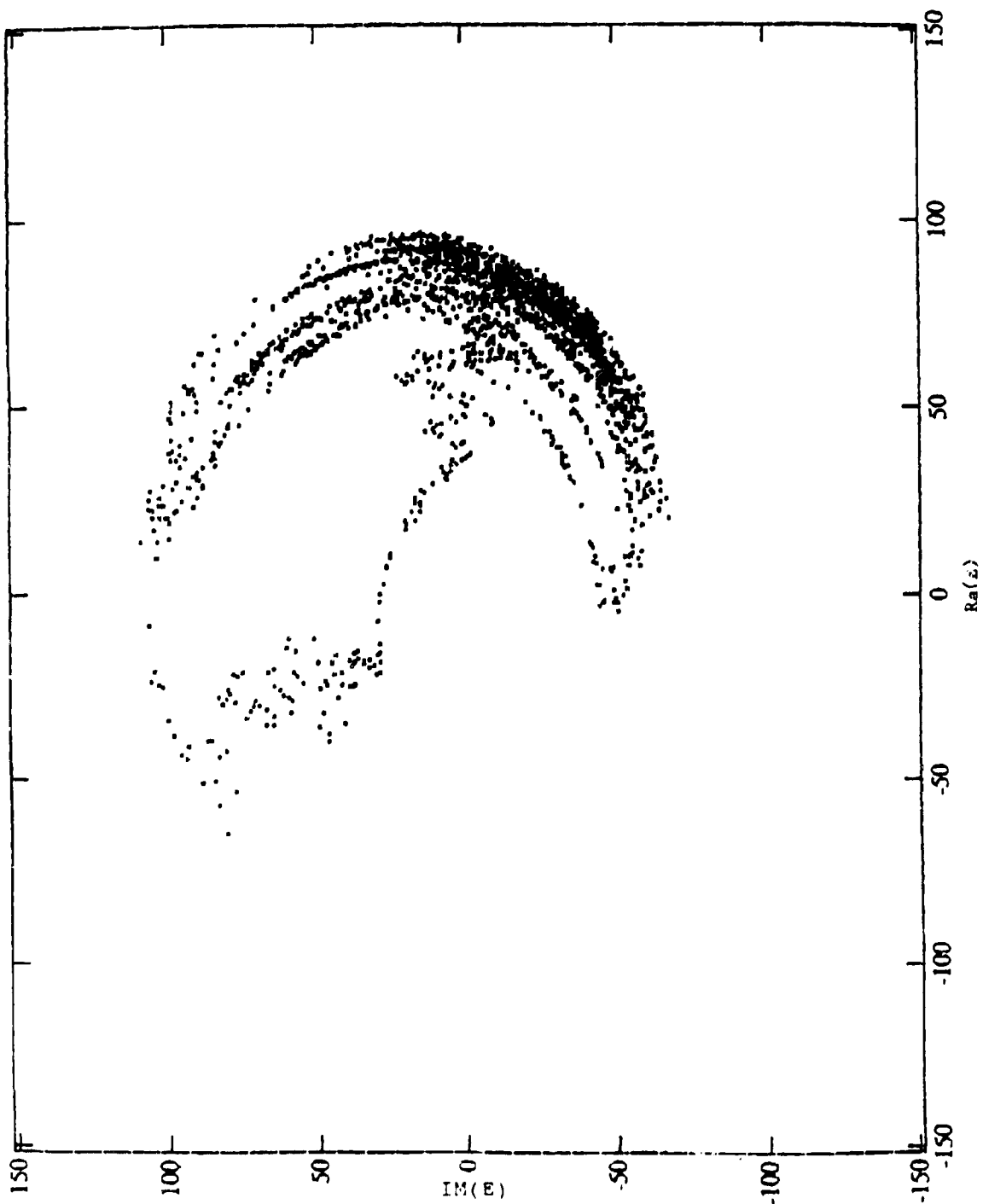


Figure - 3. Output Field in Complex Plane for Net Gain, $K_0 = 0.99$

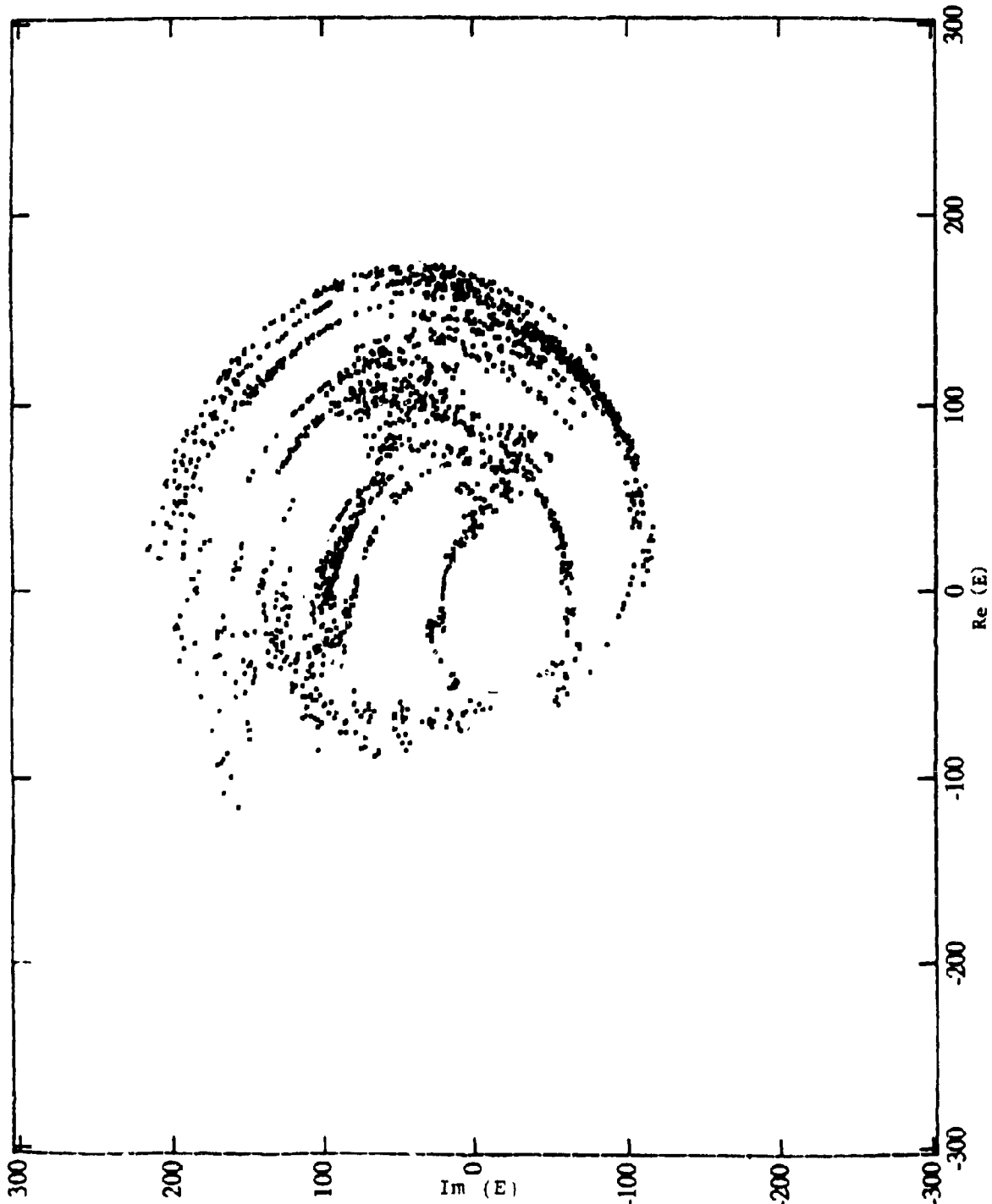


Figure - 5. Output Field in Complex Plane for Net Gain, $K_0 = 0.995$

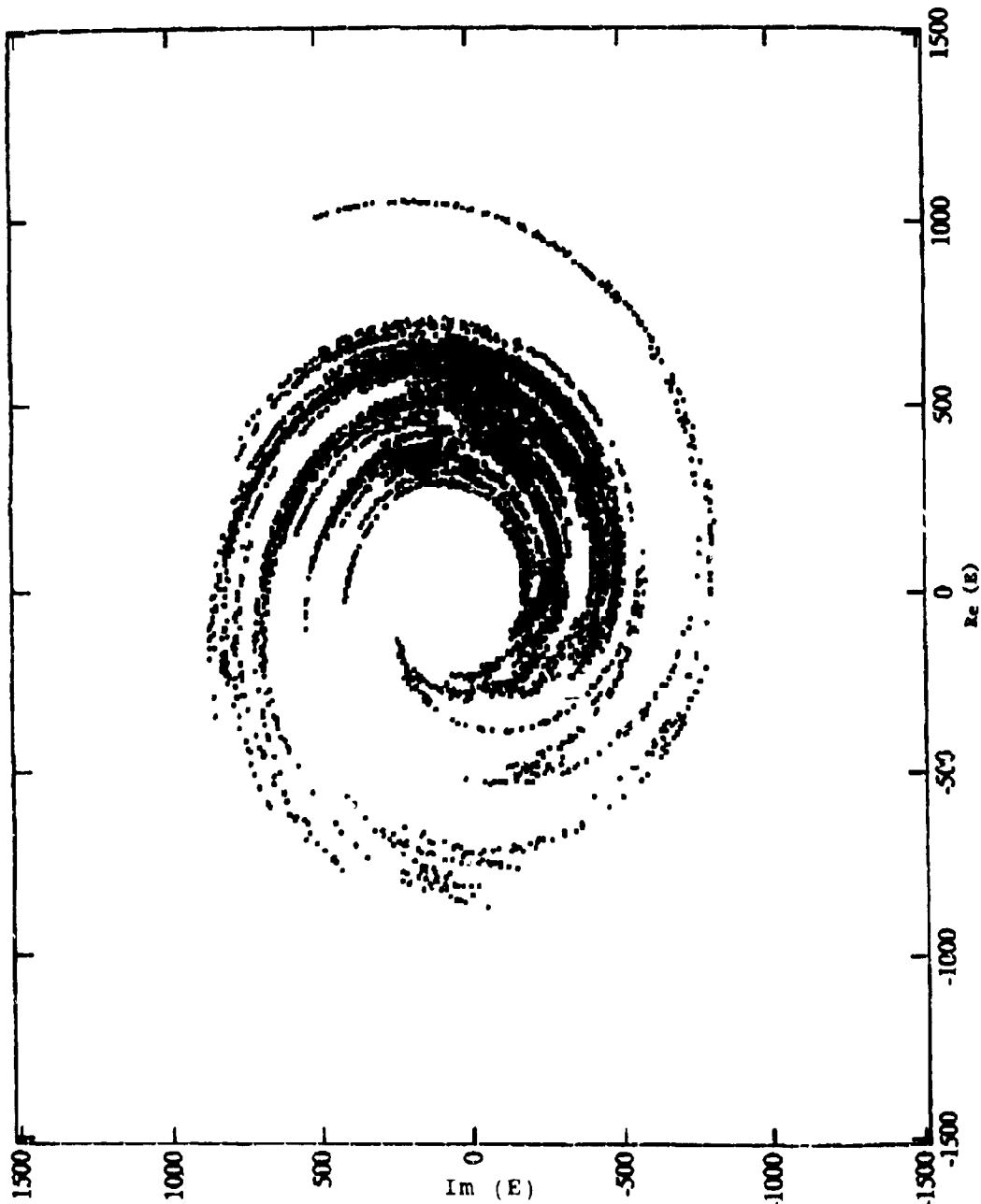


Figure - 6. Output Field in Complex Plane for Net Gain, $K_0 = 0.999$

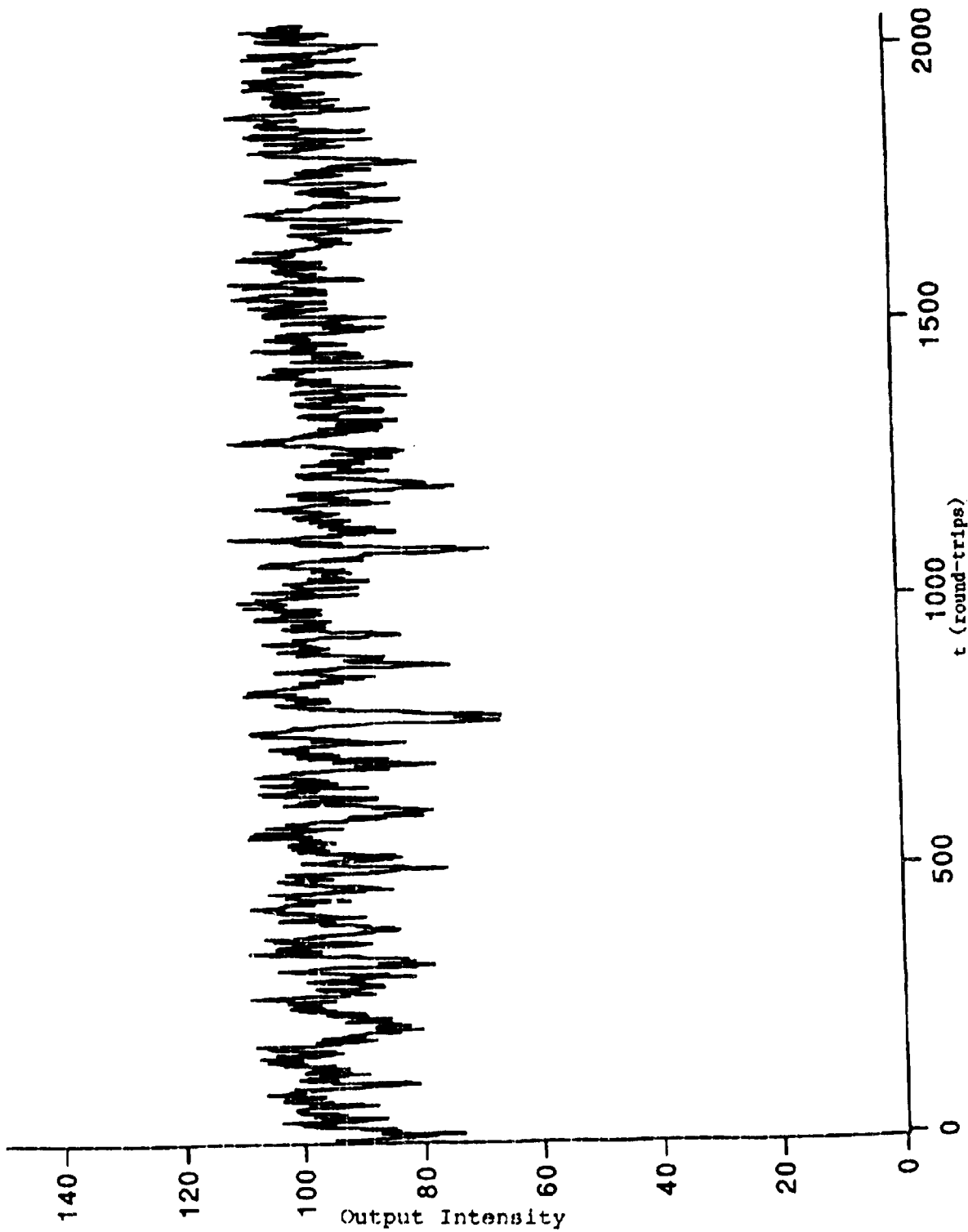


Figure - 7. Output Intensity vs. Round Trips, $K_0 = 0.9$

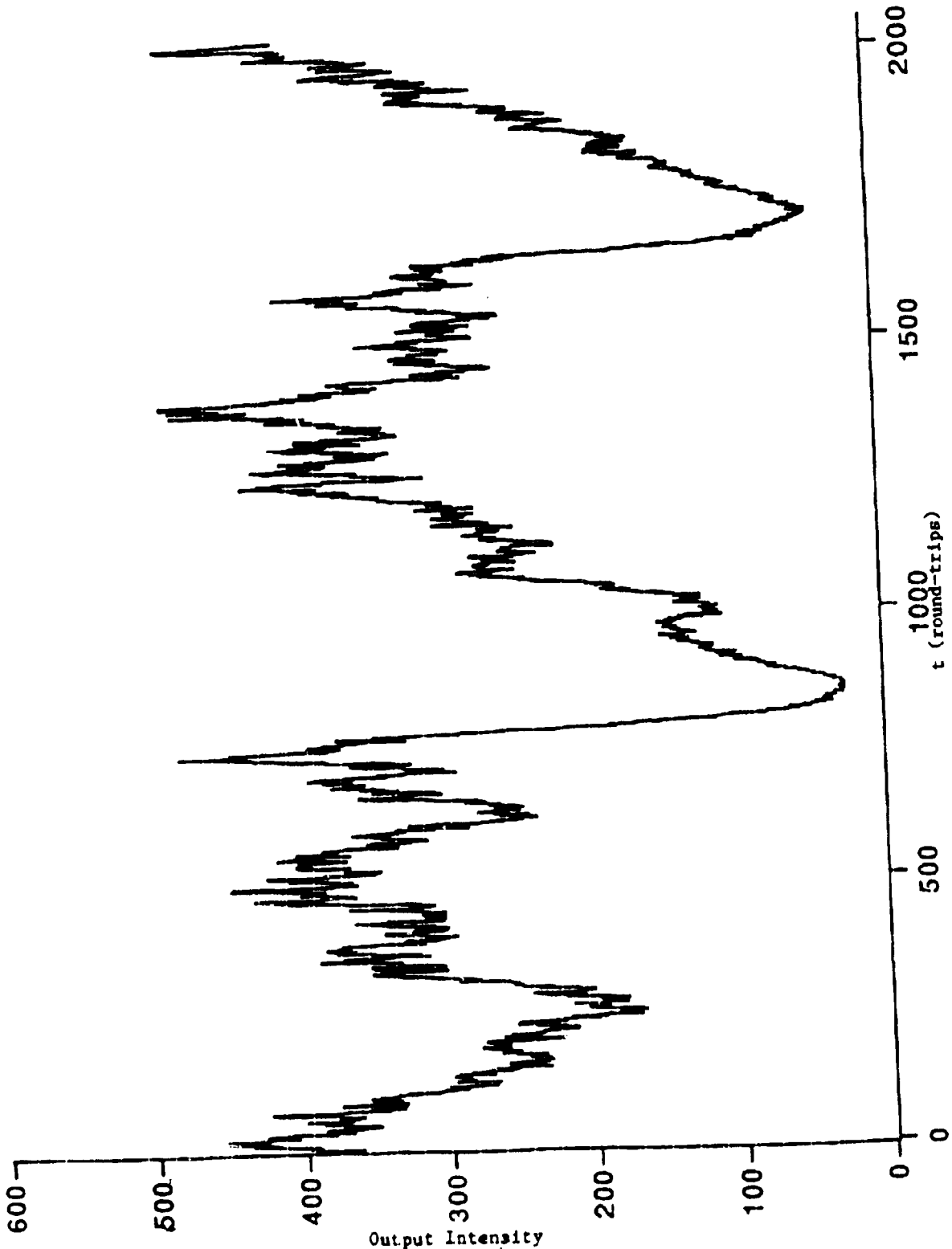


Figure - 8. Output Intensity vs. Round trips, $K_0 = 0.95$

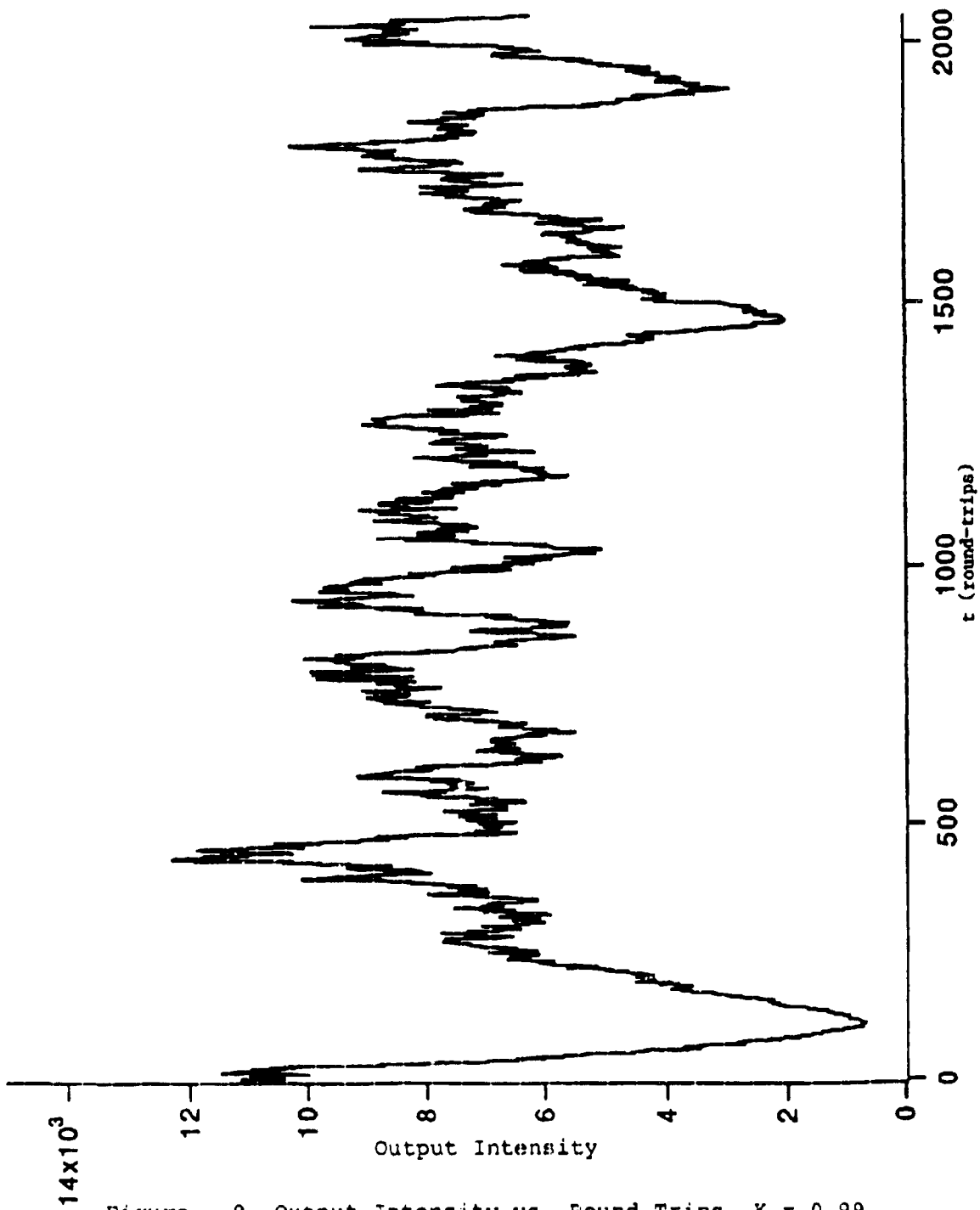


Figure - 9. Output Intensity vs. Round Trips, $K_0 = 0.99$

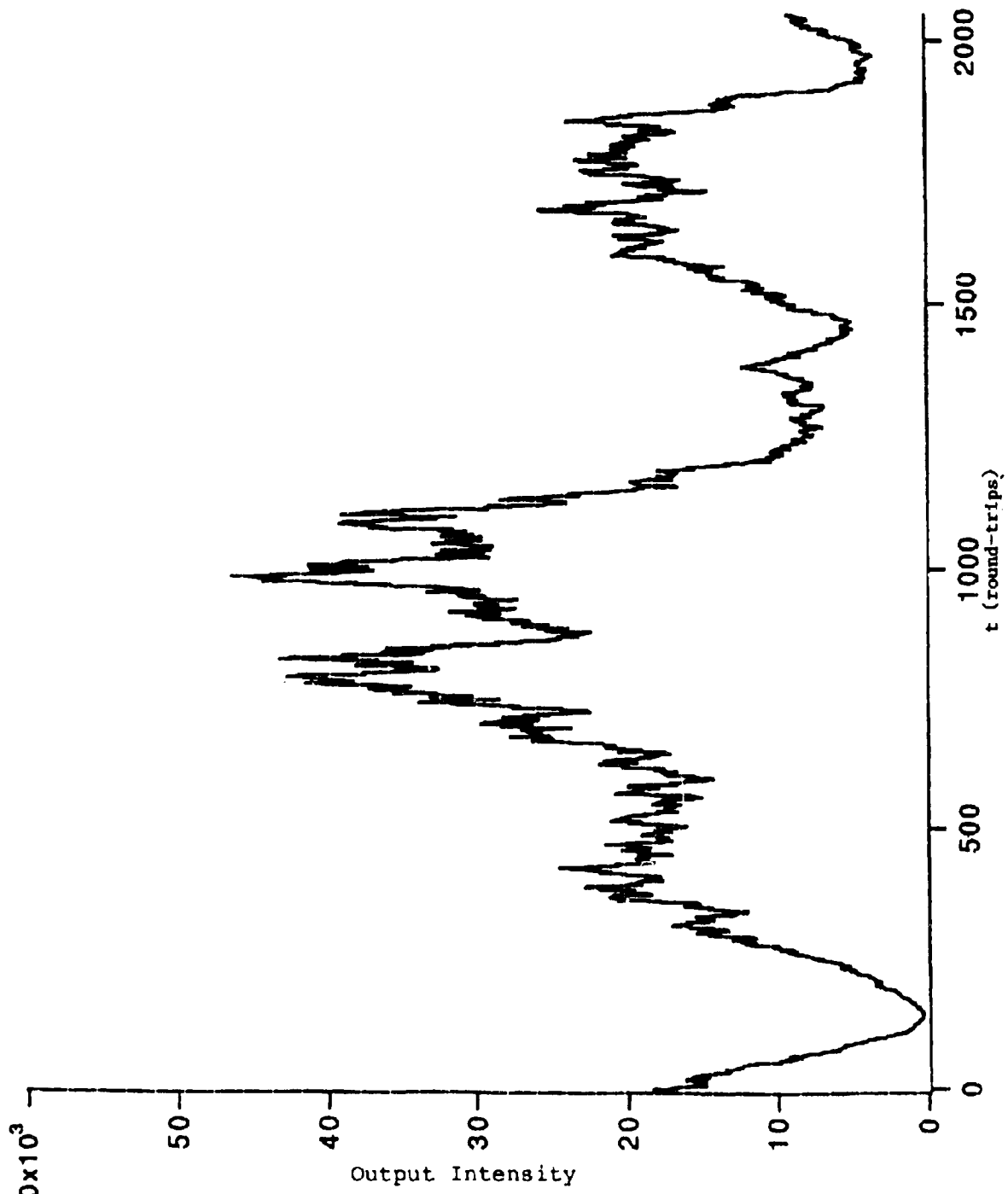


Figure - 10. Output Intensity vs. Round Trips, $K_0 = 0.995$

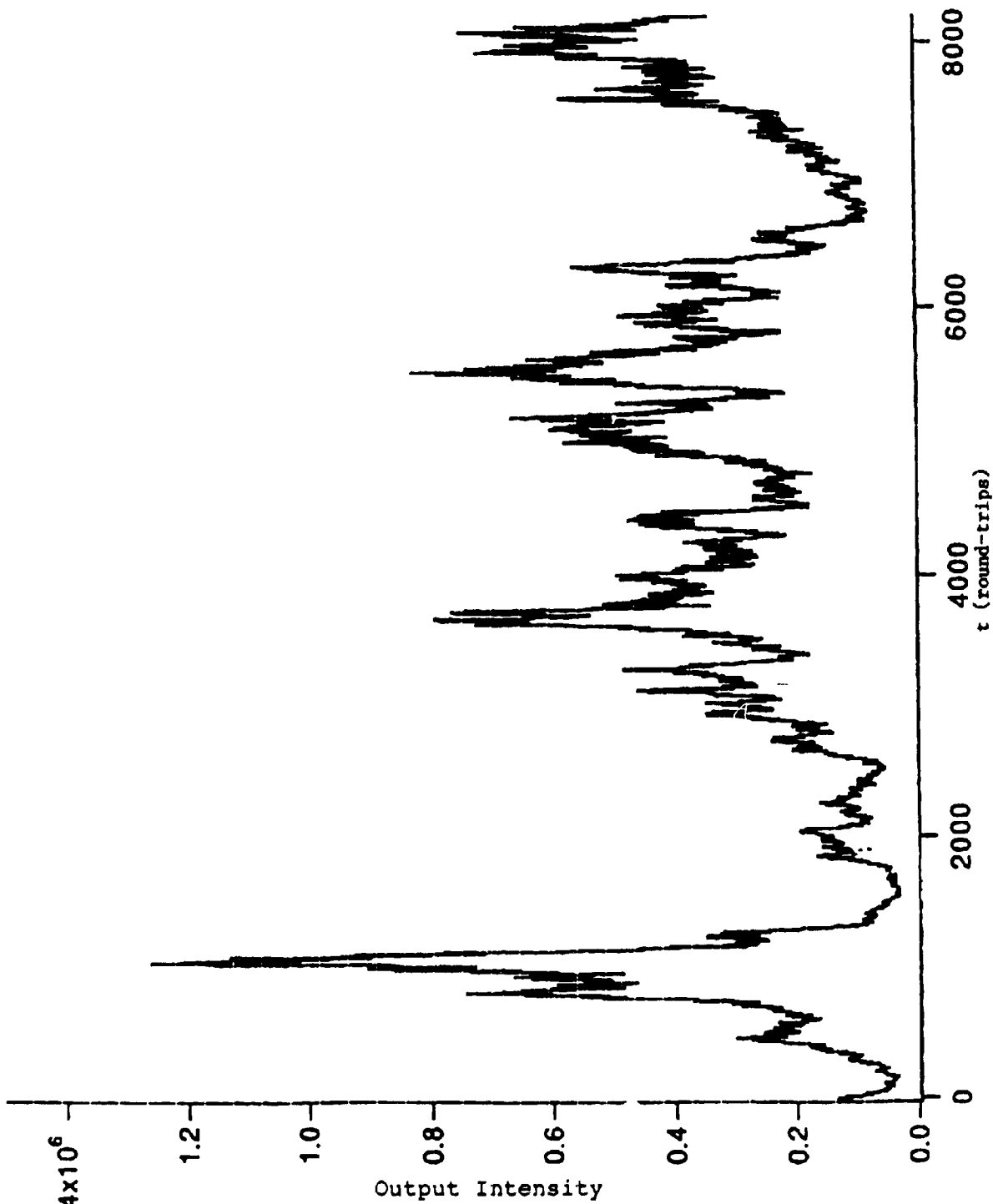


Figure - 11. Output Intensity vs. Round Trips, $K_0 = 0.999$

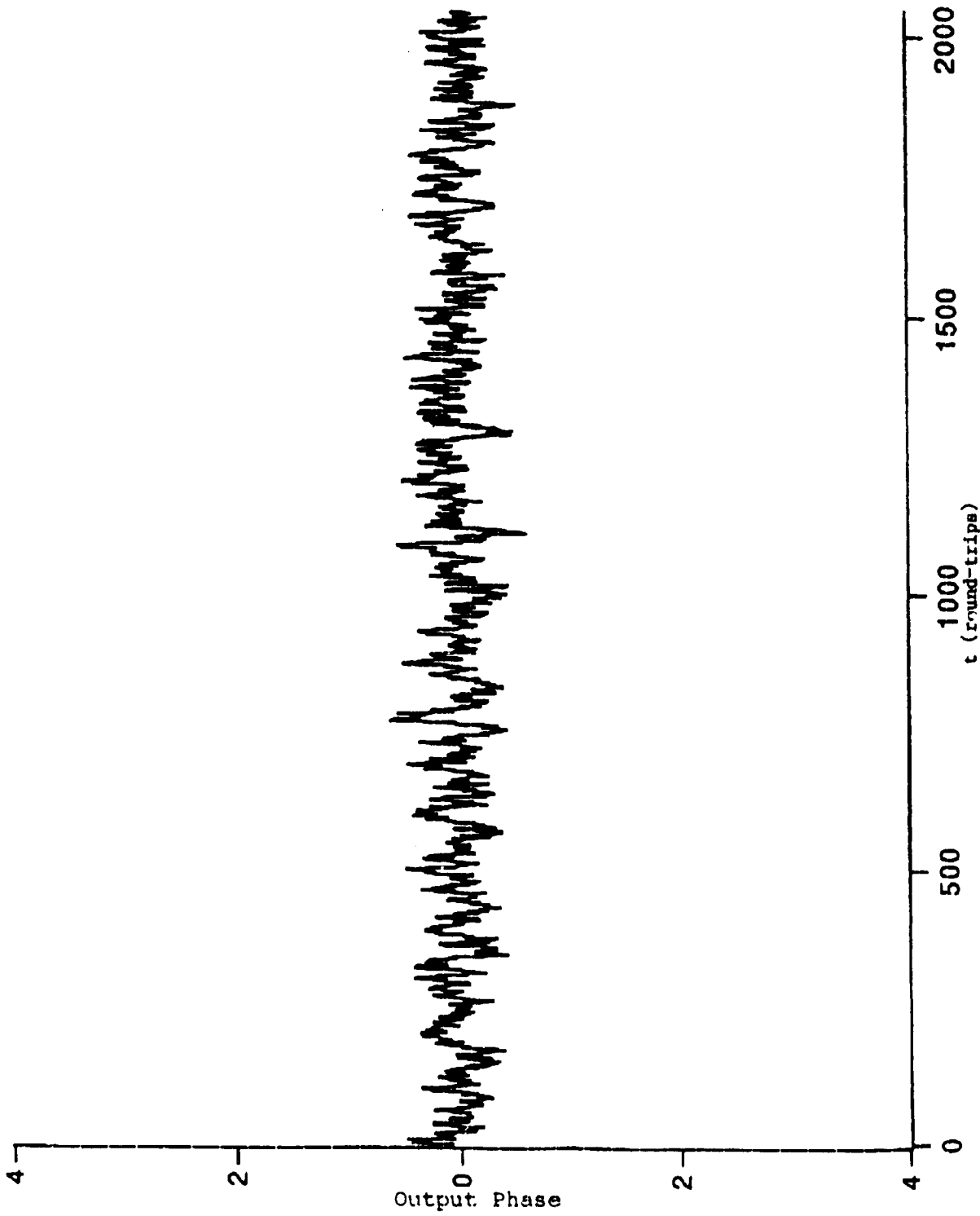


Figure - 12. Output Phase vs. Round Trips, $K_0 = 0.9$

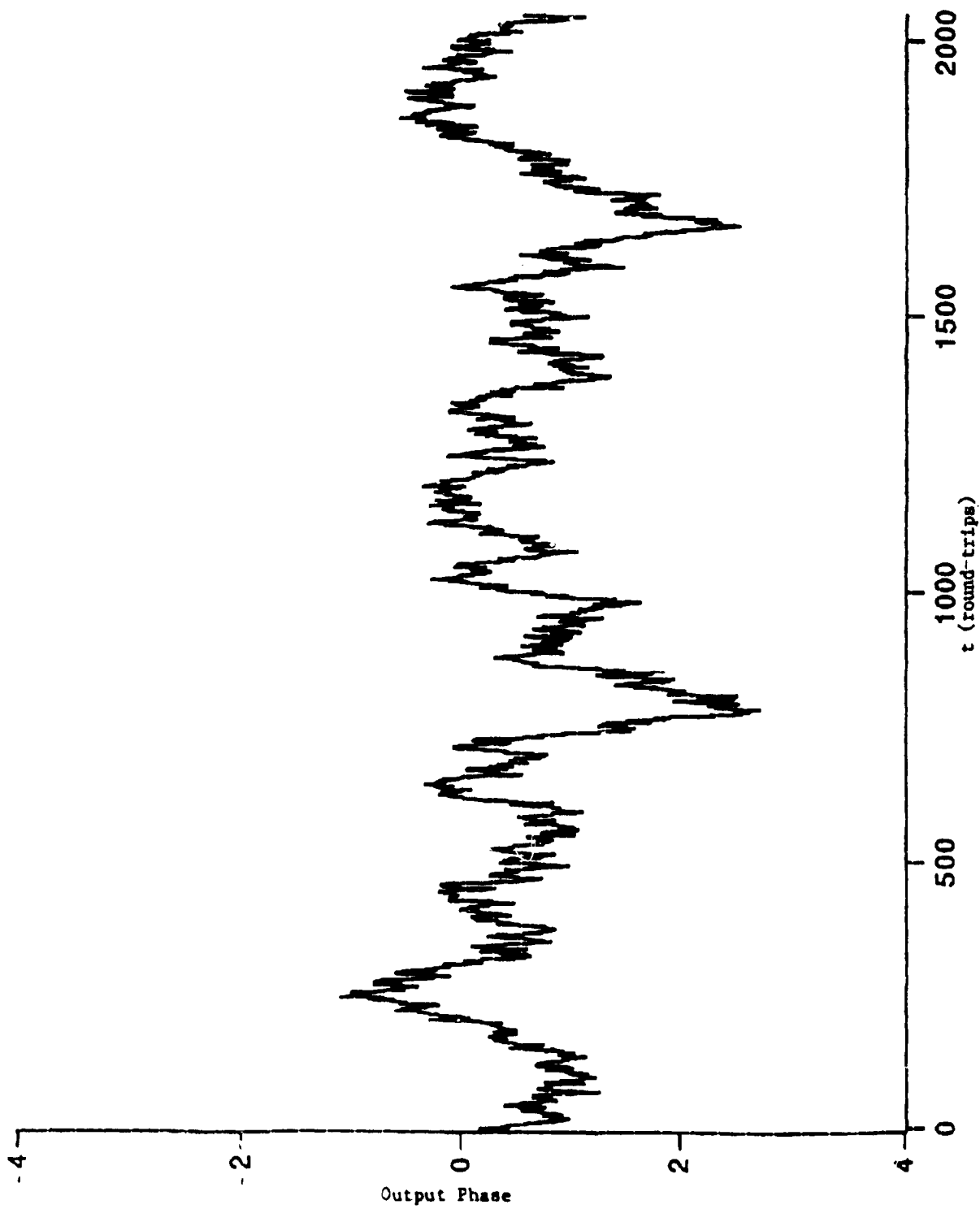


Figure - 13. Output Phase vs. Round Trips, $K_o = 0.95$

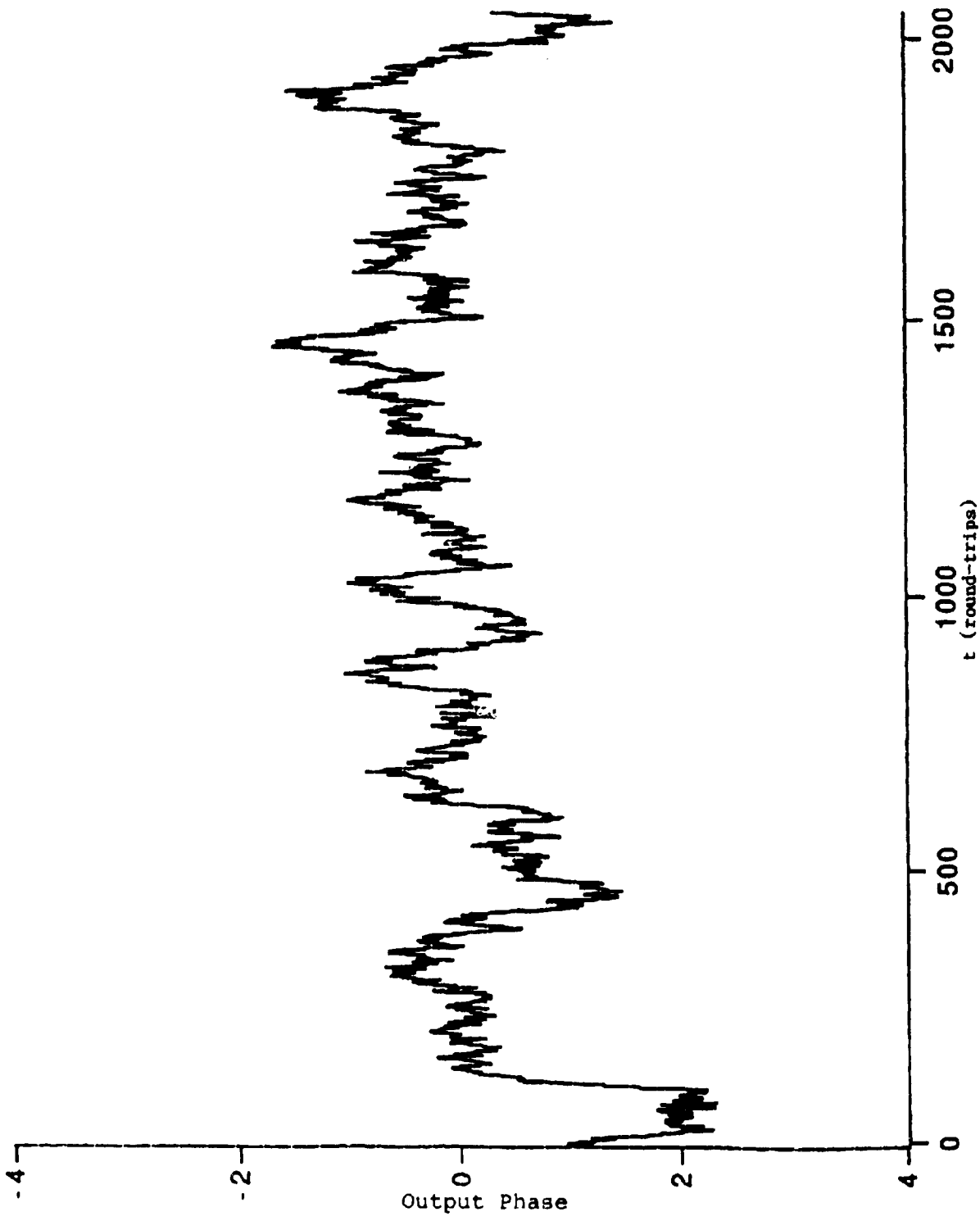


Figure - 14. Output Phase vs. Round Trips, $K_o = 0.99$

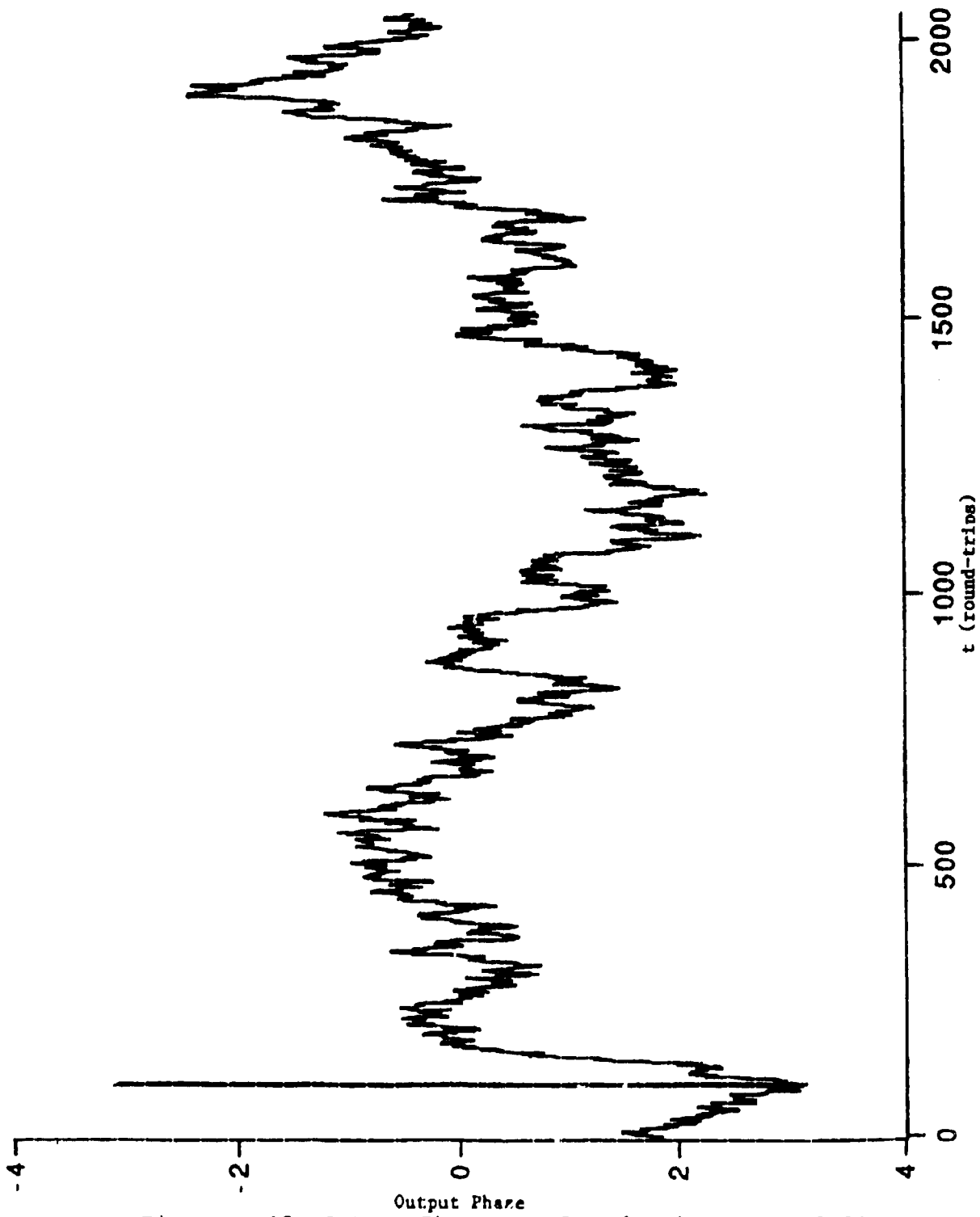


Figure - 15. Output Phase vs. Round Trips, $K_o = 0.995$

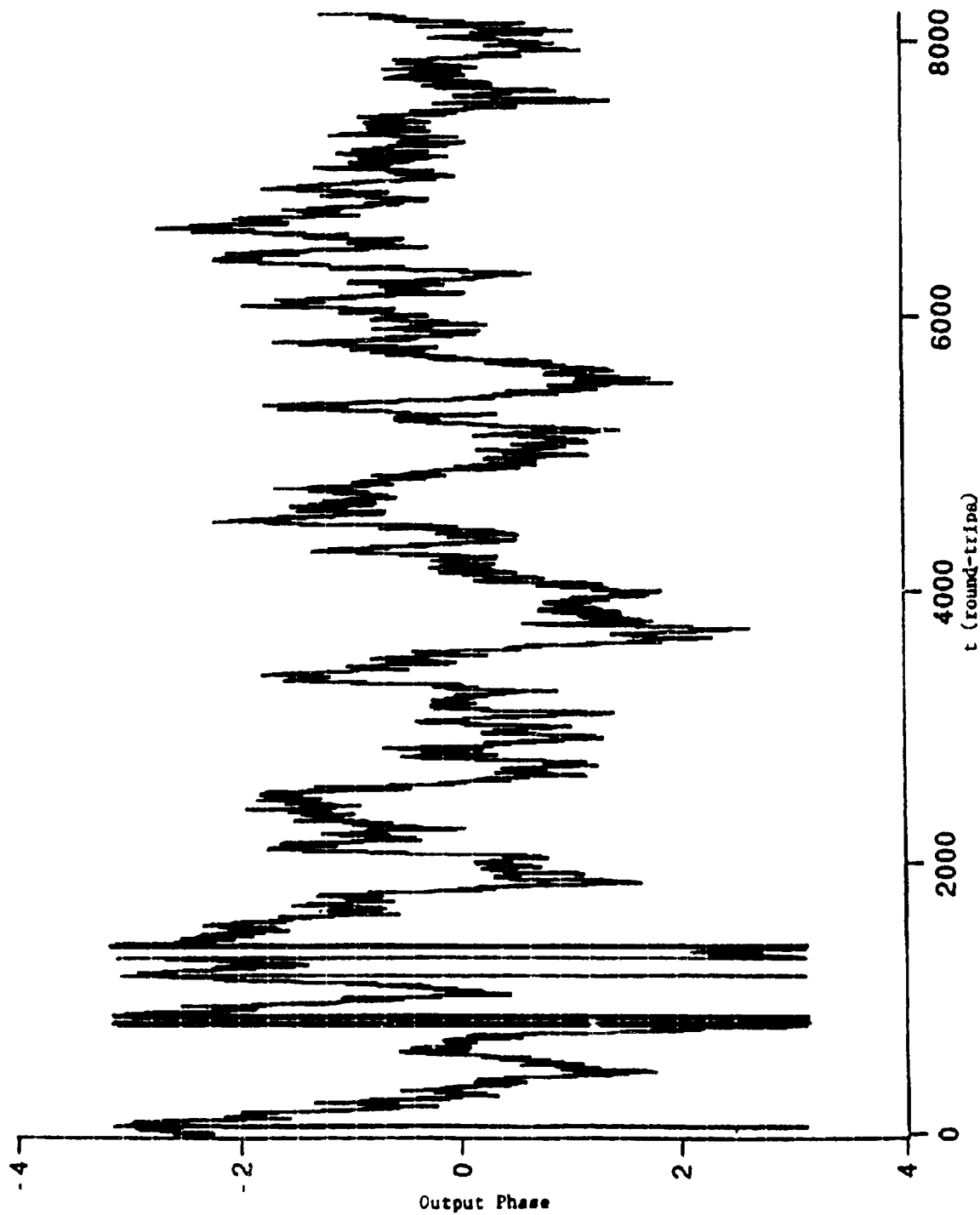


Figure - 16. Output Phase vs. Round Trips, $K_0 = 0.999$

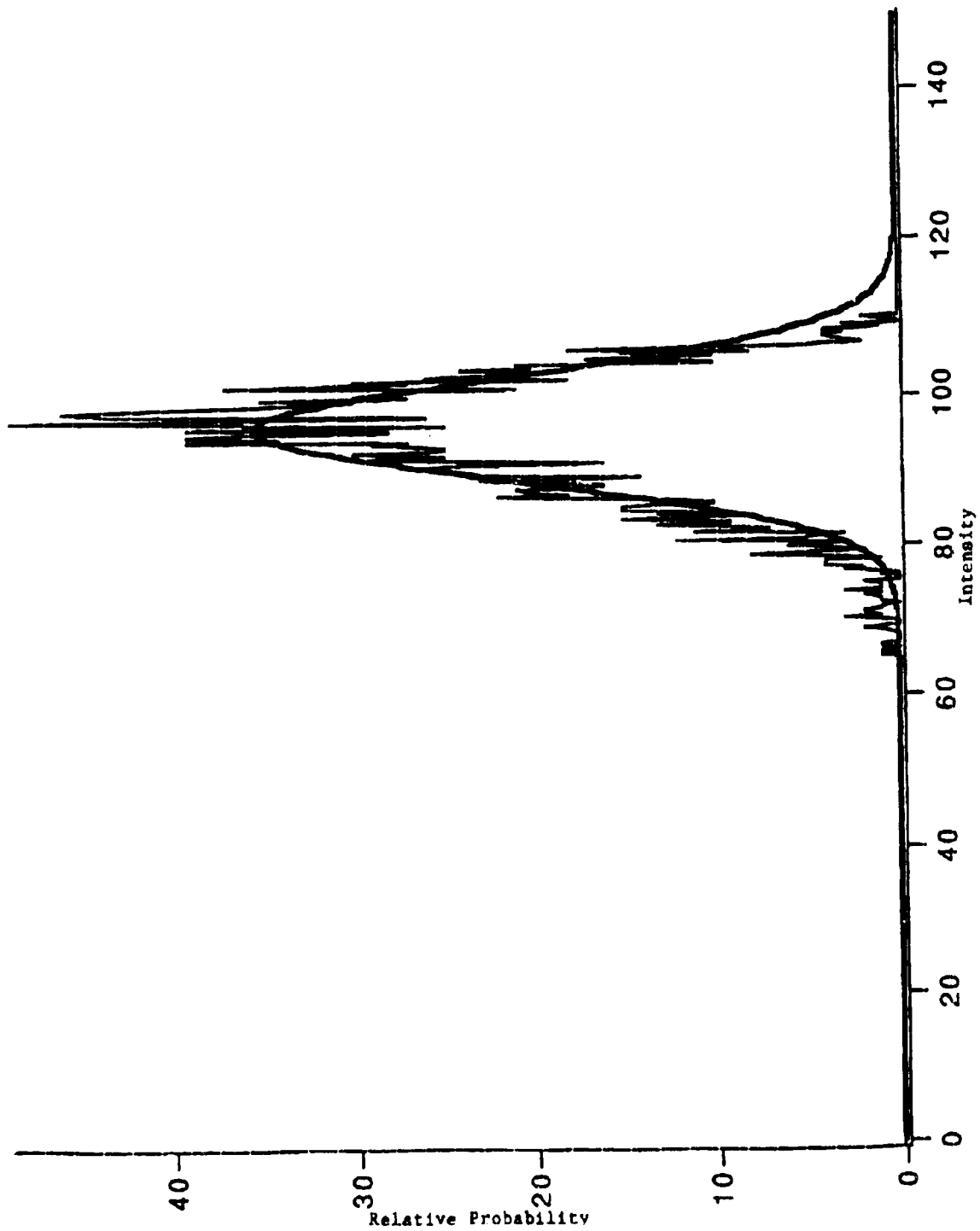


Figure - 17. Relative Probability vs, Intensity, $K_0 = 0.90$

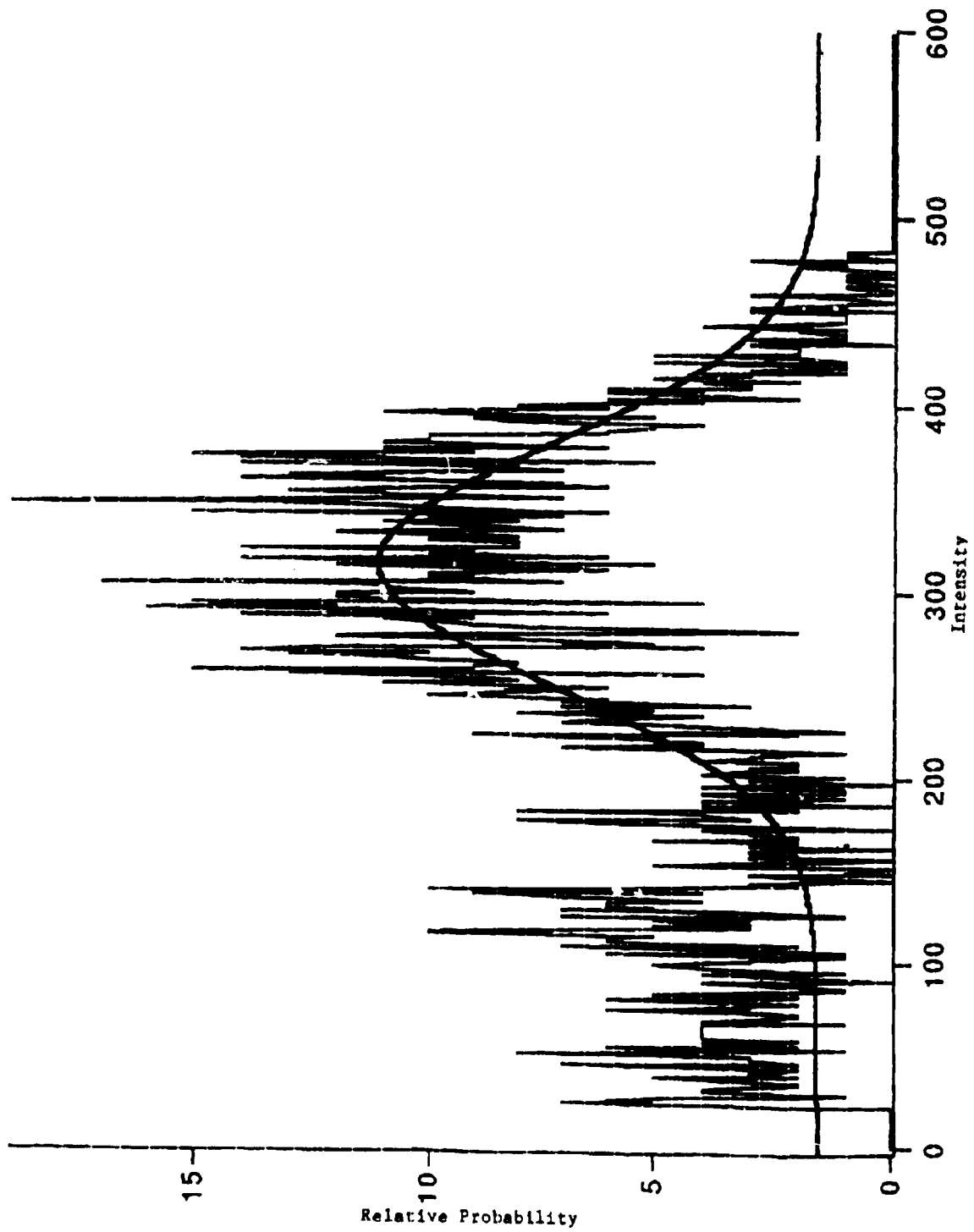


Figure - 18. Relative Probability vs. Intensity, $K_c = 0.95$

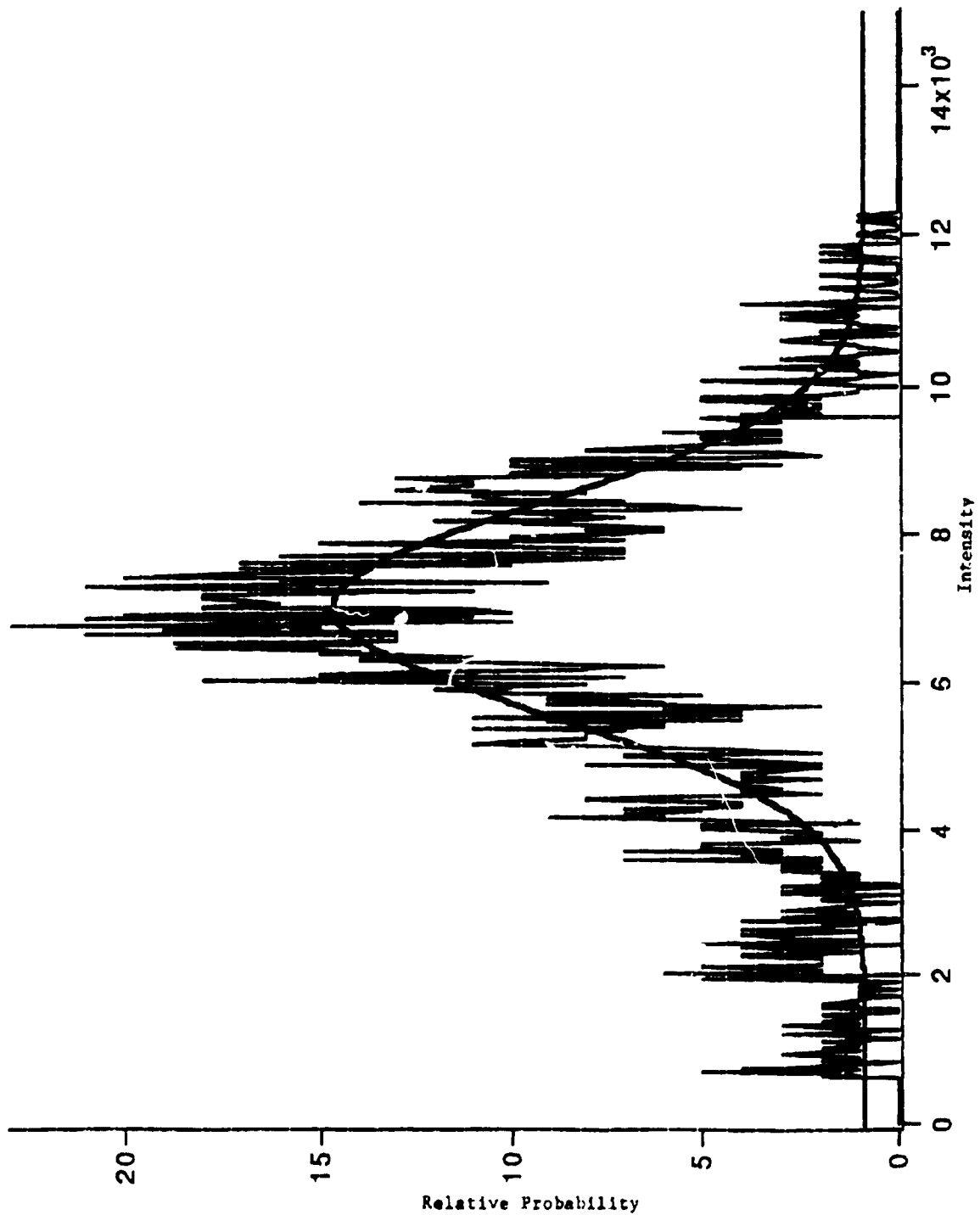


Figure - 19. Relative Probability vs. Intensity, $K_0 = 0.99$

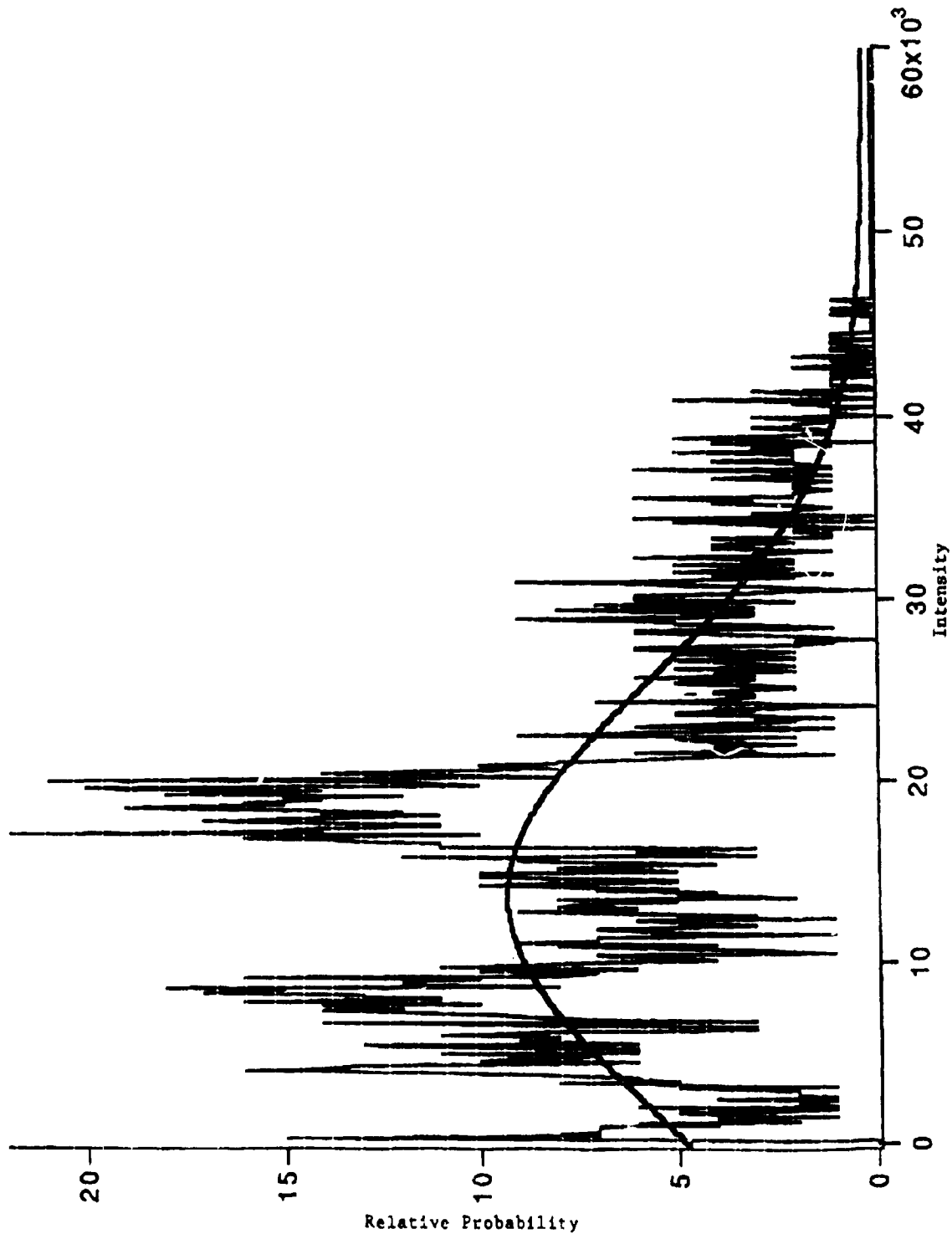


Figure - 20. Relative Probability vs. Intensity, $K_0 = 0.995$

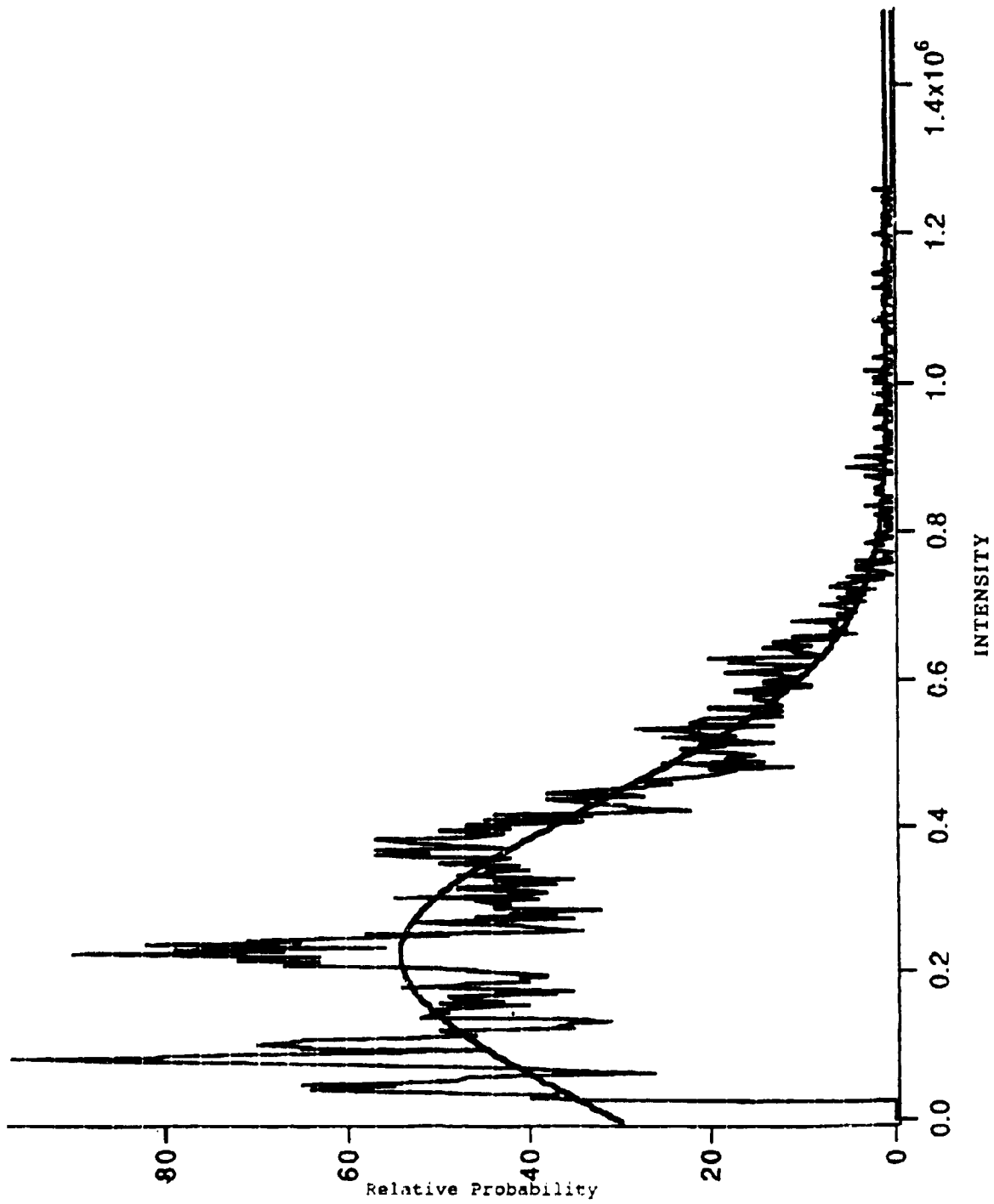


Figure - 21. Relative Probability vs. Intensity, $K_0 = .999$

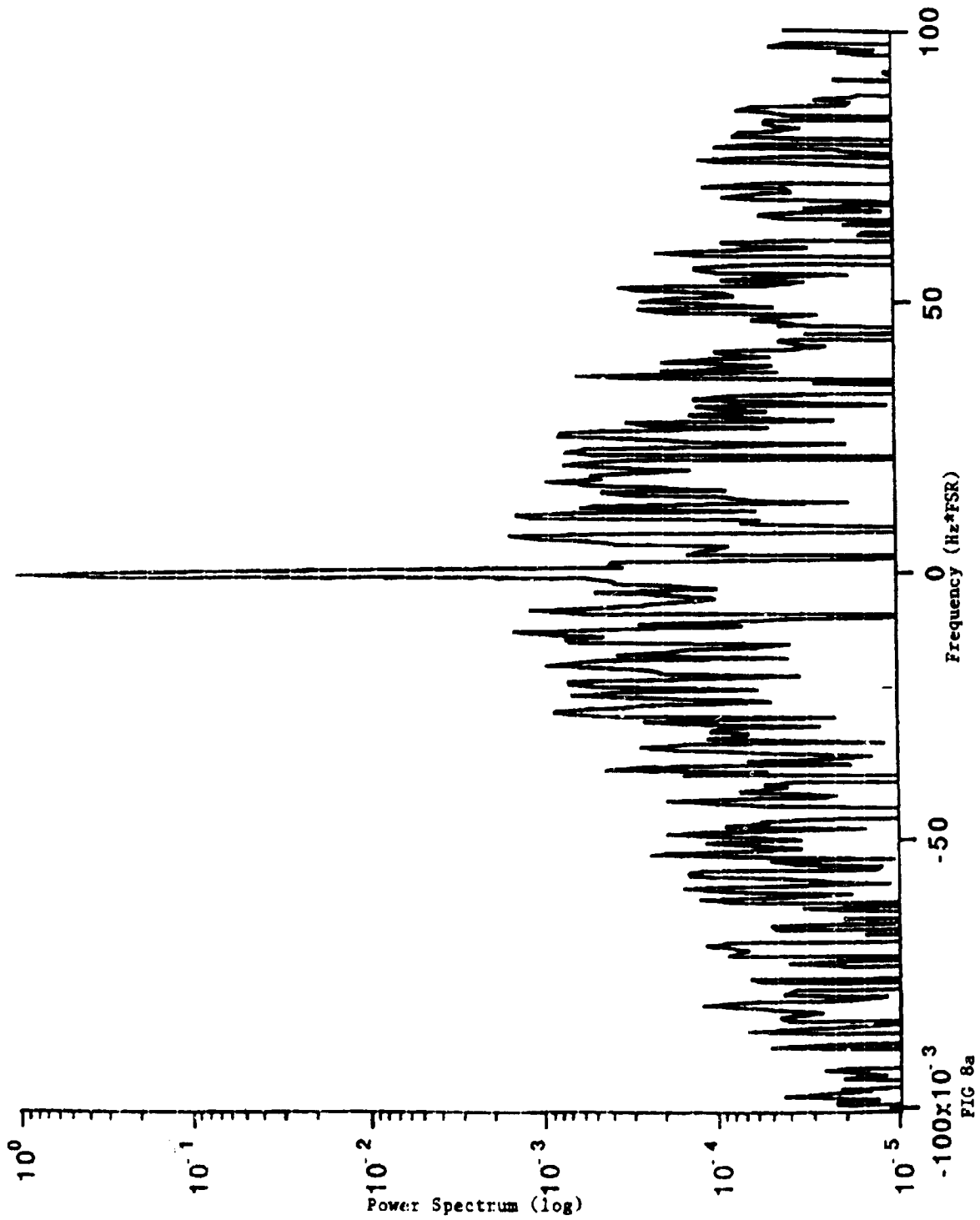


Figure - 22. Power Spectrum vs. Frequency, $K_0 = 0.90$

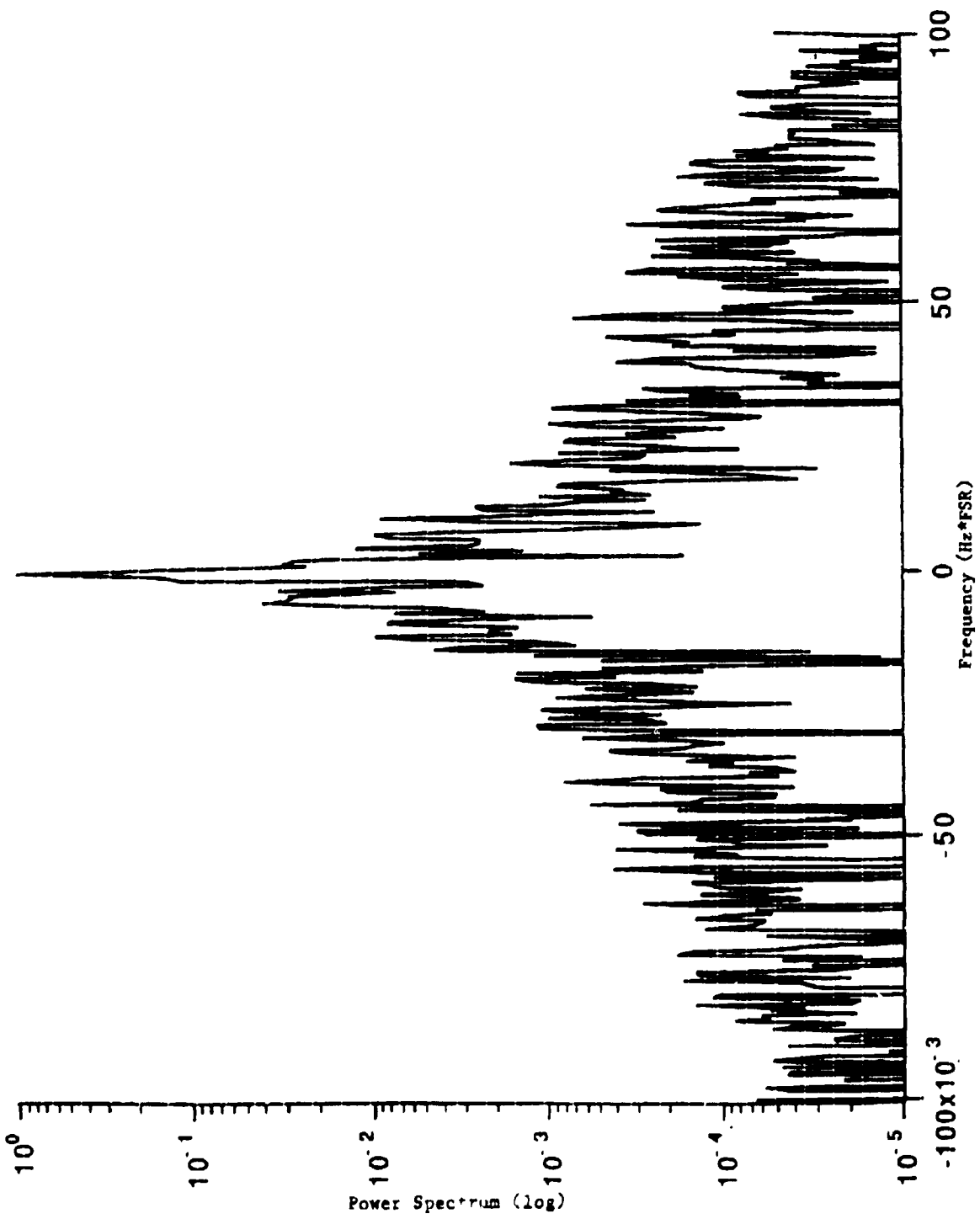


Figure - 23. Power Spectrum vs. Frequency, $K_0 = 0.95$

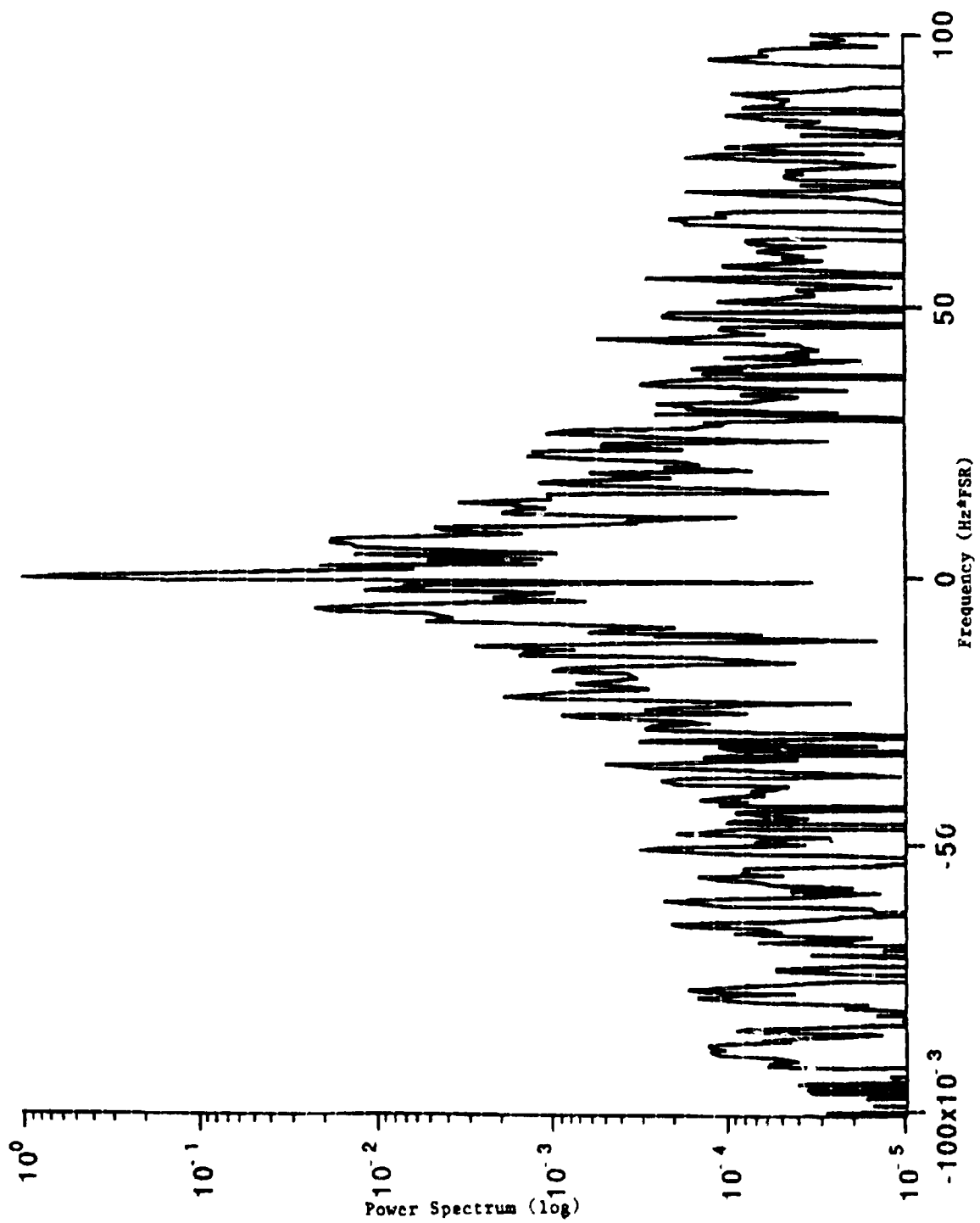


Figure - 24. Power Spectrum vs. Frequency, $K_0 = 0.99$

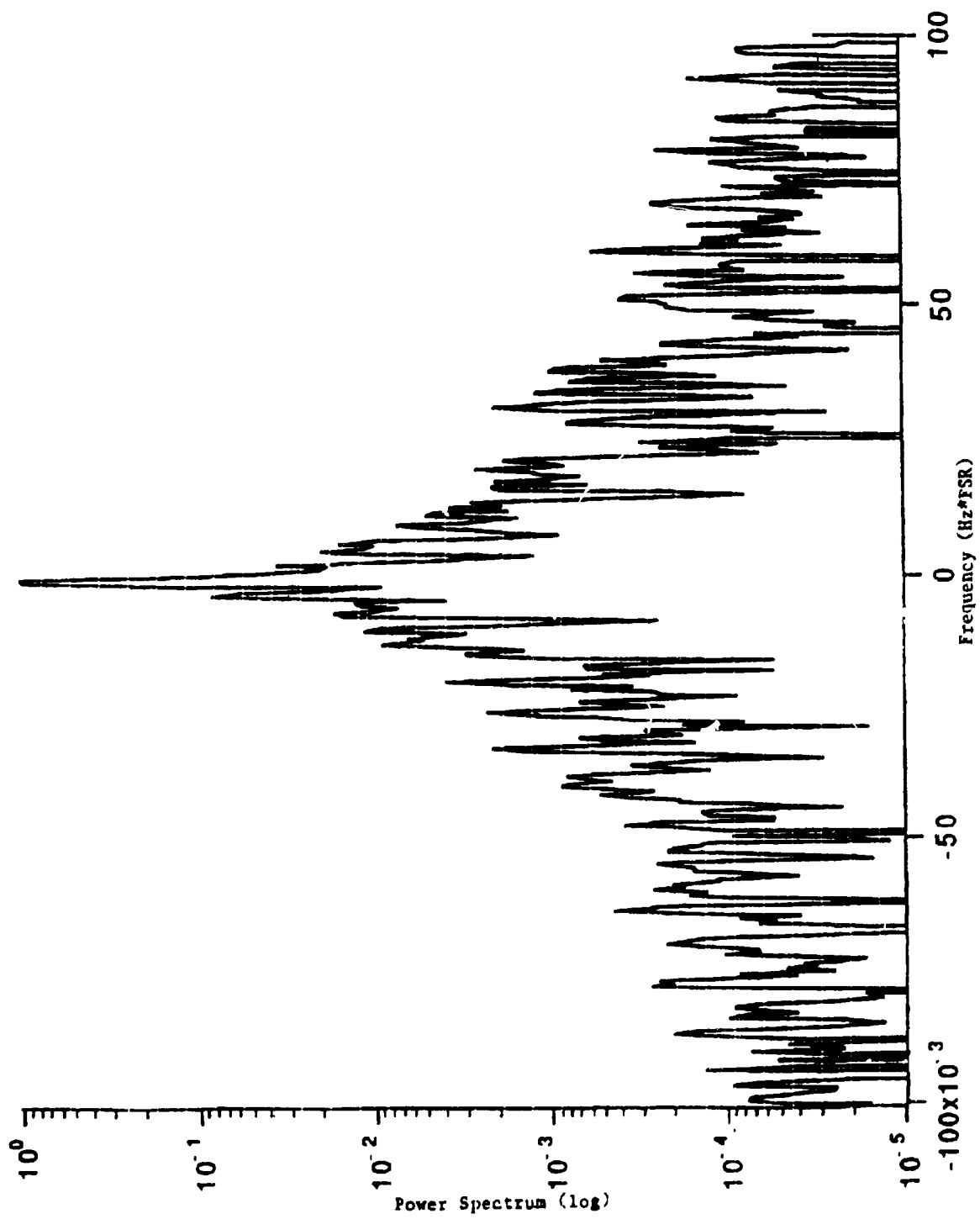


Figure - 25. Power Spectrum vs. Frequency, $K_0 = 0.995$

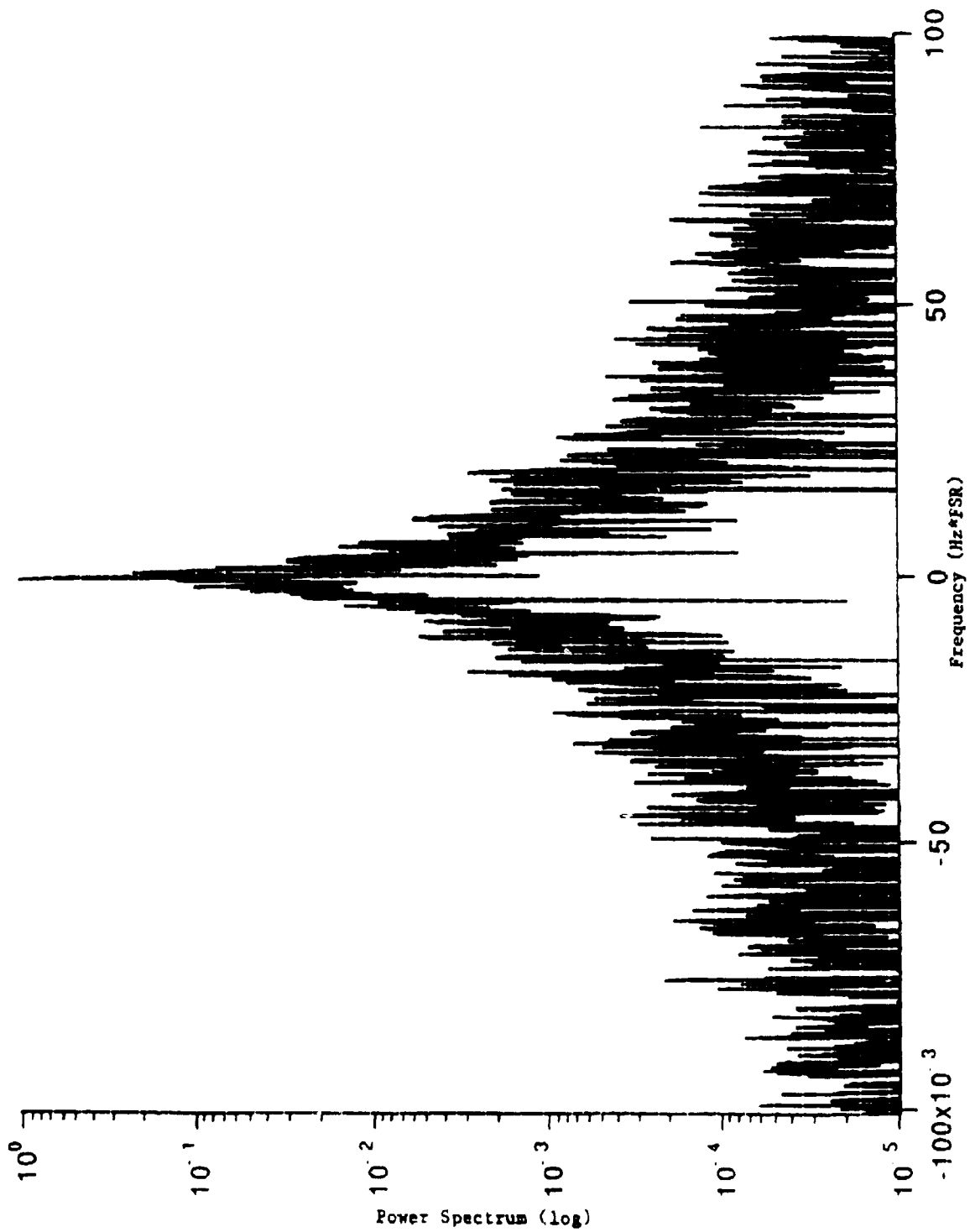


Figure - 26. Power Spectrum vs. Frequency, $K_0 = 0.999$

***MISSION
OF
ROME LABORATORY***

Mission. The mission of Rome Laboratory is to advance the science and technologies of command, control, communications and intelligence and to transition them into systems to meet customer needs. To achieve this, Rome Lab:

- a. Conducts vigorous research, development and test programs in all applicable technologies;
- b. Transitions technology to current and future systems to improve operational capability, readiness, and supportability;
- c. Provides a full range of technical support to Air Force Materiel Command product centers and other Air Force organizations;
- d. Promotes transfer of technology to the private sector;
- e. Maintains leading edge technological expertise in the areas of surveillance, communications, command and control, intelligence, reliability science, electro-magnetic technology, photonics, signal processing, and computational science.

The thrust areas of technical competence include: Surveillance, Communications, Command and Control, Intelligence, Signal Processing, Computer Science and Technology, Electromagnetic Technology, Photonics and Reliability Sciences.